Pharmaco-chemical investigation of *Erythrina caffra*: extracts, isolated compounds and their biological activities

A thesis submitted for the fulfilment of the requirements for the degree of

Master of Science (Chemistry)

At

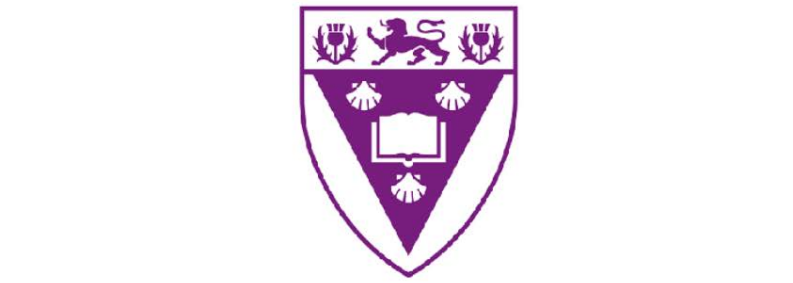

By Simnikiwe Nogqala

Supervisor: Dr. Xavier Siwe-Noundou

Co-supervisor: Prof. Rosalyn Klein

Abstract

In this study, secondary metabolites isolated from *Erythrina caffra*, a medicinal plant indigenous to South Africa, were investigated. *E. caffra* is well-known for its healing properties and it is traditionally used for treating bacterial infections like tuberculosis (TB), abscesses, tooth aches and ear infections. Its extracts have also been used to treat cancer. Though many studies have been done on this plant, most of them tended to focus solely on the isolated compounds. In the present study however, extracts, fractions and isolated compounds from *E. caffra* were evaluated for their anticancer, anti-oxidant, anti-enzymatic, antibacterial and cytotoxicity.

The methanol crude extract (B1) from the stem bark of *E. caffra* was used to extract alkaloidic fractions (B2 and B3) using ethyl acetate and *n*-butanol respectively, a third fraction (B4) was also extracted using ethyl acetate this fraction was called a neutral fraction. The neutral fraction (B4) was fractionated and through a sequence of column chromatography three active secondary metabolites were isolated. The isolated compounds included Lupeol (**1**), stigmasterol (**2**) and 5,7-Dihydroxy-4'-methoxy-3',5'-diprenylflavanone (**3**). These isolated compounds were characterized and identified using spectroscopic techniques including IR, NMR and high-resolution Mass Spectrometry. Using the cell line HCC-70, isolated from a primary ductal carcinoma, *in vitro* anticancer assays were carried out on the crude extract from the bark, fractions, isolated compounds and an unseparated mixture of two compounds. These samples were also evaluated for their anti-oxidant, anti-enzymatic, antibacterial and cytotoxicity activities. The crude extract inhibited the cell viability by over 30% and had no effect on the HeLa cells at concentrations of 20μM.

Abyssinone V' 4-methyl-ether (**3**) and the mixture of stigmasterol (**2**) and an unidentified compound exhibited potent anticancer activity against the HCC-70 cell line with IC_{50} of 18.05μM and 9.04μM respectively. Antibacterial assays were also carried out on the crude extracts, fractions and concoctions made from the fractions with the best activity combined with the ones that performed poorly. The concoctions were prepared as two separate series (S and N series). The crude extract inhibited more than 80% of the *Staphylococcus aureus* cells at a concentration of 20μM with only minimal damage to the HeLa cells. In the concoctions however, the N series managed to inhibit over 96% of the *S. aureus* while exhibiting no cytotoxicity towards HeLa cells. The extract and its fractions also showed good anti-oxidant activities.

Molecular docking of these compounds was done on the Human estrogen receptor (PDB ID:3ERT) and Abyssinone V' 4-methyl-ether (**3**) showed the best docking score of -6.6 Kcal/mol, for the simulation against Epidermal growth factor receptor (PDB ID: 1M17) Stigmasterol (**2**) showed the best docking score of -3.8 Kcal/mol. *In silico* docking on 3ERT and 1M17 were done to test the binding affinity of the isolated compounds to the proteins which are well known to be overexpressed in some types of cancer.

Flavonoids isolated from *Erythrina* species have been reported to possess good antiplasmodial activity. However, due to the minute amounts isolated in the present study *in-vitro* assays could not be carried out. Nevertheless, in-silico assays were conducted on the most prominent protozoal parasite which causes malaria in the majority of African countries.

In-silico simulations were done against *Plasmodium falciparum* protein (PDB ID: 7KJH), of the tested compounds Abyssinone V' 4-methyl-ether (**3**) was found possess the best docking score of -4.4 Kcal/mol. The molecular docking of 7KJH was done to assess the inhibitory potential of the isolated compounds on protozoal parasites.

Pharmacokinetic properties of the isolated compounds were also assessed *in silico* to assist in evaluating the drug likeness of these compounds. The compounds showed a percent human oral absorption of 100% except for Abyssinone V' 4-methyl-ether (**3**), which showed 93.83%, this indicates a remarkable oral bioavailability. Stigamsterol (**2**) exhibited a Caco-2 cell permeability (QPPCaco) greater than 500 which indicates outstanding results for good intestinal absorption. The compounds also displayed a blood-brain partition co-efficient (QPlogBB) ranging from -1.433 to 0.128 suggesting they will have less potential to cross the blood-brain barrier, thus reducing any CNS related toxicity.

Molecular networking of the crude extracts and the fractions was done through GNPS which allowed the identification of known compounds including one isolated in the present study, Abyssinone V' 4-methyl-ether (**3**). Possible derivatives that have not been isolated from this plant before were also putatively identified.

Acknowledgements

I would like to acknowledge the support from everyone who helped me in different ways to achieve this MSc.

Dr. Xavier Siwe-Noundou, my supervisor I would like to express my sincere gratitude for taking me under your wing, always finding time to help me and explaining even the basic concepts. Your patience, in-depth remarks and supportive guidance made this a success. I would also like to thank Professor Krause for accepting me in your group with warm arms, and helping me with all the chemicals I needed for my project.

I would also like to thank Professor Rosalyn Klein for the invaluable assistance provided in this research and the constructive criticism on the departmental presentations.

I am very thankful to the Henderson scholarship for giving me an opportunity to do my Masters by granting me a bursary covering all my expenses and academic fees, this work would never have been possible without the financial assistance.

I am also grateful to all the Chemistry Department members. My labmates in F22 for helping me with the problems I had in my research. I would also like to thank Professor Lobb's group, specifically Mr. Mofeli for the great help with the molecular docking simulations. I would also like to thank Dr. Kemboi for the lessons in column chromatography and analysing NMR, I would also like to thank Dr. Jarmo for taking his time teaching me about molecular networking. A special thanks to Mrs Michelle Isaacs for conducting the antibacterial and cytotoxicity assays and Dr. Jo-Anne de la Mare for running the anticancer assays.

I am thankful to my family for believing in me. I am also very grateful to my friends, Mojahi Motaung, Choonzo Chiyumba and Jaxx Edwardes for being my support system and making my stay in Grahamstown pleasant. My younger sisters, especially Zusibonise Nogqala and Sibahle Sngcoli Kewuti for their uplifting words when I was down.

But most of all I would like to thank God for “I can do all things through Him who strengthens and empowers me”

List of abbreviations

1D	1 dimensional
2D	2 dimensional
3D	3 dimensional
NMR	Nuclear Magnetic Resonance
MS	Mass Spectrometry
HR-ESI-MS	High Resolution Electrospray Ionisation Mass Spectrometry
$CDCl_3$	Deuterated chloroform
COSY	Correlated Spectroscopy (^1H -^1H)
δ_H	delta (Chemical shift of proton)
δ_C	delta (Chemical shift of carbon)
DCM	Dichloromethane
DMSO	Dimethyl sulfoxide
DEPT	Distortionless Enhancement by Polarization Transfer
FT-IR	Fourier-Transform Infrared Spectroscopy
HeLa cells	Henrietta Lacks cells

HMBC	Heteronuclear Multi-Bond Coherence (^{1}H- ^{13}C)
HSQC	Heteronuclear Single Quantum Coherence (^{1}H-^{13}C)
IC_{50}	50% Inhibitory Concentration
m	multiplet
MeOH	Methanol
MHz	Megahertz
mg	milligram
mL	Millilitres
NOESY	Nuclear Overhauser Effect Spectroscopy (^{1}H -^{1}H)
NOE	Nuclear Overhauser Effect
PDB	Protein Data Bank
ppm	parts per million
s	Singlet
d	Doublet
t	triplet
TLC	Thin Layer Chromatography
TM	Traditional Medicine

WHO	World Health Organisation
μM	micromolar
μL	Microlitre
IR	Infrared
m.p	Melting point
P. E	Petroleum Ether
S. aureus	*Staphylococcus aureus*
PIA	Polysaccharide Intercellular Adhesin
EPS	Extracellular Polymeric Substances
CNS	Central Nervous System
DNA	DeoxyriboNucleic Acid
DALY's	Disability Adjusted Life Years
eDNA	extracellular DNA
DCIS	Ductal Carcinoma *In-situ*
LCIS	Lobular Carcinoma *In-situ*
MBC	Metastatic Breast Cancer

ADH	Atypical Ductal Hyperplasia
IDC	Invasive Ductal Carcinoma
Acetyl-CoA	Acetyl coenzyme A
EC/ *E.Caffra*	*Erythrina caffra*
nM	Nanomolar
UV	Ultraviolet
PTLC	Preparative Thin Layer Chromatography
EtOAc	Ethyl acetate
STD	Sexually Transmitted Disease
AO	Anti-oxidant activity
HSV	Herpes simplex virus

“Nature hangs green curtains round the edges so that we shan’t probe into the secrets that are hidden somewhere in the depths of space beyond the range of sight. But if we only turn the key, we will unlock the gold.”

Anonymous

Table of contents

List of figures

Chapter 1. Introduction

1.1. Medicinal plants as antimicrobial and anticancer agents

Throughout history, medicinal plants have been a source of hope for humanity in the fight against infectious diseases. Medicinal plants have been found to possess antimicrobial properties that help combat certain illnesses. They are known as broad-spectrum antimicrobial agents, which means that they can target a wide range of microorganisms (Etkin, 2005). Researchers have extracted chemical constituents from medicinal plants that have been demonstrated to be effective in treating different types of infections (Mahady, 2005) . This has generated significant interest in exploring the biological activities of medicinal plants, leading to a multitude of studies being conducted in this area.

Not only have medicinal plants been used for threating antimicrobial diseases but they have also been used to treat cancers. Studies have found these plants to have a wide range of biological properties and, as a consequence, a new approach was taken called ‘combination chemotherapy’(Tyagi *et al.*, 2002). This approach uses nontoxic phytochemicals or less toxic phytochemicals in combination with chemotherapeutic agents to amplify its effectiveness as well as to have reduced cytotoxicity to normal tissues (Tyagi *et al.*, 2002).

An exuberant number of compounds from natural products have been used as frameworks for numerous clinically proven drugs in treating various types of infectious diseases (Mahady, 2005). This section will shed more light on applications of medicinal plants in general including the plant investigated in this study. A large number of compounds isolated from natural sources has been evaluated for their activities *in vitro*.

1.1.1. Traditional applications of medicinal plants

The utilization of medicinal plants dates back to the beginning of human civilization (Fabricant and Farnsworth, 2001). Medicinal plants were first used by our ancestors as remedies to assuage a wide range of ailments from mere joint pains to liver troubles (Avhad, Tiwari and Ushir, 2019). For many decades medicinal plants were mostly used for their health benefits on both humans and livestock by numerous communities around the world. Each part of the plant contains compounds having different medicinal properties (Bruschi *et al.*, 2014). A typical

example of this is *Erythrina Abyssinica* which is commonly used in traditional medicine to treat snake bites, cough, sexually transmitted diseases (STD's) etc. Some parts of the plants are used to treat peptic ulcers, flowers to treat dysentery whereas its bark is used as an anthelmintic and to treat asthma and meningitis respectively (Aerts, 2009). This knowledge was of course mostly confidential and kept among traditional healers in ancient times also the administration of these medicines was somewhat arbitrary (Cowan, 1999). However, as civilizations progressed times changed and the knowledge was passed on from generation to generation either in writing or simply by word of mouth, thus building vast libraries of medicinal plants with known traditional applications (Mishra *et al.*, 2011; Ningthoujam *et al.*, 2012; Fredriksson, 2021).

A large number of studies has been done to better understand the biological properties of medicinal plants (Tyagi *et al.*, 2016). To ameliorate the pharmacological properties of the parts of the plants with poor biological activity were often combined with the parts that have moderate activity, the resulting concoction would occasionally give remarkable pharmacological properties due to the stupendous synergistic effect (Aerts, 2009). Over 80% of the world's population have been estimated to rely on traditional medicine for primary health care, this is especially true for developing countries (low and middle income) countries (WHO, 2019). The increase in the use of traditional medicine (TM) as primary health care has been noted and is mostly due to them being easily accessible, affordable and because they are deemed effective (Tugume *et al.*, 2016). A minority of these people is more interested in autarchy than the medicinal care (Cowan, 1999).

The emergence of antibiotic resistant infectious diseases has rendered commonly used drugs ineffective making it harder to treat common disease thus leading to increased morbidity and mortality (WHO, 2020). This has in turn increased the need for novel effective drugs to fight against microbial diseases. This has led to extensive investigations on plant extracts and chemical constituents from medicinal plants with known antimicrobial properties, which has significantly affected therapeutic treatment (Tyagi *et al.*, 2016). The main reasons for using medicinal plants as sources of therapeutic agents are:

- To use isolated bioactive compounds as drugs e.g., morphin, vinblastine and vincristine;
- To produce novel or known compounds or known structures of bioactive compounds as lead compounds using chemical synthesis to provide

patentable synthetic analogues with higher activity and/or lower toxicity e.g., oxycodone, taxotere and verapamil;

- To use them as pharmacological tools e.g., mescaline, yohimbine, lysergic acid diethylamide (LSD);
- To use parts or the whole plant as herbal medication. Only about 6% of the known plants in the world have been screened for biological activities and 15% has been evaluated phytochemically (Joshi and Kaur, 2016). Even though most plants have been extensively investigated, there are plants that require thorough investigation of their composition and corresponding activities. The use of medicinal plants is not only limited to being used as therapeutic agents; they can also be used as preservatives during food processing to prevent food borne microorganisms.

Various medicinal plants contain different classes of compounds that have biological activity. However, for the purposes of this study, we will only focus on four specific classes of compounds: alkaloids (**1.1.2**), polyphenols (**1.1.3**), flavonoids (**1.1.4**), and terpenoids (**1.1.5**).

1.1.2. Alkaloids

Alkaloids are a class of organic compounds that are structurally diversified and containing a heterocyclic nitrogen atom. These compounds are naturally occurring and they are mostly derived from amino acids. This class of compounds is most basic in nature as a consequence of the nitrogen atom; however, it also includes some compounds that are neutral even weakly acidic. These compounds were first discovered in 1819 by Carl F.W. Meissner (Kaur and Arora, 2015), they make up about 40% of a plants' secondary metabolites. On account of their physiological effects and pharmacological properties, these compounds have been used frequently throughout history (Ziegler and Facchini, 2008). Alkaloids are not always heterocycles as there are also non-heterocyclic alkaloids (Barnes, 2010).

Previous reports showed that as many as 12 000 alkaloids have been isolated from various genera of the plant kingdom (Dey *et al.*, 2020). Alkaloids are classified into different categories namely, indole, tropane, piperidine, purine, imidazole, pyrrolizidine, pyrrolidine, quinolizidine, quinoline and isoquinoline alkaloids (**Figure 1**). Each of the aforementioned categories can be distinguished from one another by their different structures, presence, or absence of certain moieties which leads to each of them having its unique chemistry ultimately

influencing their diverse pharmacological properties (Yan and Liu, 2019). For instance, an indole alkaloid can be easily identified by the presence of 5-hydroxytryptamine or 5-HT whereas a tropane alkaloid has 8-azabicyclo [3.2.1] octane core structure (Ziegler and Facchini, 2008). There are more than 2000 different compounds that belong in the indole category, including vincristine, vincamine, and vinblastine which are intensively researched for their biological and pharmacological properties (Kainsa *et. al*, 2012). Compounds like vinblastine and vincristine are mostly used as anticancer drugs (Aryan, 2018).

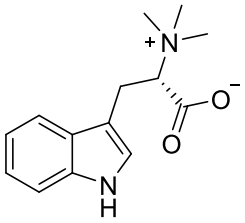

Hyperphorine

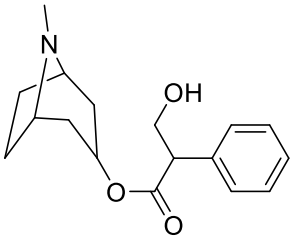

Atropane

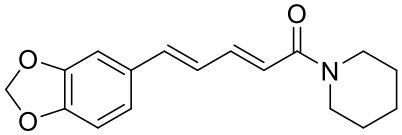

Piperine

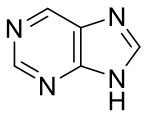

Purine

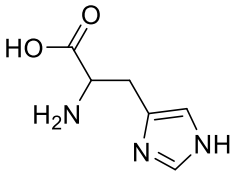

Histidine

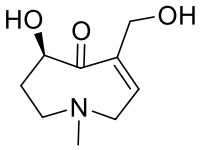

Otenecine

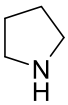

Pyrolidine

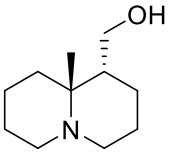

Lupinine

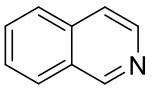

Quinoline

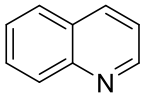

Isoquinone

Figure 1. Different classes of alkaloids

A large number of alkaloids have been isolated from plants of different families including the genus *Erythrina*. *Erythrina* alkaloids have also been found to exhibit excellent biological and pharmacological properties (Fahmy *et al*., 2020). These compounds can be easily identified by their unique core structure as they consist of a tetracyclic spiroamine skeleton. These are also divided into 3 categories namely, dienoid, alkenoid, and lactonic alkaloid (**Figure 2**). These compounds are distributed throughout the plant's bark, seeds, leaves, and flowers. However, they are usually isolated in very small amounts. A great deal of literature reports the astounding pharmacological properties of these alkaloids which corroborate with the traditional uses of the *Erythrina* species. Alkaloids isolated from the seed, bark and flower of these species have been reported to have remarkable antimicrobial and anticonvulsant activities (Wanjala *et al.*, 2002; de Ávila *et al.*, 2018; Ahmed *et al.*, 2020).

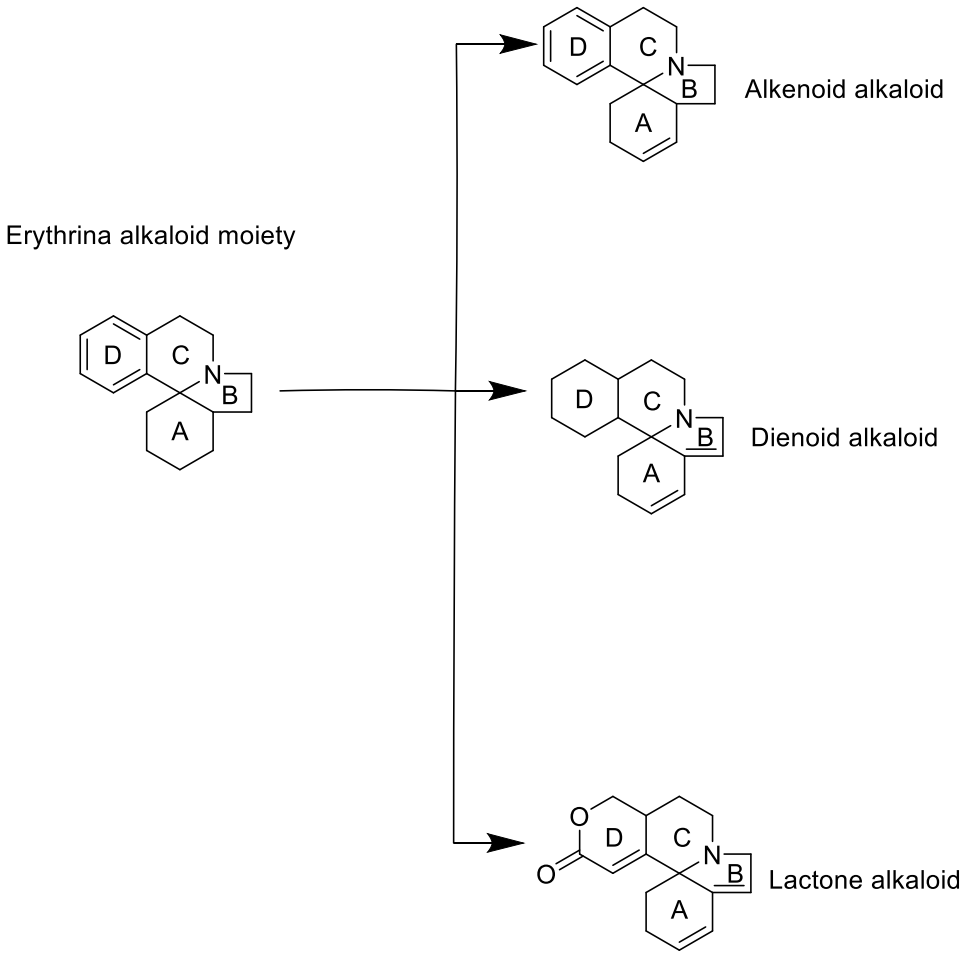

Figure 2. Three categories of Erythrina alkaloids

Over the past decade, there has been a controversy about the biosynthetic pathway of *Erythrina* alkaloids. However, a study conducted on *Erythrina crista-galli* using a series of experiments has demonstrated that (*S*)-norreticuline plays a vital role as a precursor in the biosynthesis of *Erythrina* alkaloids (Tan *et al*., 2017).

1.1.3. Polyphenols

Phenols, also known as polyhydroxyphenols are naturally occurring organic compounds with a wide range of complex structures however they can also be synthesized. These organic compounds can be mainly characterized by the large number of phenol structural units they have. Basic units of polyphenols like a phenolic ring can be generally classified as phenolic acids or phenolic alcohols. The classification of these complex structures mainly depends on the phenolic ring strength, the main classes of these compounds consist of phenolic acids, flavonoids, stiblins, lignans and phenolic alcohols (Dragovic-Uzelac *et al.*, 2007; Quideau, 2009).

These compounds are unique for their biological properties, consisting of wide range of biological properties. They are commonly found in the human diet and originate from plants like fruits and vegetables mostly in minute amounts. They can however be found in other plants like the *Erythrina* species. Their different classes have been found to possess good antibacterial activity, anti-oxidant as well as antiplasmodial activities (**Table 1**) (Nkengfack *et al.*, 1997; Daglia, 2012; Tjahjandarie *et al.*, 2014).

Table 1. Some classes of phenolic compounds with associated activities (Abbas *et al.*, 2017).

Bioactive Compounds	Activities and pathogens
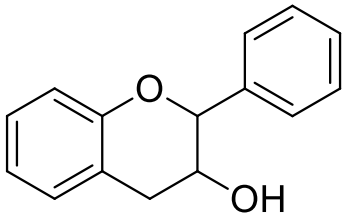 Flavan-3-ol	**Antibacterial** *Vibiro Cholerae, Strptococcus. mutans; Campylobacter. jejuni, Clostridium perfringens,*

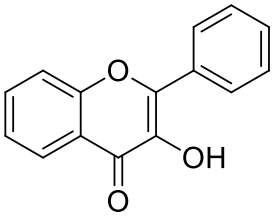 Flavonol	*Escherichia coli, Bacillus Cereus, Helicobacter pylori, Staphylococcus aureus, Lactobacillus acidophilus, Actinomyces naeslundii, Prevotella oralis, Porphyromonas gingivalis, Prevotella melaninogenica, Fusobacterium nucleatum, Chlamydia pneumonia* **Antiviral** Adenovirus, Enterovirus, Flu virus **Antifungal** *Candida albicans, Microsporum gypseum, Trichophyton mentagrophytes, Trichophyton rubrum*
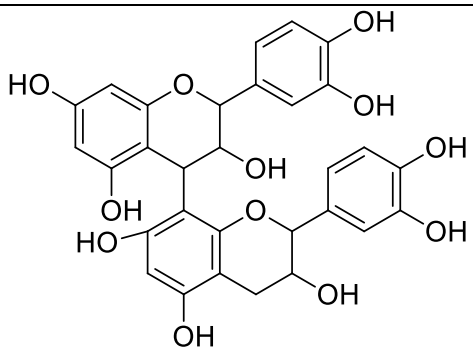 Condensed tannins	**Antibacterial** *Staphylococcus aureus, Escherichia coli, Streptococcus mutans* **Antiviral** Influenza A virus, type-1 herpes simplex virus

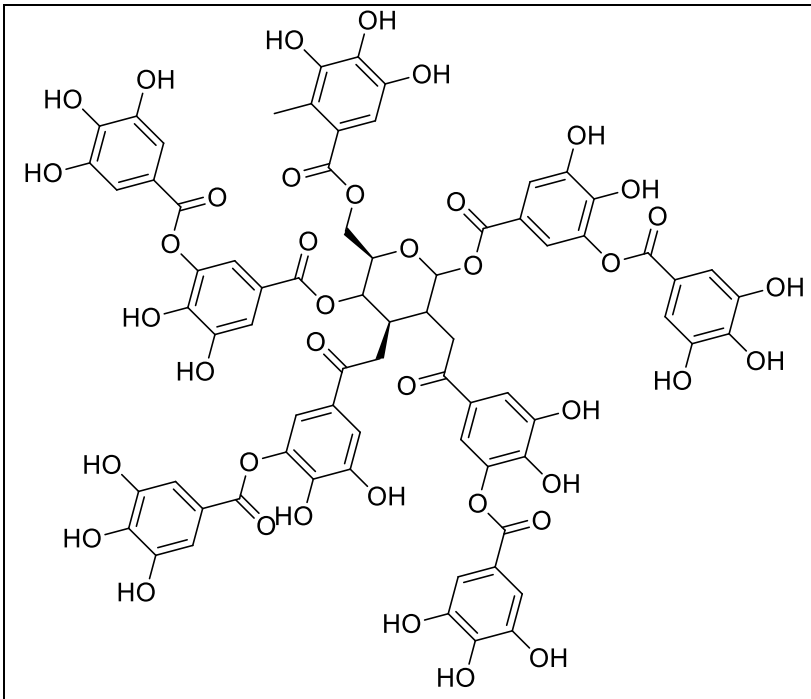 Hydrolyzable tannins	A**ntibacterial** *Salmonella species, Staphylococcus helicobacter, Escherichia coli, Bacillus clostridium, Campylobacter lysteria* **Antiviral** Epsein-Barr virus, Herpes virus, Herpes simplex virus-1 and herpes simplex virus-2 **Antifungal** *Candida parapsilosi*
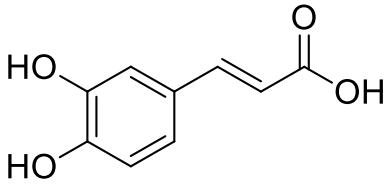 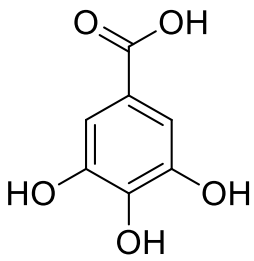 Phenolic acids	**Antibacterial** *Staphylococcus aureus, Listeria monocytogens, Escherichia coli, Pseudomonas aeruginosa*

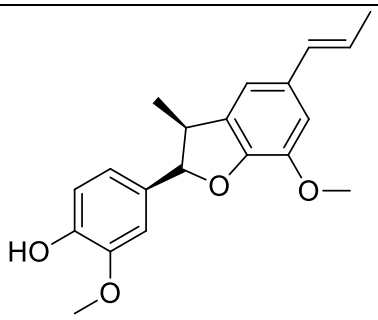 Neolignan	**Antibacterial** Different strains of *Mycobacterium tuberculosis*

1.1.4. Flavonoids

Flavonoids are a diverse group of polyphenolic compounds which are naturally occurring. These compounds can be found in almost every plant (Kumar and Pandey, 2013). The first flavonoid (rutin) was first isolated in 1930 by Dr. Albert Szent-Gyorgyi. The basic flavonoid structure consists of a 15-carbon skeleton with two benzene rings (A & B) connected by a heterocyclic pyran ring (C) (**Figure 3**). Depending on the position where the aromatic ring is connected to the benzopyrano (chromano) moiety these compounds can be classified into various classes such as flavones (e.g apigenin, chrysin, and 6-hydroxyflavone), flavonols (e.g myricetin, fisetin, and kaempferol) and flavanone (e.g., Abyssinone V-4' methyl ether and hesperetin), flavan-3-ols (e.g., Catechin and epigallocatechin gallate), isoflavones (e.g., Daidzin and genistin) and anthocyanins (e.g., Malvidin and cyanidin).

These different classes of flavonoids differ from one another in many ways including the pattern of substitution of the C-ring. However, the main difference between compounds of the same class is determined by the substitution pattern of the A and B rings (Tomás-Barberán, 2001). The position at which a substituent connects to the chromone skeleton divides the flavonoid class into different categories (flavonoid and isoflavonoids). For a flavonoid, the chemical structure consists of a 2-phenylchromen-4-2*H*-1-one core skeleton whereas for isoflavonoids their chemical structure consists of 3-phenylchromen-4-2*H*-1-one (**Figure 3**).

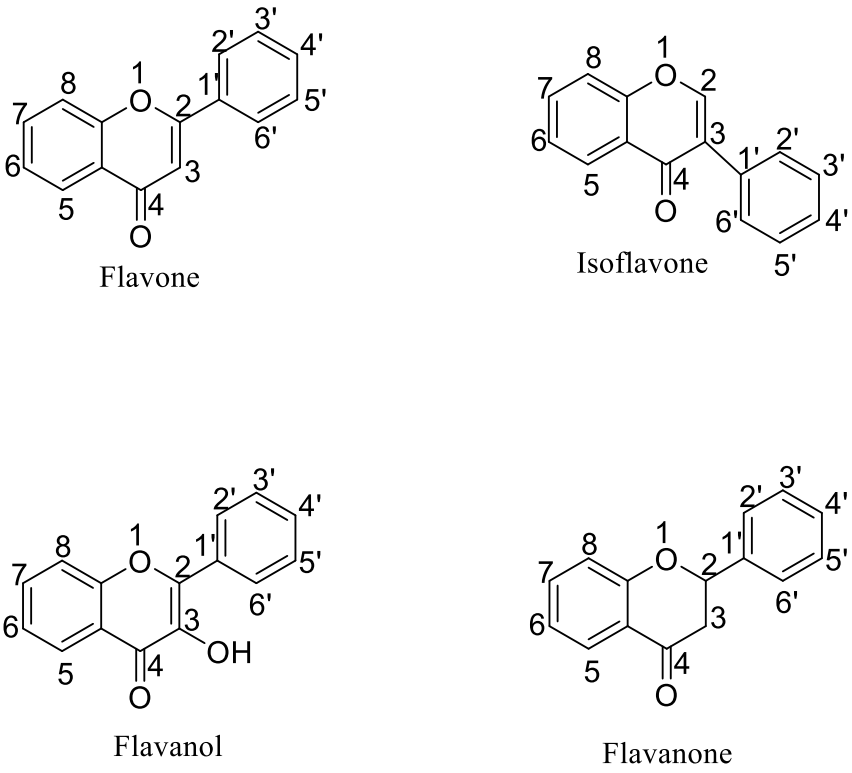

Figure 3. Different groups of flavonoids

Flavonols can be distinguished from flavanones by the hydroxy group at position-3 and the double bond present between C2-C3 (**Figure 3**) (Narayana *et al.*, 2001). There are three different ways to name flavonoids, the most commonly used method of naming is trivial naming which occasionally signifies the flavonoid class or plant source. A typical example of this can be seen in compounds like tricin and hypolaetin, where the ending '-etin' denote a flavanol and a compound with the ending '-inidin' denotes an anthocyanidin. Another way of naming flavonoid is the systematic naming using this way of naming a flavan would be named 2,4-dihydro-2-phenyl-2H-1-benzopyran, however this method of naming is at times complicated and thus seldomly used. Lastly, flavonoids can also be named using a hybrid naming method known as semi-systematic/semi-trivial. In this method the name of the compound consists at least one part systematic and one part trivial. Compounds like flavone would be named 3,5,7,3', 4'-pentahydroxyflavone or 3,3',4',5,7-pentahydroxyflavone (**Figure 4**) (Tomás-Barberán, 2001).

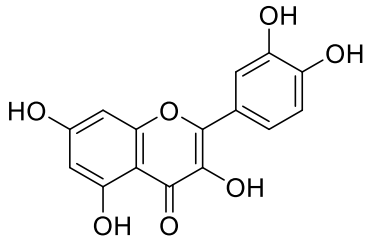

3,5,7,3',4'-pentahydroxyflavone

Figure 4. Semi-trivial naming of a flavone

These compounds have drawn the attention of many researchers due to the vast range of their pharmacological properties such as enzyme inhibition, antimicrobial activity (Havsteen, 1983; Tomás-Barberán, 2001), anti-oxidant activity (Middleton and Kandaswami, 2017) and cytotoxic antitumor activity (Harborne and Williams, 2000). Their ability to inhibit various enzymes has been hypothesized to be as a consequence to the interaction of enzymes with different parts of the flavonoid molecule (Havsteen, 1983; Harborne and Williams, 2000; Middleton, Kandaswami and Theoharides, 2000). The biological activities of several plants including *E. caffra* are mostly due to a high flavonoid content in that specific plant (Atanassova and Georgieva, 2011).

1.1.5. Terpenoids

Terpenoids also known as terpenes are one of the largest and diversified group of naturally occurring compounds. These compounds are a class of natural products that are derived from mevalonic acid (MVA) (**Figure 5**) (Bergman, Davis and Phillips, 2019) which are made up of many isoprene (C5) structural units (Sobral *et al.*, 2014).

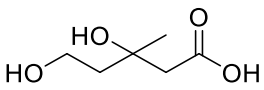

Figure 5. Melavonic acid

Depending on the number of the isoprene units present in their structures they can be classified as monoterpene (C10), sesquiterpenes (C15), triterpenes (C30), tetraterpenes (C40), and polyterpenes (>C40) (**Table 2**).

Table 2: Classes of terpenoids (Tong, 2013)

Classification	**Carbon atoms (Isoprene units)**	**Chemical structure**
Hemiterpenes	5 (1)	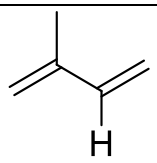
Monoterpenes	10 (2)	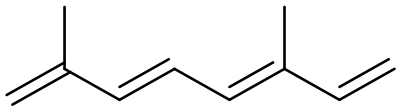
Sesquiterpenes	15 (3)	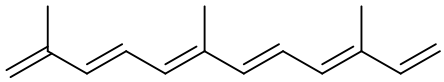
Diterpenes	20 (4)	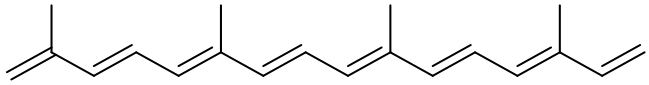
Sesterterpenes	25 (5)	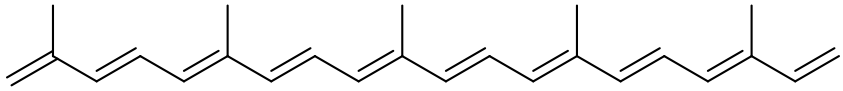
Triterpenes	30 (6)	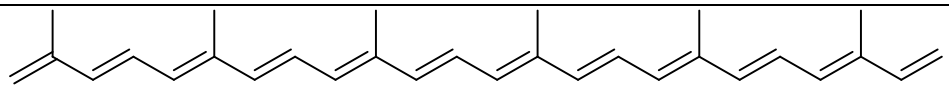
Sesquaterpenes	35 (7)	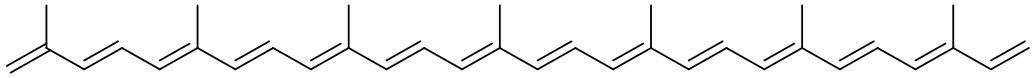
Tetraterpenes	40 (8)	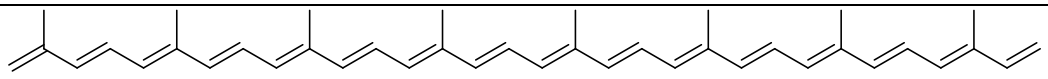

There are thousands of these compounds isolated from natural sources over the years. In most cases these compounds can be found in various oxygen-containing derivatives (**Figure 6**) (Tong, 2013). Terpenoids are naturally produced via a biosynthetic pathway that is known as the mevalonate pathway which includes mevalonic acid as an intermediate. This pathway exists in the cytoplasm and secondary metabolites like sterols, sesquiterpenes and triterpenes are

largely produced through this pathway. In this pathway acetyl-CoA is the starting primary metabolite which goes through a chain of reactions to ultimately convert three molecules of acetyl-CoA to mevalonic acid (**Figure 7**) (Habtemariam, 2019).

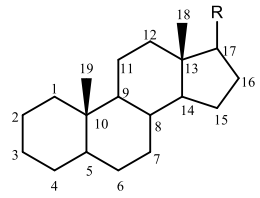

a. Chemical structure of steroids:
Steroid nucleus

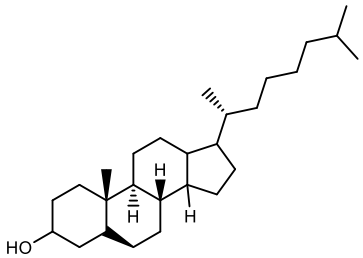

b. Sterol: Cholesterol

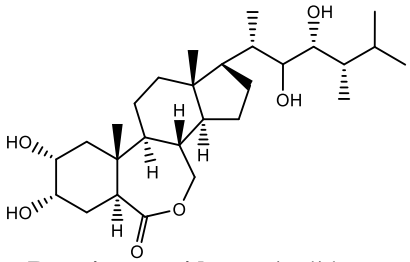

c. Brassinosteroid: Brassinolide

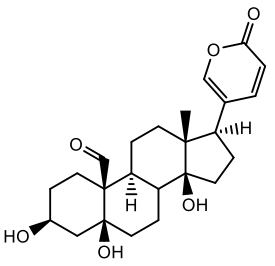

d. Bufadienolide: Hellebrigenin

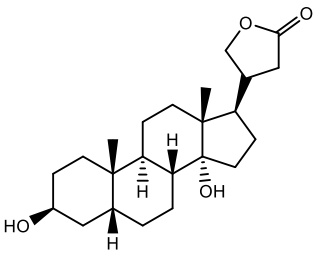

e. Cardenolide: Digitoxigenin

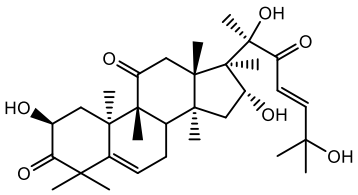

f. Cucurbitacin: Cucurbitacin D

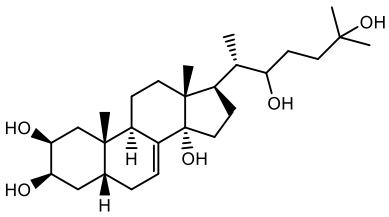

g. Ecdysteroid: Ecdysone

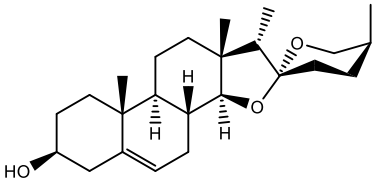

h. Sapogenin: Diosgenin

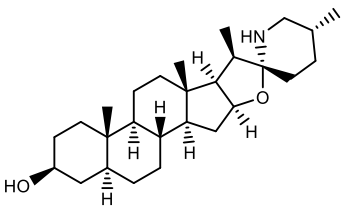

i. Steroid alkaloid:
Salasodine

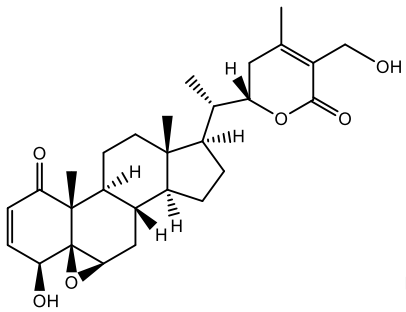

j. Whithasteroid:
Whithaferin A

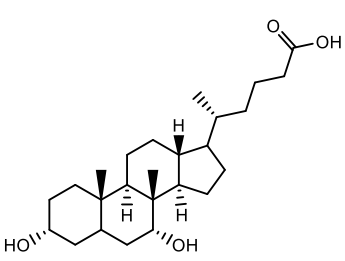

k. Bile acid:
Chenodeoxycholic acid

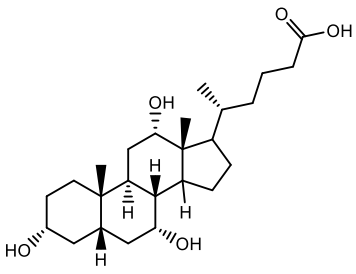

k. Bile acid:
Cholic acid

Figure 6: Some of the oxygen containing derivatives of terpenoids

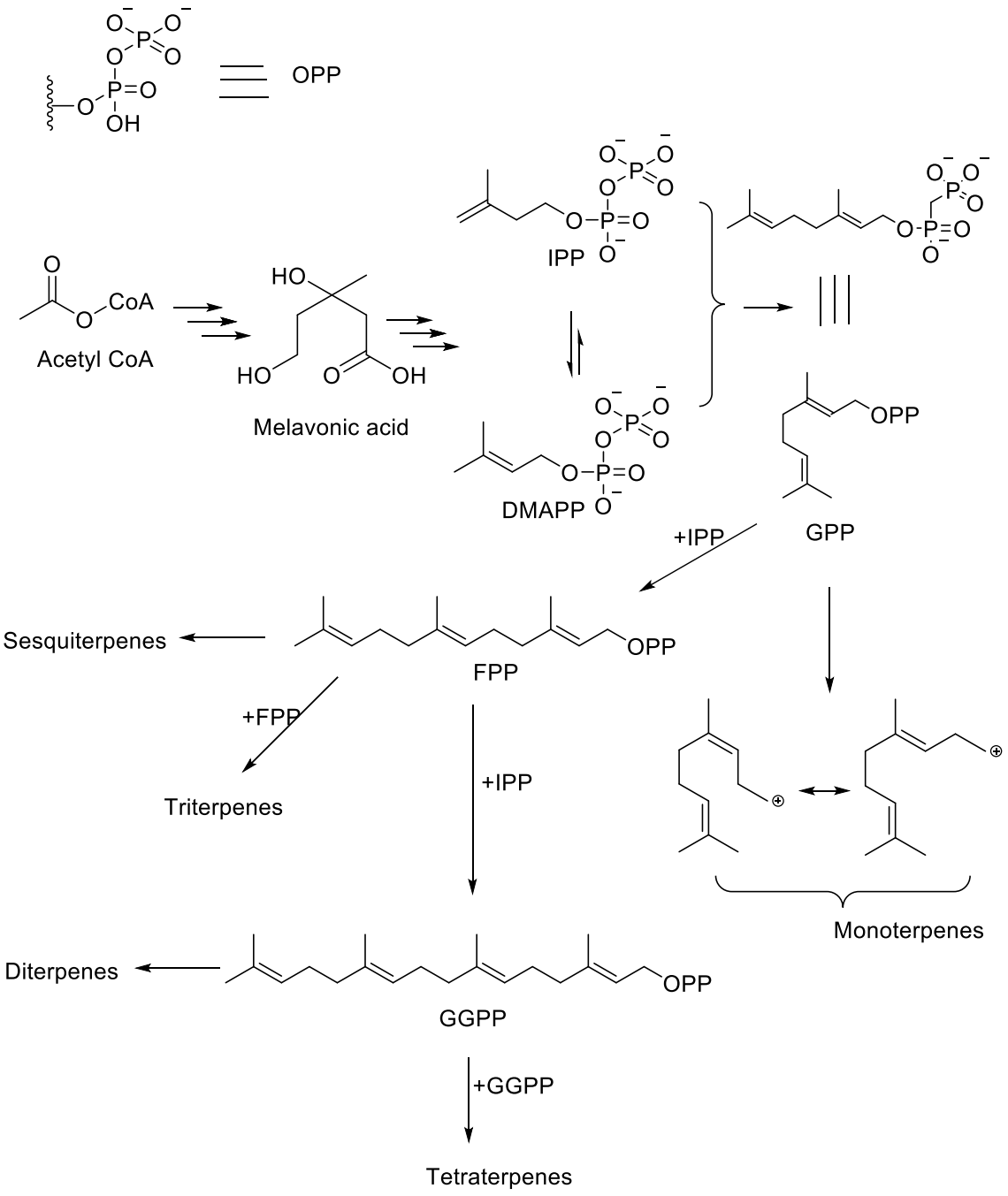

Figure 7: Biosynthetic pathway of terpenoids (Habtemariam, 2019)

Terpenoids have been found to have good antitumor activity. Their peculiar structural features have attracted the interests of many medicinal chemists (Yang *et al.*, 2020). Studies have

revealed that some terpenoids have strong antibacterial activities (**Figure 8**) (Sobral *et al.*, 2014; Chen, da Fonseca and Schönthal, 2015; Oturanel *et al.*, 2017). Some compounds in this class have also been found to consist of excellent antitumor activity (**Figure 9**) (Sebei *et al*., 2015; Shahbazi, 2015; Wang *et al*., 2016).

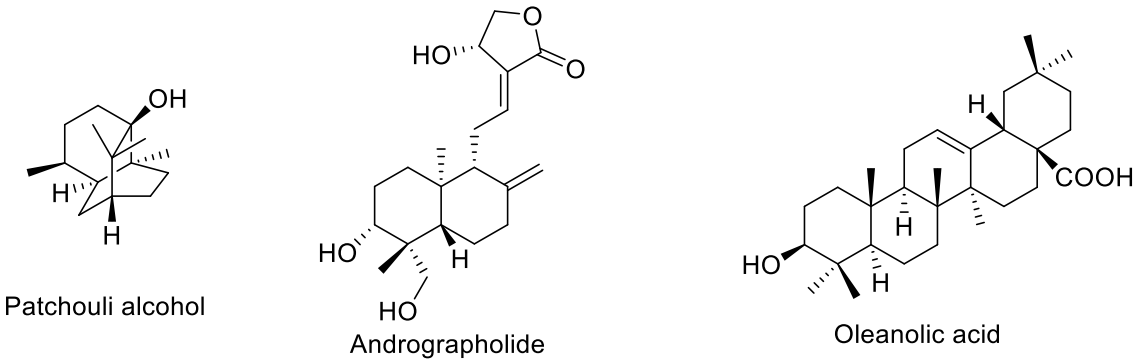

Figure 8: Some structures of terpenes with antibacterial activity.

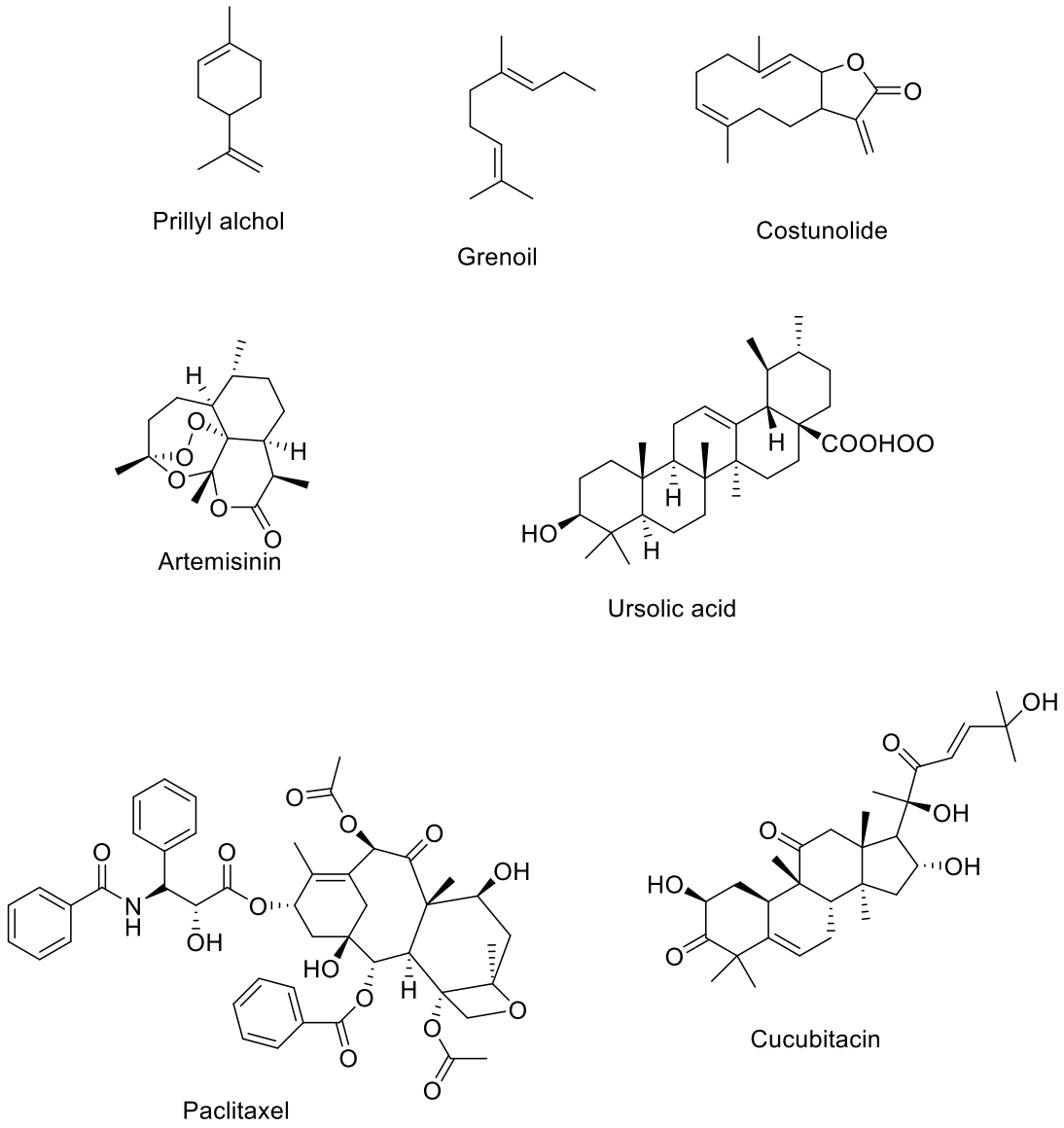

Figure 9: Some structures of terpenoids with antitumor activity.

1.2. Microbial and cancer diseases

1.2.1. Bacterial disease

There are many human diseases that are caused by bacteria. Common examples include tuberculosis, pneumonia, endocarditis, osteomyelitis etc. Bacteria that cause diseases in humans are regarded as pathogenic bacteria. However, not all bacteria are pathogenic, a considerable amount of bacteria are present on top of the skin and inside our bodies and completely are harmless to humans (Reynolds *et al.*, 2012), these bacteria are known as “good

bacteria", in fact some bacteria have been found to be beneficial to humans (Linares *et al.*, 2016).

It has been found that an average human being can live with pathogens without getting sick, the human microbiome is reported to comprise of up to trillions of microorganisms (Sender *et al.*, 2016). The intrinsic immunity provided by the body's defense mechanism allows us to sustain that many bacteria (Paludan *et al.*, 2021).

Pathogenic bacteria however can be very deadly as they are able to infiltrate the body tissues and fluid by substantially overwhelming the body's natural defenses (Laing, 2019). Bacteria can enter the human body in number of ways including ingestion, inhalation, wounds and through sexual transmission (Yates *et al.*, 2016; Kurtz *et al.*, 2017; Smolarczyk *et al.*, 2021). Once they enter the body they can damage the host cells through direct or indirect effects (Guerrant *et al.*, 1999). Most bacteria are intracellular pathogens which means that they need to invade the cell in order to multiply (Uribe-Querol and Rosales, 2020). They do this by utilizing the bacterial adhesion factors or adhesins in their surface to attach to proteins located at the host cells. This ultimately causes the cell to engulf the bacterium forming a thin layer around the bacterium. When the thin layer, called a vesicle, separates from the membrane it becomes a phagosome which can destroy the bacteria. However, the bacteria avoid this by using specific enzymes to break the membrane of the phagosome and escape into the cytoplasm (Haas, 2007).

In the cytoplasm these bacteria are free to undergo the cell division and proliferate, the newly formed cells go on to invade the neighboring healthy cells and continue causing cell damage. Some bacteria have been known to proliferate inside the cell causing the cell to burst (Ribet and Cossart, 2015; Turco and Winkler, 2021).

Modern medicine has been used to treat these diseases for decades. However, they seem to have developed resistance against commonly used drugs making them even more dangerous. Even diseases like skin infections, which is caused by S*taphylococcus aureus*, will in time be difficult to treat (Rao *et al.*, 2022).

1.2.2. *Staphylococcus aureus*

Staphylococcus aureus (*S. aureus*) is one of the most well-known and widespread Gram-positive pathogenic bacteria. It is the major cause of a wide variety of infectious diseases in humans and animals making it hard to estimate the number of mild infections like skin infection

and likely hundreds of thousands of more intense infectious diseases globally a year (Klevens, 2007; Temkin *et al.*, 2018; Limmathurotsakul *et al.*, 2019). These infections may range from simple, easy to treat infection to more severe and life-threatening illnesses like osteomyelitis (Rasigade *et al.*, 2014; Schaumburg *et al.*, 2015; Gimza and Cassat, 2021; Pimentel de Araujo *et al.*, 2021).

Staphylococcus is the major human pathogen that has one of the highest morbidity rates among pathogenic bacteria (Eisenstein, 2020). It is also a leading cause of bacteremia, pneumonia and device related infections, where microbial pathogens stick onto am indwelling implant causing a foreign body reaction which ultimately leads to an infection (Limmathurotsakul *et al.*, 2019; Bai *et al.*, 2022; Samura *et al.*, 2022). Bacteremia caused by *Staphylococcus aureus* has been reported to have a higher number of deaths as compared to the acquired immune deficiency syndrome (AIDS), tuberculosis (TB) and hepatitis (Hal *et al.*, 2012). It is a significant threat to people with serious skin disease like *epidermolysis bullosa* or chronic diabetic foot and venous ulcers. While the mild *Staphylococcus* infections may not be life-threatening, they are accompanied by pain.

Like many other bacteria, *Staphylococcus aureus* can be mostly found in skins of unhealthy patients. They can enter the human body through a compromised skin barrier and become pathogenic causing a wide range of illnesses (**Figure 10Error! Reference source not found.**) (L. S. Miller and Cho, 2011; Nowicka and Grywalska, 2019; Eisenstein, 2020;). They have to go through our innate immune system and if they manage to overwhelm the defensive mechanisms of the immune system, the bacteria can spread to other tissues and ultimately lead to death. This is a more significant threat to patients with a compromised immune system like children and the elderly (Regev-Yochay *et al.*, 2004; Nowicka and Grywalska, 2019).

This bacterium has managed to mutate over the years as a consequence of its fast adaptation skills (Gajdács, 2019). *Staphylococcus aureus* excretes biofilms, which are extracellular polymeric substances (EPS) that help it to withstand and diminish the effects of antimicrobial drugs (Kaplan *et al.*, 2018) (**Figure 11**). The EPS mainly consist of organic matter of the biofilm and different polymeric substances such as extracellular DNA (eDNA), protein and polysaccharides (Donlan, 2002; Idrees *et al.*, 2020) (**Figure 11**). The EPS is commonly known as the polysaccharide intercellular adhesin (PIA) on account that the bacteria cells use it for intercellular adhesion. The cationic PIA plays a very important role in colonizing the cell, forming the biofilm and biofilm-related infection, immune evasion and resistance to antimicrobials (Reffuveille *et al.*, 2017; Nguyen, Nguyen and Otto, 2020). This raises the need for alternative therapeutic drugs preferably from naturally occurring sources as these not only

have a long-standing history of being proven to be effective but they are also easily accessible and efficient (Veeresham, 2012).

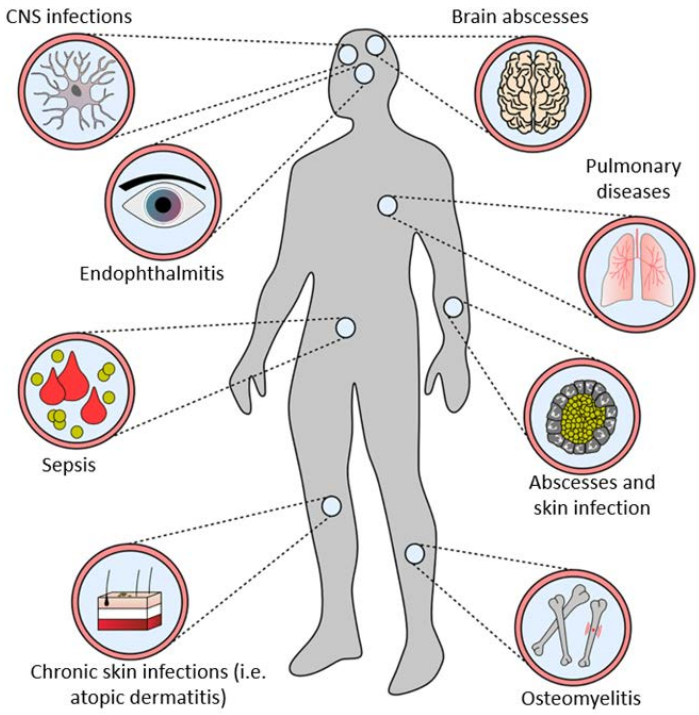

Figure 10. Different diseases caused by *Staphylococcus aureus* (Missiakas and Winstel, 2021). CNS- Central nervous system

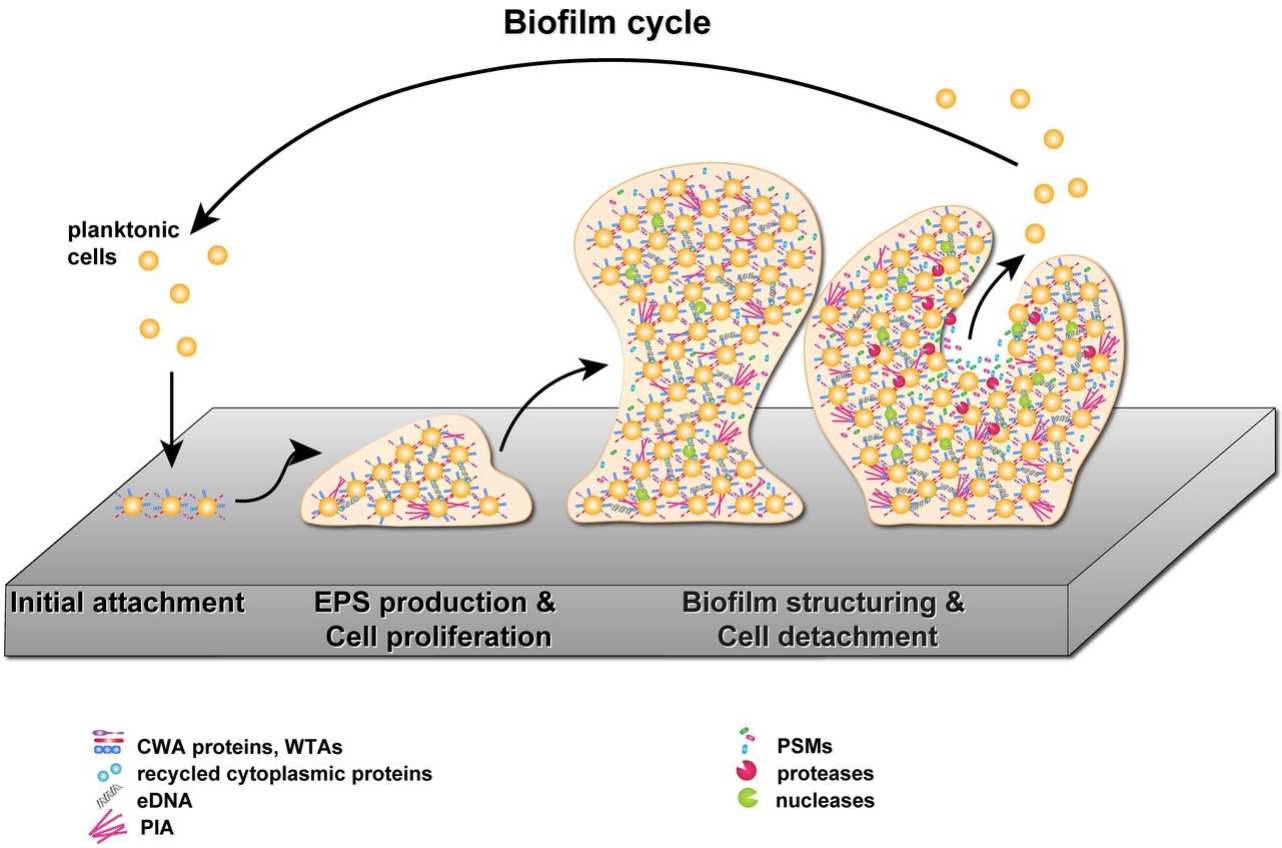

Figure 11. Biofilm formation (Schilcher and Horswill, 2020)

1.2.3. Cancer

Cancer is one of the diseases with high mortality rate worldwide. In 2020 it was reported to be responsible for approximately 10 million deaths (WHO, 2022). The word cancer is an inclusive term used to refer to a number of complex diseases affecting every part of the body and potentially life-treating, which arises due to an uncontrollable division and spread of some of the body cells to surrounding tissues. Cancer is not a modern era disease. Earliest reports dates back to ancient Egypt, 3000 BC, showing that even then cancer was a burden disease. The word cancer was first coined by Hippocrates in 400BC. He used the term ‘karkinos’ or ‘crab’ to describe a malignant tumour. The network of blood vessels on a tumour resembles the claws of a crab reaching out to its surrounding (Faguet, 2015).

It is of great significance that we understand how this uncontrollable cell division occurs. To do that one must first understand the normal functions of cell growth and reproductions as the transformation of a healthy to a cancerous cell does not occur overnight. By obtaining certain genetic mutations or genetic changes a normal cell can slowly transform into a cancerous cell. The changes are called the drivers of cancer, there are three known drivers of cancer namely; proto-oncogenes, tumour suppressor genes and DNA repair genes. Modifying the functions and regulations of these genes essentially leads to the uncontrollable and rapid cell division which in turn causes neoplasm. The growth of these neoplastic cells is completely independent of the growth factors and regulatory mechanisms that govern a normal tissue (Hoda and Hoda, 2005). The uncontrollable growth of these neoplastic cells often leads to a formation of mass. However, this is not always the case. When a mass forms it is commonly called a tumour. There are different kinds of tumour, they all have different sizes and they are altogether different to other swellings (Pérez, Raimondi and Itoiz, 2005; McLaughlin and Shafritz, 2011).

When a tumour mass occurs on or near the surface of the skin it can be easily felt as a lump, however there are some tumours located deep within the body. These types of tumours are very difficult to examine. Typical examples of these are internal organ tumours (Östman and Augsten, 2009; Iyer and Chaichana, 2018). The growth and aggressiveness of the tumours is mainly controllable by the biological cross-talk between the parenchyma which consist of neoplastic cells and the reactive stroma composed of immune cells, fibroblasts endothelial cells and specialized mesenchymal cells (Schäfer and Werner, 2008; Kojima *et al.*, 2010). The role played by the stromal cells in the tumour microenvironment in cancer development has been fairly researched to bring about sufficient knowledge about cancer. Recent research has revealed the important roles played by the tumour stromal cells that it is responsible for initiation, progression and metastasis. It has also been reported that the most frequent component of tumour stroma is cancer associated fibroblasts (CAF), this is especially true for breast and pancreatic cancer (Hoda and Hoda, 2005; Östman and Augsten, 2009).

There are different kinds of cancer and the most common types of cancer are breast cancer, prostate cancer, lung cancer colon and rectal cancer (Siegel *et al.*, 2022). This study will mainly focus on breast cancer.

1.2.3.1. Breast cancer

Among the various types of cancers breast cancer is one of the diseases that has a highest mortality rate. In 2020 it has accounted for 685 000 deaths. The WHO reported that by the end

of the year 2020 there were 7.8 million women alive who were diagnosed with breast cancer in the previous 5 years making it the most widespread cancer of all the cancers.

There are more lost disability adjusted life years (DALY's) by women to breast cancer globally than any other type of cancer (WHO, 2022). Breast cancer occurs globally in women at any age after puberty, however the chances of having it as a woman increase with increasing age. Breast cancer is a heterogenous disease caused by an uncontrollable growth of cells in the breast. There are different types of breast cancer. The kind of breast cancer depends on which cells in the breast have turned cancerous (DeSantis *et al.*, 2015; Ginsburg *et al.*, 2020; Mccormack *et al.*, 2020; Stoltenberg *et al.*, 2020).

A breast mainly consists of 3 parts: lobules, ducts and connective tissue (**Figure 12Error! Reference source not found.**). Each of these different parts have different functions: the lobules are the epithelial structures that produce milk, the ducts are tubes that transport the milk to the nipple and the connective tissue (which is made up of fibrous and fatty tissue) holds everything together. Breast cancer can arise in any of these different parts, however most breast cancers arise in the ducts or lobules (Weigelt, Geyer and Reis-Filho, 2010). Empirical evidence from previous scientific reports also suggest that breast cancer is, in fact, a group of different diseases with differing risk factors, physical signs and symptoms, pathological features, and therapeutic response which affect the same organ (Li, Uribe and Daling, 2005; Weigelt, Geyer and Reis-Filho, 2010). Breast cancers can be classified based on their histological grade (Eliston and Ellis, 1991) histological type (Ellis *et al.*, 1992). Histological grade is an evaluation of the degree of growth and differentiation of a tumour and reflects its aggressiveness (Eliston and Ellis, 1991). Histological grade has been integrated in multiple

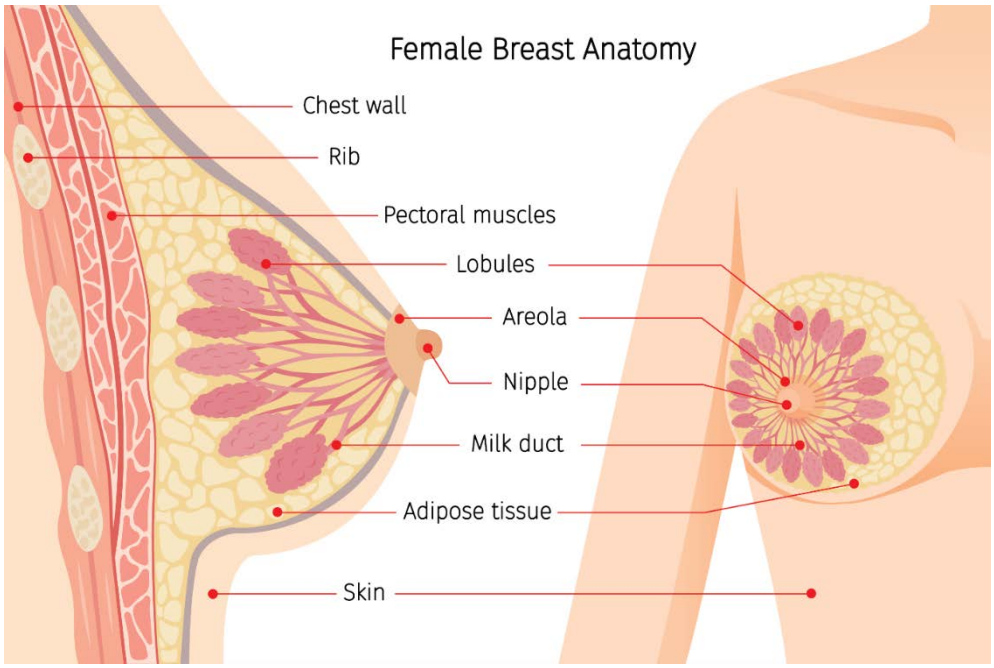

scientific reports including but not limited to Mook and colleagues and Armando and colleagues (Mook *et al.*, 2009; Esquivel *et al.*, 2018; D'Angelo *et al.*, 2021).

Figure 12. Three main parts of the outer breast.

https://www.breastaugmentation101.com/parts-of-outer-breasts/

There is evidence showing the correlation between the grade and the transcriptomic features of breast cancers and microarray-based genomic signatures for the histological grade (Ivshina *et al.*, 2006; Sotiriou *et al.*, 2006; Sotiriou and Pusztai, 2009; Weigelt, Baehner and Reis-Filho, 2010). The histological type examines the growth pattern of the tumours with specific structural and cytological patterns that are responsible for different symptoms and physical signs. Breast cancer histology reveals different classifications of breast cancer like ductal carcinoma in-situ (DCIS), lobular carcinoma in-situ (LCIS), metastatic breast cancer (MBC) etc each with different clinical presentations (Irvin, Muss and Mayer, 2011; Taffurelli, 2018; Wen and Brogi, 2018; Lin *et al.*, 2021). However, for the scope of this project only ductal carcinoma in-situ (DCIS) will be further expounded.

When the cells that line the milk ducts of the breast have become cancerous, but have not spread to the surrounding tissue in the breast this type of breast cancer is known as ductal carcinoma in-situ (DCIS) (**Figure 13**)

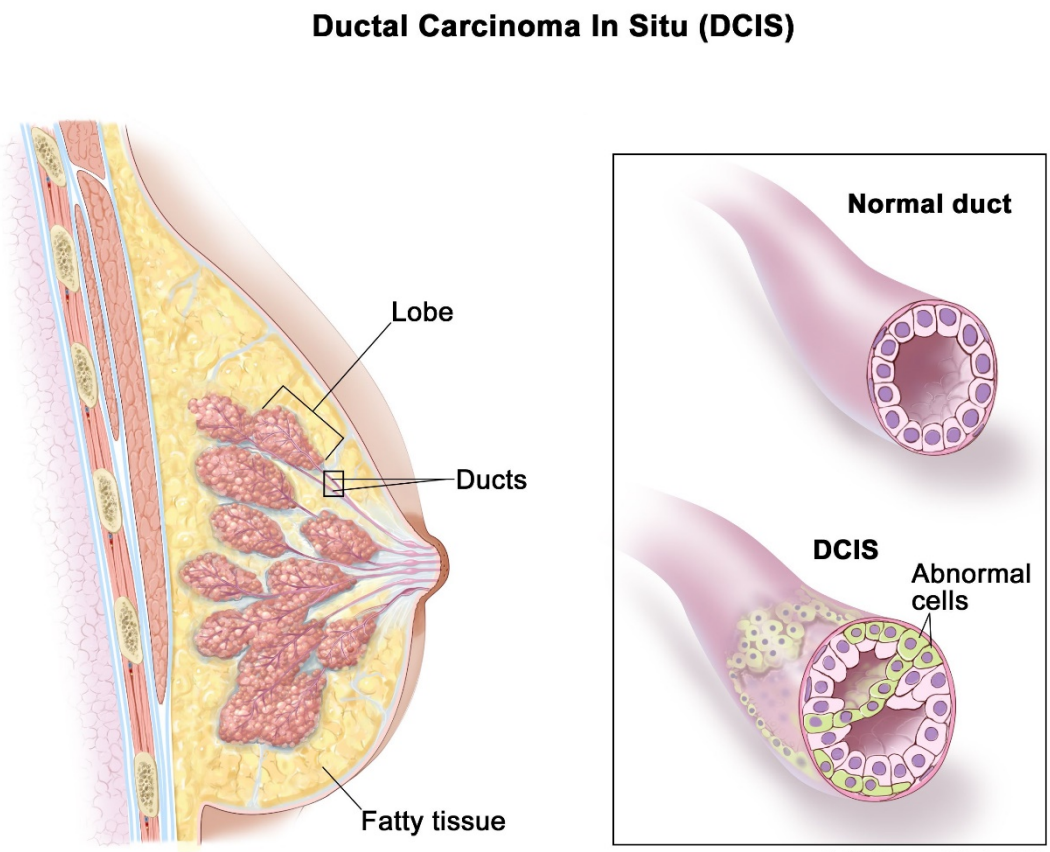

Figure 13. Illustration of Ductal Carcinoma *In-Situ* (DCIS).
https://www.cancer.gov/publications/dictionaries/cancer-terms/def/ductal-carcinoma-in-situ

Some scientific reports suggest that the formation or development of these cancers (DCIS and IDC) starts from hyperplasia, which occurs because of the disruption of the normal processes that cause the development and growth of normal cells leading to an overproduction of normal looking cells. This then continues until a surplus of normal-looking cells are produced and stack upon each other forming an abnormal appearance this process is known as atypical hyperplasia. This is not yet cancer, however it increases the chances of a patient developing cancer in the future. The normal looking (abnormal) cells continue to develop into a more advanced condition and multiply advancing into *in situ* cancer. In this state the cancer is still confined within the milk ducts. When these abnormal cells amass within the duct and continue to multiply and advance to became an even more aggressive cancer known as invasive ductal cancer (IDC) (**Figure 14**). Over 70 – 80% of all breast cancer is as a result of IDC (Eliyatkin *et al.*, 2015).

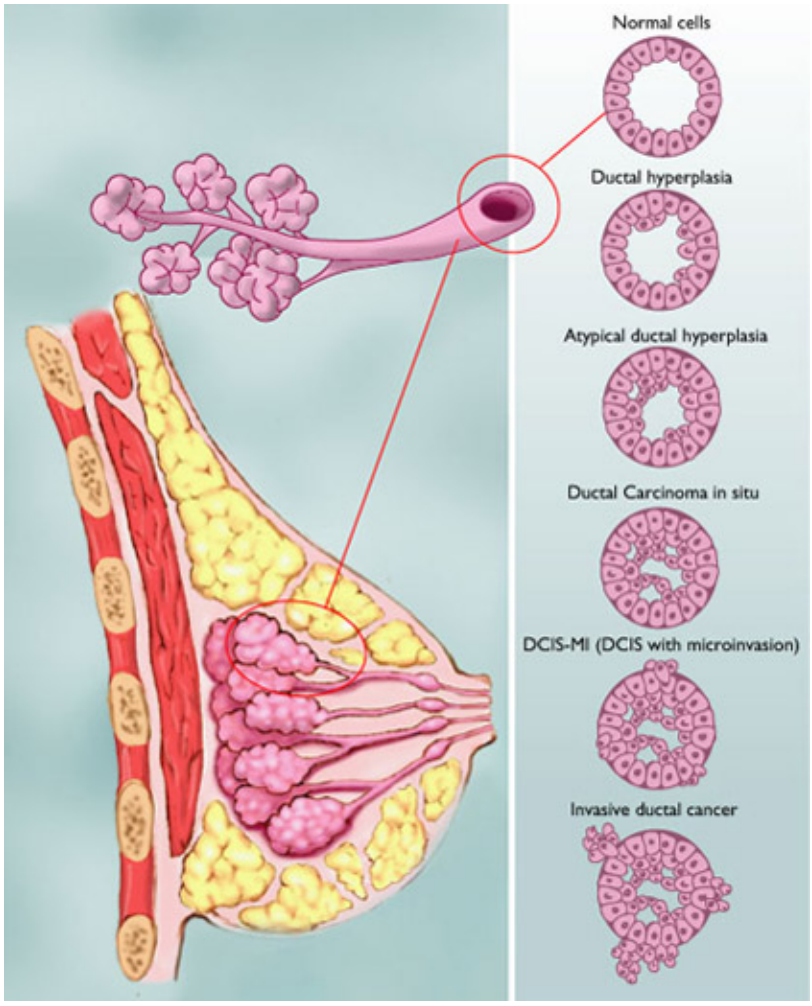

Figure 14. Ductal hyperplasia and invasive ductal cancer (Irshad, 2014)

Studies done by researchers show that about 7% of women diagnosed with atypical hyperplasia may develop breast cancer 5 years after being diagnosed with ADH (Hartmann *et al.*, 2014). The number of women that may be affected has been observed to almost double as the number of years after diagnosis increases. Researchers have found that for every 100 women disgnosed with hyperplasia about 30 of them can be expected to develop breast cancer within 25 years. (Hoda and Hoda, 2005; Hartmann *et al.*, 2014; Hartmann *et al.*, 2015) . Some studies however claim there is no direct proof that epithelial hyperplasia and atypical hyperplasia (ADH) are direct precursors to ductal carcinoma *in situ* or invasive carcinoma (Rosai, 1991; Tavassoli, 1998). Thus, rejecting the use of the terms intraepithelial neoplasia and ductal intraepithelial hyperplasia which insinuate the continuous progression from epithelial hyperplasia to ductal carcinoma *in situ* (Sloane *et al.*, 1999) (**Figure 14**).

Breast cells consists of proteins called hormone receptors. These hormones are essential for cell growth in the breast. The hormone receptors commonly found in breast cells are known as estrogen receptor (ER), progesterone (PR) and human epidermal growth factor receptor 2 (HER2). HER2 is overexpressed in 20% of all breast cancer (Maennling *et al.*, 2019). When these different types of breast cancer arise, there is usually an over-expression of some or all of these hormones in the infected breast (Gebre-Medhin *et al.*, 2001). Though a majority of breast cancers show an upregulation of ER and PR there are some that show none.

The type of breast cancer that have receptors (protein) for estrogen and progesterone are known as ER and PR positive breast cancers. There are also some breast cancers that are positive to all 3 hormones. Those types of breast cancer are known as triple positive breast cancers. These types of cancers have proteins in their cells for all the hormones (ER, PR and HER2). They use these hormones to help them grow, multiply and spread. These types of breast cancers have proteins which can be easily treated by simply lowering the levels of that specific hormone or by stopping it using target specific drugs like tamoxifen. In a case of estrogen positive breast cancer drugs like tamoxifen are used to block estrogen from connecting to the cancer cells and this in turn stops them from growing and dividing further.

There are many accepted and experimental therapies for these types of cancers (Rosai, 1991). There is however a type of breast that does not have estrogen or progesterone (ER and PR) receptors in its cells and also doesn't have any receptors for the protein HER2, this type of breast cancer accounts for about 10-15% of all breast cancers. This cancer is known as triple negative breast cancer (TNBC). This invasive breast cancer tends to be commonly found in black women under the age of 40 years (Huo *et al*., 2009; Stead *et al*., 2009; Jhan and Andrechek, 2017; Li *et al*., 2017; Siddharth and Sharma, 2018;). Triple negative breast cancer (TNBC) is more aggressive and has a faster growth rate with exacerbated risk of metastasizing, it is non-responsive to the commonly used drugs to treat cancer thus its treatment options include chemotherapy, surgery and/or radiation therapy (Al-Mahmood *et al.*, 2018).

1.3. Previous reported biological activity of *Erythrina caffra* extracts and compounds

The genus *Erythrina*, a member of the Fabaceae family, subfamily of Papilionideae consists of over 108 species of red or orange flowered trees, shrubs and herbaceous plants. The genus is mostly found along the tropical and the sub-tropical regions of the world (Raven, 1974). *Erythrina* species are famous for their good biological activities. These species are used traditionally to treat a number of diseases like tuberculosis, malaria, inflammation, anaemia and jaundice (Saidu *et al.*, 2000; Lee *et al.*, 2009; Schultz *et al.*, 2020). Numerous studies have conducted biological testing and have confirmed the traditional uses of the *Erythrina* species (Musau, Mbaria and Gakuya, 2006; Lillian Mukandiwa, 2012).

Erythrina caffra which is commonly known as a coral tree (English); "kuskoraalboom" (Afrikaans); "umsinsi" (Zulu); "umsintsi" (Xhosa) with the scientific name *Erythrina caffra* Thunb. is a medium-sized to large deciduous subtropical tree that is indigenous to South Africa. Its warm red to scarlet-coloured flowers which mostly appear in from winter to spring are what makes this tree more distinctive. It is mostly found in the warm frost-free coastal regions of the Eastern cape and in the light frost coastal regions of Northern KwaZulu-Natal. This species can be found in different type of soils from wet, well-drained, humus-rich to dry, clayey soils in most cases. The size of this tree is determined by the climate and the soil type (Hutchings, 1997; Macintyre, 2020).

As other species in its genus, *E. caffra* is also popular for its strong biological activities (Kone, Solange and Dosso, 2011). The bark of *E. caffra* is traditionally used by the indigenous people of South Africa to treat a myriad of diseases like sores, tuberculosis, respiratory infections, arthritis, abscesses and toothache (Chukwujekwu *et al.*, 2016; O. O. Olajuyigbe, 2012). While infusions of the leaves can be used to treat ear infections, they are also used as a paste for urinary infections and venereal diseases. The decoctions of the roots are used for sprains.

Various crude extracts from the bark of this plant have shown to possess strong antibacterial, antifungal and antitumor activity *in-vitro*. The acetone extract from *E. caffra* stem bark was found to consist of moderately good antibacterial activity against *Staphylococcus aureus* and good antifungal activities (Olajuyigbe, 2012). Impressive antibacterial activities were also

found in the ethanol and ethyl acetate extracts (Pillay *et al.*, 2001; Olajuyigbe and Afolayan, 2012). The ethanol extract was also found to consist of good anticancer activity (Hsu *et al.*, 2016). Compounds isolated from this plant have also shown remarkable antibacterial and anti-oxidant activities. Flavonoids isolated from the stem bark of *E. caffra* have been tested *in-vitro* and proved to possess strong antibacterial activities (Olajuyigbe and Afolayan, 2012) **Error! Reference source not found.**. Flavonoids like **Error! Reference source not found.a** isolated from *E. caffra* have been also reported to have good antibacterial activity (Chukwujekwu *et al.*, 2011; Desta, Sewald and Majinda, 2016; Farhadi *et al.*, 2019). Compounds like **Error! Reference source not found.c** have also been found to consist of anticancer activity (Desta, Sewald and Majinda, 2016).Previous reports show the promising antibacterial, antifungal and anticancer activity of various extracts from different parts of *E. caffra* individually. However, no studies have been found to report the biological activity of concoctions from different parts of *E. caffra*. In the present study anticancer, antibacterial, anti-oxidant, anti-enzymatic activities and the cytotoxicity of different *E. caffra* extracts, fractions, concoctions and isolated compounds were tested against medically important pathogens.

Quantitative phytochemical analyses done by previous investigators on *E. caffra* extracts has revealed that this species is a rich source of natural products (El-Masry *et al.*, 2010a; Wintola *et al.*, 2021). A myriad of different classes of compounds have been previously isolated from this species including alkaloids (hyperphorine), flavonones (euchrenone b10), isoflavonones (alpinumisoflavone), triterpenoids (oleanolic acid), sterols (stigmasterol) and hydroxycinnamic acids (coumaric acids). These are the classes of compounds with some of the previously

isolated compounds from this species (Amer *et al.*, 1991; El-Masry *et al.*, 2010a; Desta and Majinda, 2014).

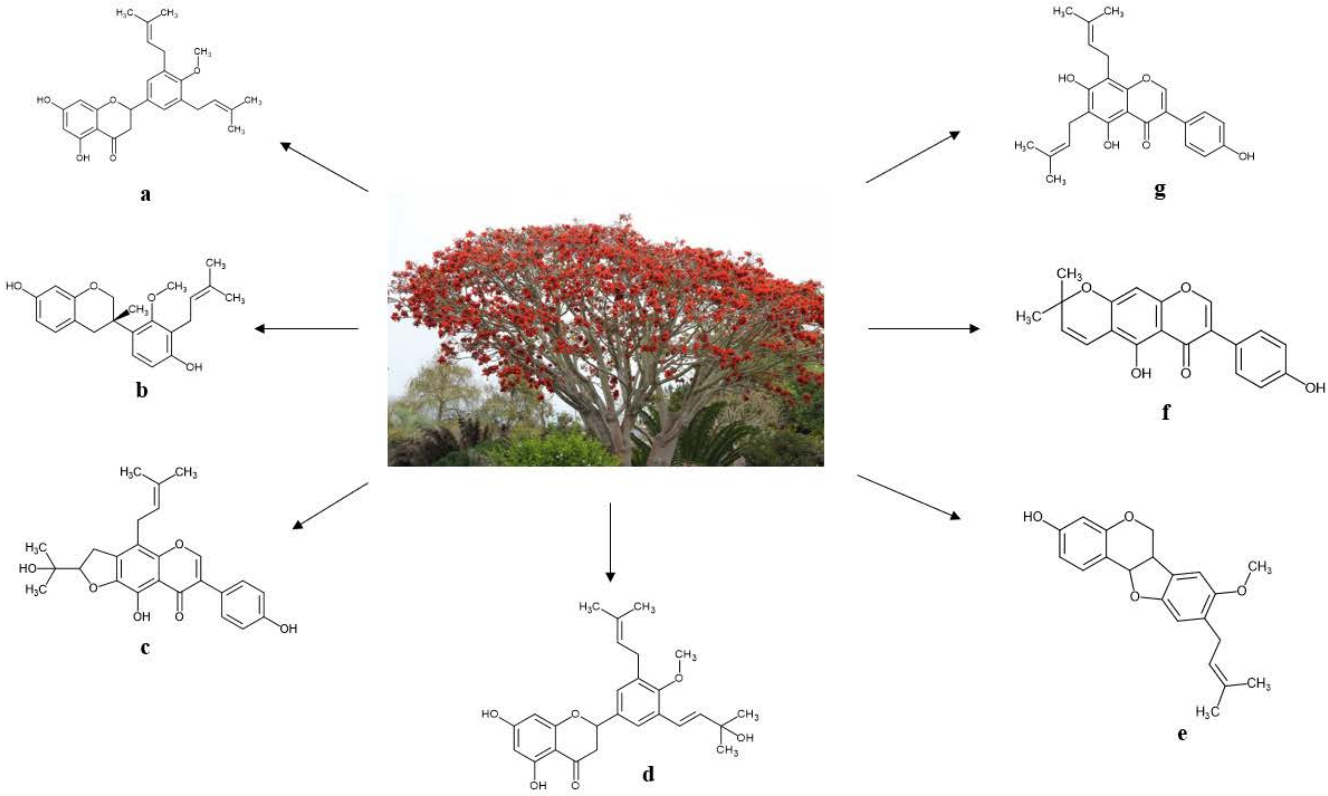

Figure 15. Some bioactive compounds isolated from *Erythrina caffra*

1.4. Study objectives

The aim of this study was to conduct an investigation for the anticancer, anti-oxidant, anti-enzymatic, antibacterial activity and cytotoxicity of the crude extracts, fractions, concoctions and isolated compounds of *E. caffra* as well as to characterize and identify the isolated compounds

The objectives of the study were to:

a) Extract alkaloidic fractions (B2 and B3) and a neutral fraction (B4) from the crude stem bark extract of *E. caffra* (B1).
b) Isolate the compounds through column and Preparative Thin Layer Chromatography and characterize them using LC-ESI-MS, NMR and IR.
c) Carry out the biological assay on the isolated compounds to test their:
    i. Activity against cancer cells (HCC-70).
    ii. Activity against bacterial pathogens.
d) Carry out biological assays on the crude extracts and fractions from *E. caffra* to test their:
    i. Activity against cancer cells (HCC-70).
    ii. Anti-oxidant activity.
    iii. Anti-enzymatic activity.
    iv. Activity against bacterial pathogens.
    v. Cytotoxicity against HeLa cells.
e) Visualize the interrelationship between extracts and fractions using their MS data and putatively identify potential derivatives available in the samples through molecular networking (using Cytoscape).
f) Study the interaction of some of the isolated compounds with the pathogens' proteins through molecular docking.

Chapter 2. Results and discussion

2.1. Extraction and fractionation

The brown crude extract from the stem bark (B1, 20.795 g) was used to extract two alkalodic fractions (B2 and B3) and a neutral fraction (B4) (**Table 3**). The neutral fraction (B4) was then separated by gradient elution using a column chromatography yielding a number of subfractions which were pooled based on their TLC profiles to obtain 8 subfractions.

Table 3. Fractions obtained from the crude extract from the stem bark

Name of fraction	Mass (g)	Solvent used (%)
B1	20.79	Methanol
B2	0.155	Ethyl acetate
B3	0.161	*n*-butanol
B4	20.08	Ethyl acetate

2.2. Phytochemical screening

In order to better understand the behaviour of the fractions and extracts from *E. caffra* they were phytochemically screened for their respective phytochemicals using the methods outlined in **Section 3.4**. **Table 4** shows the results obtained from the phytochemical screening of the *E. caffra* extract and fractions. In **Table 4** the screening of B1 did not give a positive response to the alkaloidic test even though it is a crude extract from which the alkaloidic fractions were taken. This might be because, in the crude extract the alkaloids were a relatively significantly small proportion such that they were present below the limit of detection of this very crude technique and could not give a positive test. However, B2 and B3 gave a strong positive test for alkaloids, this might be because since the B2 and B3 fractions were concentrated alkaloidic fractions with the major steroid components removed. The alkaloids were overexpressed such that they could give a positive test for alkaloids. The other fractions tested negative for alkaloids.

Table 4: Phytochemical screening of *E. caffra* extracts and fractions

Fractions and extracts	Classes of secondary metabolites			
	Steroids	Alkaloids	Phenolics	Flavonoids
B1	+	-	+	+
B2	-	+	+	-
B3	-	+	+	+
B4	-	-	-	+
SA2	+	-	+	+

(+): positive for the tested class, (-): negative for the tested class.

Further separation of the neutral fraction (B4) yielded three compounds which were dried, weighed and tested for their melting points. The obtained results are shown in **Table 5**.

Table 5: Compounds isolated from *Erythrina caffra*

Compound	Isolated mass	Melting point
1	17.1	210-215℃
2	21.3	210-215℃
3	65.2	145-146℃

2.3. Structure elucidation of isolated compounds

The neutral fraction was identified for further study because it the results from its phytochemical screening exhibited different classes of compounds which had a potential of being bioactive. Compounds of different classes were isolated from the neutral fractions (B4) of the crude extract. The first two compounds were faintly visible in TLC analyses under UV however, when the TLC plate was sprayed with an acid reagent, they were more prominent. These were characterized as terpenoid and steroid, respectively. Compound **1** was found to be a pentacyclic triterpenoid, whereas compound **2** was characterized as a type of 3β sterol. Terpenoids are known to give dark purple spots when sprayed with a vanillin-sulphuric acid solution (Gogoi *et al.,* 2016).

Compound **3** was characterized as a flavanone and was visible under UV light due to the presence of the high conjugation within its structure. This meant that this compound absorbed within the visible region of the electromagnetic spectrum (Pavia *et al.*, 2000) and were visible on the TLC plates altogether, indicating the presence of aromatic rings.

To elucidate the structures of the isolated compounds, their HR-ESI-MS, NMR (^{1}H, ^{13}C, DEPT 135, COSY, HMBC, HSQC, and NOESY) as well as IR spectral data were obtained and interpreted.

2.3.1. Structure elucidation of compound 1

Compound **1** was isolated as a white amorphous powder with a melting point of 210-215°C.

HR-ESI-MS of compound **1** (**Appendix 3.1:** Mass spectrum for compound **1**) detected in the positive mode at *m/z* = 427.1622 $[M+H]^+$ (calculated for $C_{30}H_{51}O^+$: 427.3934). Corresponding to the molecular formula $C_{30}H_{50}O$. The molecular formula indicated the presence of six degrees of unsaturation.

The IR spectrum of compound **1** (**Appendix 1.1.1:** Infrared for compound **1**) presented strong absorption bands at 3372.8 (OH stretch), 2917.4 (aliphatic C-H stretch), 1713.3 (C=C aliphatic) this data correlated with (Emaikwu *et al.*, 2020).

The ^{13}C NMR (**Error! Reference source not found.**) and DEPT 135 spectra (**Appendix 2.1.1:** DEPT-135) of compound **1** exhibited thirty carbon atoms, including two olefinic carbon signals at 150.8 (C-20) and 109.2 (C-29) and one oxymethine at δ_C 78.9 (C-3).

The ^{13}C NMR data further revealed signals for six quaternary carbons at δc 38.5 (C-4), 40.7 (C-8), 37.0 (C-10), 42.7 (C-14), 42.8 (C-17), and 150.8 (20); eleven methylenes (CH_2) at δc 38.7, 27.3, 18.2, 34.1, 20.8, 25.0, 27.2, 35.4, 29.5, 39.8, 109.2 and seven methyl (CH_3) groups at δc 27.8, 15.4, 15.8, 15.9, 14.4, 17.8 and 19.1. The experimental values were compared with the published values, and they were consistent with the compound previously reported to be lupeol (Gandagule *et al.*, 2018; Imam *et al.*, 2007)**.**

The chemical shifts at δc 109.2 and 150.8 (C-29 and C-20) indicated the presence of both an olefinic methylene group and a quaternary carbon, respectively (Shwe *et al.*, 2019). The chemical shift at δc 78.9 was assigned as an oxymethine due to it appearing more downfield as a consequence of high deshielding effect caused by the oxygen atom from the hydroxyl group.

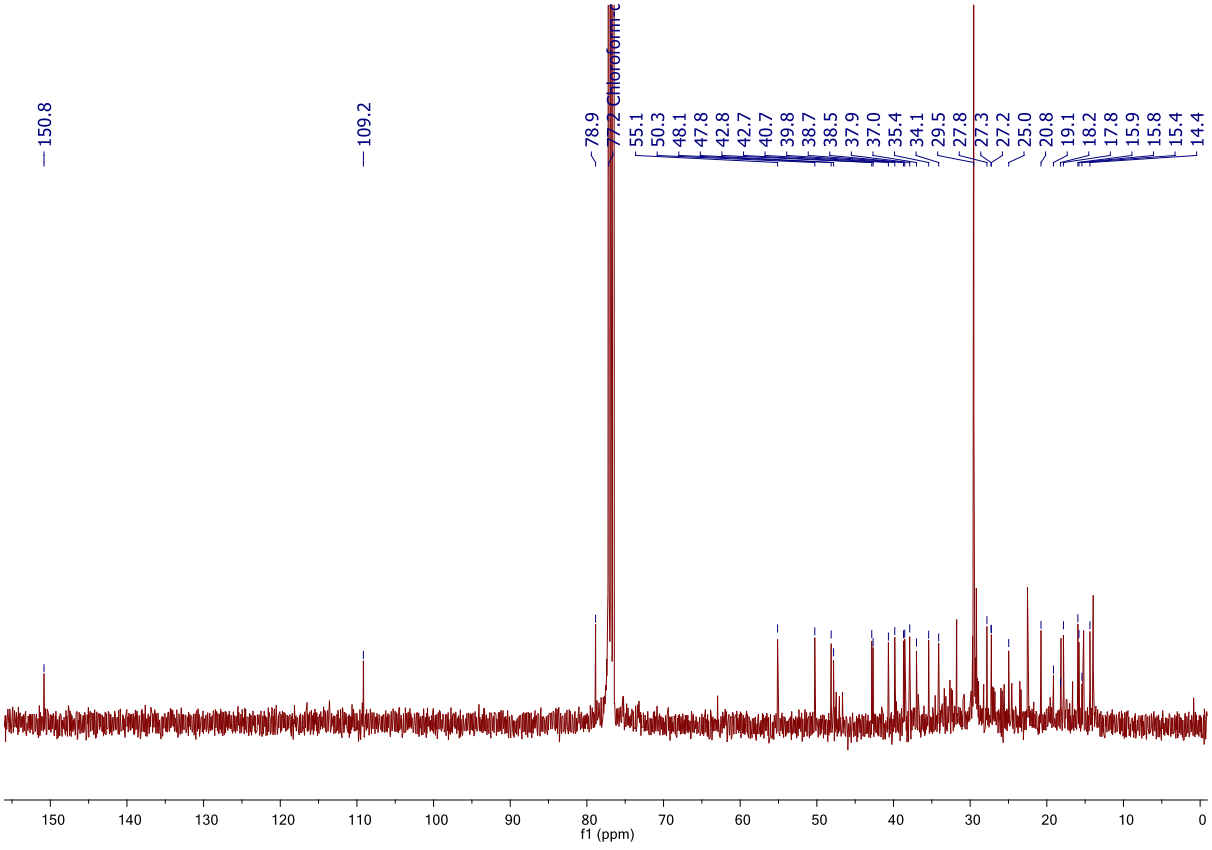

Figure 16. ^{13}C NMR spectrum (in $CDCl_3$) of compound **1**

On the ^{1}H NMR spectrum (**Error! Reference source not found.**) of compound **1**, the protons of the methyl group at δ_H 1.68 (H-30) showed a signal more downfield than it is expected of a methyl group, however this unusual behavior is indicative of an adjacent aliphatic olefin (C=C) group near the methyl group which causes it to resonate downfield (Shwe *et al.*, 2019).

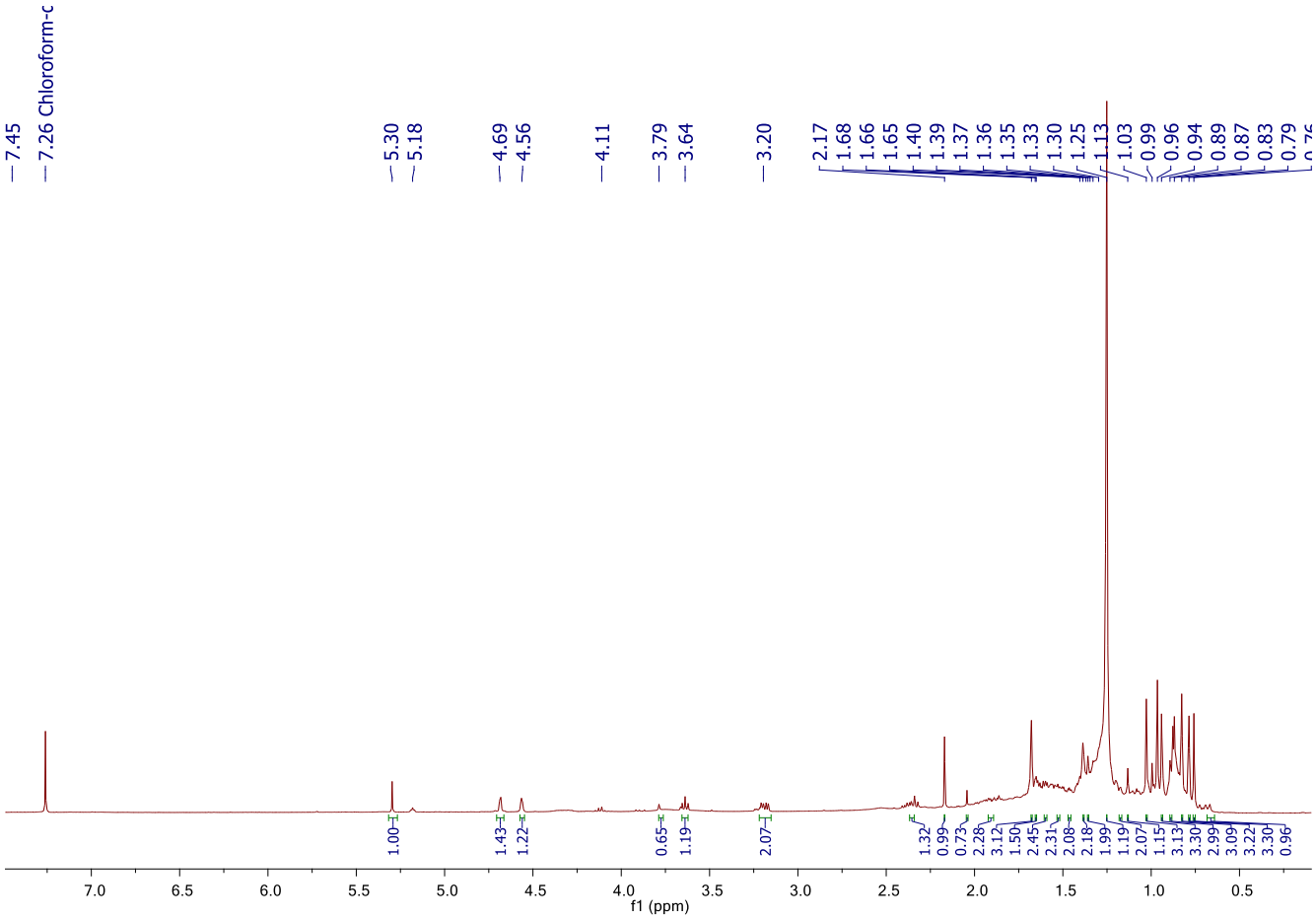

Figure 17. ^{1}H NMR spectrum (in $CDCl_3$) of compound **1**

The protons resonating at δ_H 4.50 and 4.62 (H-29a and 29b) were the most deshielded in the spectrum and were assigned as the exo methylene hydrogens from the double bond between C-29 and C-20 (δ_C 109.2 and 150.8). This was mainly due to the deshielding effect of the alkene group. The π electrons in the alkene group have higher electron density compared to sigma bonds which in turn produces a larger internal magnetic field which ultimately leads to peaks appearing downfield (higher chemical shift). However, it seems like this magnetic field was shared non-uniformly as the protons have different chemical shifts (Yuan *et al.*, 2022). These

two protons were not isochronous, they behaved like diastereotopic protons. They seemed to have undergone a geminal splitting giving off two doublets, this showed that they were not chemically equivalent (Abel, 2020). This is expected since one is *trans* to the ring and the other is *cis*.

The rest of the protons were assigned to their respective carbons with the help of the HSQC spectrum. The HSQC spectrum (**Appendix 2.2.4:** HSQC) showed that the proton at δ_H 5.30 (br.s, 3-OH) was most likely from the hydroxyl group as it was not correlated to any of the carbon atoms present on the HSQC (**Appendix 2.2.4:** HSQC) .

In the COSY spectrum (**Appendix 2.2.2:** COSY)the following correlations were found between the proton at δ_H 1.20 (H-9) and the protons at δ_H 1.40 and 1.25 (H-11); as well as the proton at δ_H 1.30, 1.91 (H-21), 2.31 (H-19). These correlations indicate that protons H-9 and H-11 couple each other, also proton H-19 and H-21 couple each other. The correlation between the protons at δ_H 1.65 and δ_H 1.36 revealed coupling between the H-13 and H-18. The COSY also showed a correlation between the two protons at δ_H 4.50 and 4.62 (H-29a and H-29b).

The HMBC spectrum (**Appendix 2.2.3:** HMBC) showed that the singlet assigned to the methyl group at δ_H 0.89 (H-23) was correlating with the carbon atom at δ_C 38.5 (C-4), it also showed correlation from the singlet at δ_H 0.76 (H-24) to the carbon atom at δ_C 38.5 (C-4), confirming that this was a quaternary carbon. The proton at δ_H 1.45 (H-19) displayed a strong correlation with the carbon signal at δ_C 150.8 (C-20) and the carbon signal at δ_C 29.5 (C-21). The correlation on the HMBC spectrum from the proton at δ_H 1.45 (H-19) to the carbon signal at δ_C 150.8 (C-20) suggested that there is a bond between C-19 and C-20.

The HMBC spectrum also further depicted correlations from the proton at δ_H 1.25 (H-9) to the carbon resonating at δ_C 37.0 (C-10), the singlet at δ_H 0.83 (H-25) to the carbon resonating at δ_C 37.0 (C-10) and the proton at δ_H 0.67 (H-5) to the carbon at δ_C 37.0 (C-10) confirming that C-10 is connected to C-5 as well as C-9. The proton at δ_H 1.17 (H-22) as well as the singlet at δ_H 0.79 (H-28) showed strong correlation to the carbon atom at δ_C 42.8 (C-17) suggesting that C-17 is probably bonded both to C-22 and C-28 as well as C-16. More correlations indicated by the HMBC are shown in **Error! Reference source not found.**.

Table 6. The ^{1}H (400MHz) and ^{13}C (400MHz) spectral data of compound **1** measured in $CDCl_3$; δ in ppm, J in Hz.

Position	δ_H (multiplicity, J in Hz)	^{13}C (δ_c)	COSY	HMBC
1	0.89(o, 1H), 1.57 (o, 1H)	38.7	1.53, 165	37.0, 27.3
2	1.53, 1.65(o, 1H)	27.3	1.53, 3.12	38.7, 79.9
3	3.12(dd, J = 11.2, 5.0)	79.9	1.53, 1.65	27.3, 38.5
4	-	38.5	-	-
5	0.62(o, 1H)	55.1	1.36, 1.53	38.5, 18.2, 37.0
6	1.36(, 1H), 1.53(o, 1H)	18.2	1.39	55.1, 34.1
7	1.39(o, 1H)	34.1	1.36, 1.53	18.2, 40.7
8	-	40.7	-	-
9	1.17(o, 1H)	50.3	1.20, 1.40	40.7, 37.0, 20.8
10	-	37.0	-	-
11	1.20(o, 1H), 1.40(o, 1H)	20.8	1.07, 1.55	50.3, 25.0
12	1.07(o, 1H), 1.55 (o, 1H)	25.0	1.65, 1.20	20.8, 37.9
13	1.65(o, 1H)	37.9	1.27, 1.07	25.0, 42.7, 48.1
14	-	42.7	-	-
15	1.05(o, 1H), 1.60 (o, 1H)	27.2	1.33, 1.46	42.7, 35.4
16	1.33(o, 1H), 1.46(o, 1H)	35.4	1.05, 1.60	27.2, 43.0
17	-	42.8	-	-
18	1.27(o, 1H)	48.1	1.65, 2.31	37.9, 42.0, 47.8
19	2.31(o, 1H)	47.8	1.27, 1.30, 1.91	48.1, 150.8, 29.5
20	-	150.8	-	-
21	1.30 (o, 1H), 1.91(m, 1H)	29.5	2.31, 1.17, 1.37	47.8, 39.8

22	1.17(o, 1H), 1.37(o, 1H)	39.8		42.8, 29.5
23	0.89(s, 3H)	27.8	-	38.5
24	0.69(s, 3H)	15.4	-	38.5
25	0.76(s, 3H)	15.9	-	37.0
26	1.03(s, 3H)	15.8	-	40.7
27	0.87(s, 3H)	14.4	-	42.7
28	0.79	17.8	-	42.8
29	4.50(d, J = 1.0, 1H) 4.62(d, J = 2.1, 1H)	109.2	4.50, 4.62	150.8
30	1.61(s, 3H)	19.1	-	150.8

s = singlet, d = doublet, o = overlap, m = multiplet

A study by Shwe and colleagues (Shwe *et al.*, 2019) has reported spectral data of lupeol that is similar to the one presented in this study **Table 7**.

Table 7. ^{13}C-NMR Data of compound **1** and lupeol (Shwe *et al*., 2019)

Position	Compound **1** δc	Lupeol δc
1	38.7	38.9
2	27.3	27.3
3	79.9	78.9
4	38.5	38.7
5	55.1	55.3
6	18.2	18.3
7	34.1	34.3
8	40.7	40.8
9	50.3	50.4
10	37.0	37.2
11	20.8	20.9
12	25.0	25.1
13	37.9	38.1
14	42.7	42.8
15	27.2	27.4

16	35.4	35.6
17	42.8	42.9
18	48.1	48.3
19	47.8	47.9
20	150.8	150.9
21	29.5	29.8
22	39.8	39.9
23	27.8	27.9
24	15.4	15.4
25	15.9	16.1
26	15.8	15.9
27	14.4	14.6
28	17.8	17.9
29	109.2	109.1
30	19.1	19.3

The structure of compound **1** was found to be identical to that of lupeol, a pentacyclic triterpenoid (Shwe *et al.*, 2019; Emaikwu *et al.*, 2020) (**Figure 18**). This compound has been previously isolated from most *Erythrina* species including but not limited to *Erythrina senegalensis* (Tchuente Djoko *et al.*, 2021) *Erythrina excelsa* (Kwamou *et al.*, 2015) and *Erythrina caffra* (Chukwujekwu *et al.*, 2016)

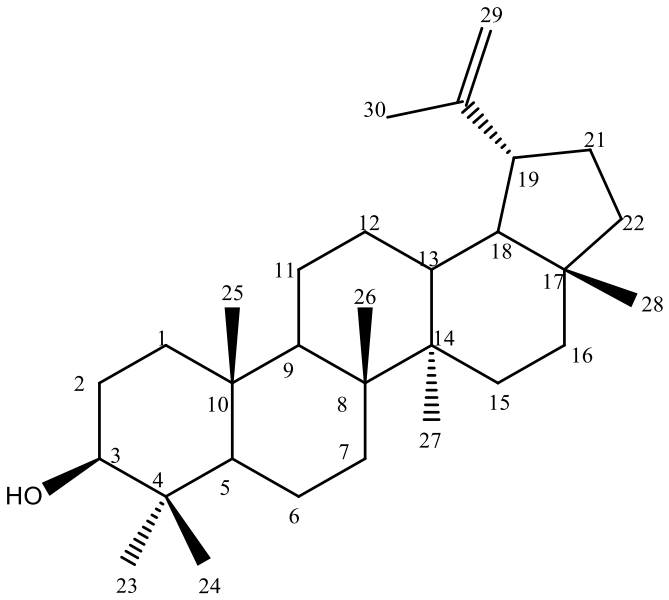

Figure 18. Structure of compound **1**

2.3.2. Structure elucidation of compound 2

Compound **2** was isolated as a white solid; melting point was 161-165°C.

HR-ESI-MS of compound **2** (**Appendix 3.2:** Mass spectrum for compound **2**) detected in the positive mode at *m/z* = 413.2669 $[M+H]^+$ (Calculated for $C_{29}H_{49}O^+$: 412.3778) corresponding to the molecular formula of $C_{29}H_{48}O$. The molecular formula depicted the presence of six degrees of unsaturation.

The IR spectrum of compound **2** (**Appendix 1.1.2:** Infrared for compound **2**) presented strong absorption bands at 3396 (OH stretch), 2925 (C-H stretch), 2851.8, 1647.7 (C=C stretch) and 1045 (C-O stretch).

The ^{13}C NMR (**Error! Reference source not found.**) and DEPT spectra (**Appendix 2.2.1**: DEPT-135) indicated compound **2** to have twenty-nine carbon atoms. The NMR data further revealed that three of these carbons were quaternary carbon atoms at δ_C 140.9 (C-5), 36.6 (C-10) and 42.4 (C-13); nine were methylene groups at δ_C 37.4 (C-1), 32.1 (C-2), 42.4 (C-4), 31.8 (C-7), 21.2 (C-11), 39.8 (C-12), 24.5 (C-15), 29.3 (C-16) and 25.6 (C-28); ten methines and

six methyl groups. The spectral data of compound **2** was compared with literature values and found to be consistent with reported stigmasterol (Pateh *et. al.*, 2009).

In the ^{13}C NMR spectrum (Error! Reference source not found.), the carbon atom at δ_C 72.0 (C-3) confirmed the presence of a hydroxyl group attached to compound **2**. The chemical shifts at δ_C 140.9, 121.9, 138.5 and 129.4 (C-5, C-6, C-22 and C-23 respectively) were indicative of the presence of two double bonds in the structure of compound **2**, as they were highly deshielded. This was further supported by the HSQC spectrum (**Appendix 2.2.3**: HMBC) which exhibited strong correlations from these carbons to protons that were highly deshielded for instance the proton at δ_H 5.34 (H-6) with the carbon atom at δ_C 121.9 (C-6). The HSQC also displayed a correlation from the proton at δ_H 3.53 (H-3) to the carbon atom at δ_C 72.0 (C-3) indicating that these two atoms are bonded and no correlation found from the proton at δ_H 6.21 (3-OH) to any carbon atom indicated that it is bonded to a heteroatom.

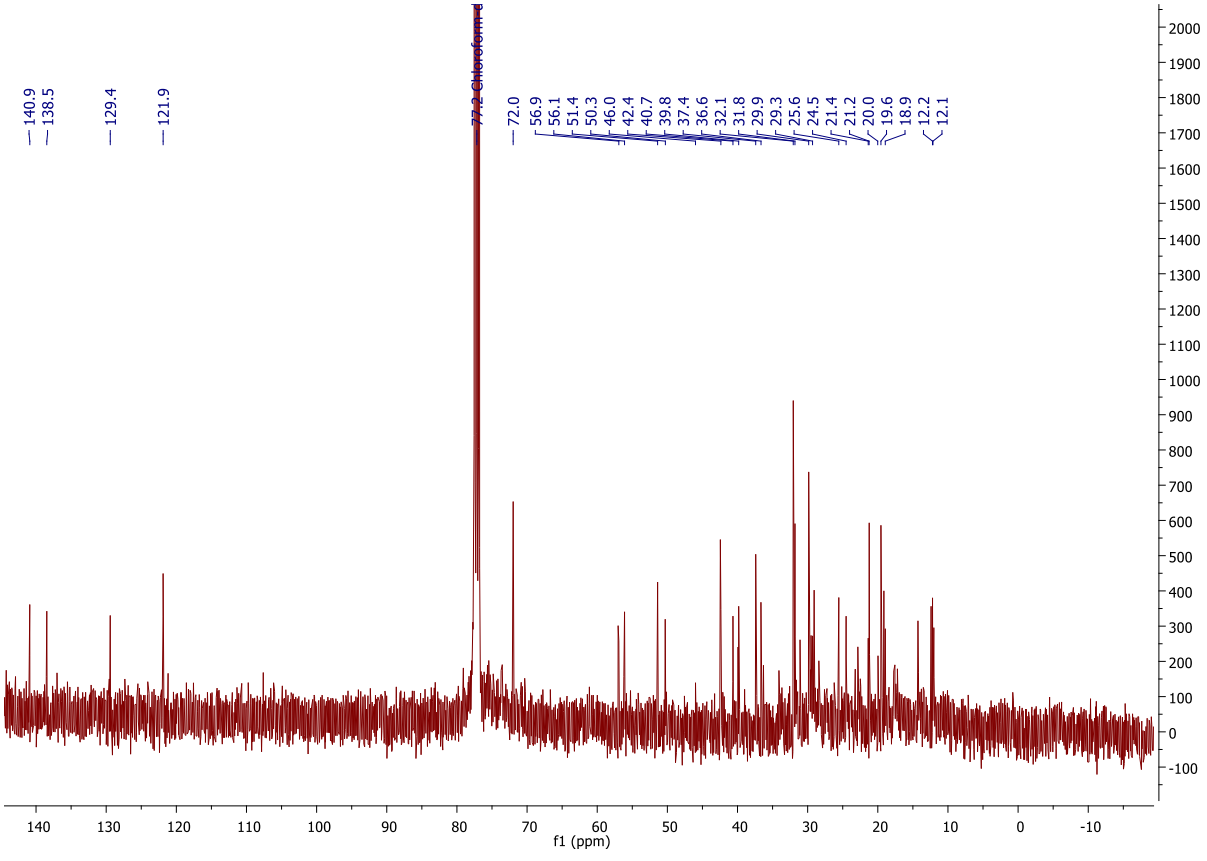

Figure 19 ^{13}C NMR spectrum (in $CDCl_3$) of compound **2**

In the ^{1}H NMR (**Error! Reference source not found.**) the signal at δ_H 6.21 can be assigned to hydroxyl proton. The HMBC (**Appendix 2.2.3**: HMBC) showed a strong correlation from the

proton at δ_H 1.60 (H-2/H-4) to the carbon atom at δ_C 72.0 (C-3) suggesting that these atoms are two bonds apart, this signal could belong to either H-4 or H-2. This was corroborated by the strong correlations shown between the proton at δ_H 1.60 with the one at δ_H 3.52 (H-3) in the COSY spectrum. The HMBC spectrum revealed a strong correlation from the proton at δ_H 1.60 to the carbon atom at δ_C 140.9 (C-5), indicating that the proton at δ_H 1.60 belongs to H-4. More correlations indicated by the HMBC are shown in

Table 8.

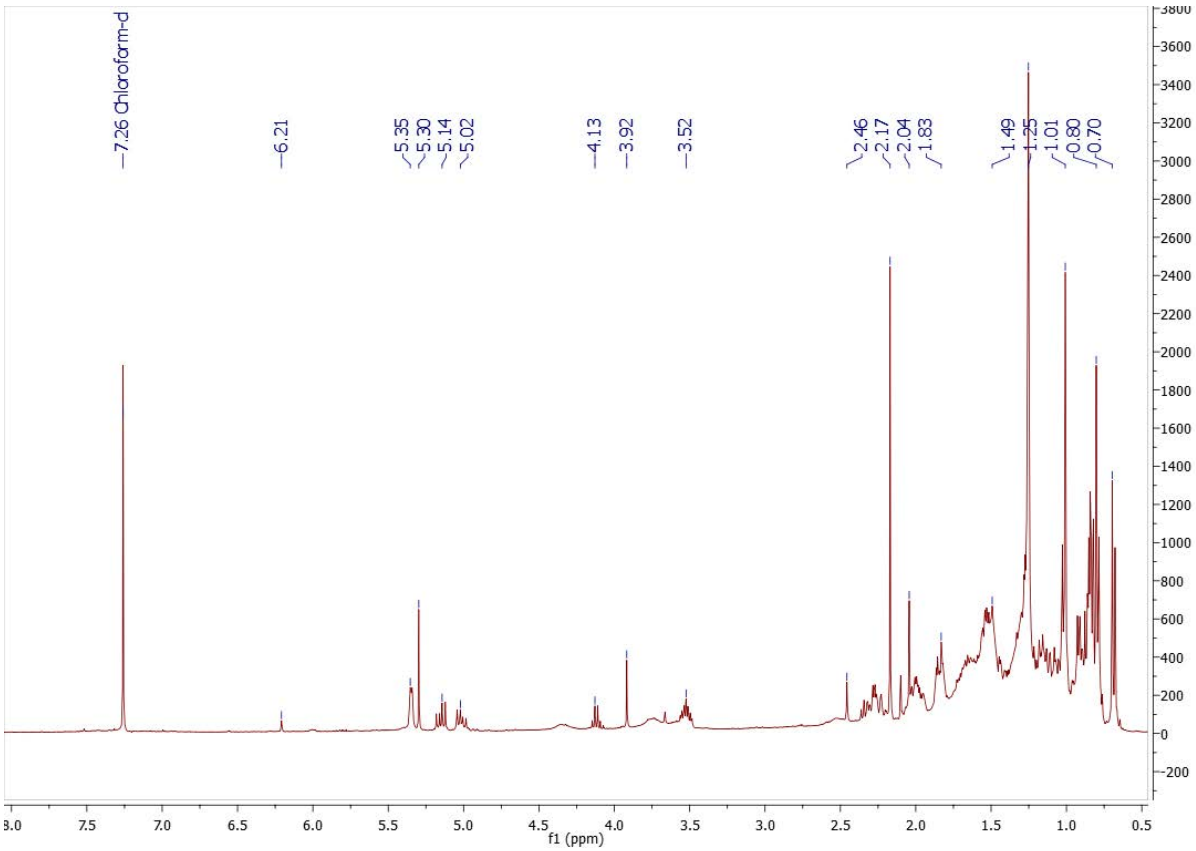

Figure 20. ^{1}H NMR spectrum (in $CDCl_3$) of compound 2

Correlations depicting ^{1}H-^{1}H coupling and more correlation from HMBC which led to the identification of compound **2** are displayed in

Table 8 below.

Table 8. The ^{1}H (400MHz) and ^{13}C (400MHz) spectral data of compound **2** measured in $CDCl_3$; δ in ppm, J in Hz

Position	δ_H (multiplicity, J in Hz)	^{13}C (δ_c)	COSY	HMBC
1	-	38.7	-	32.1, 36.6
2	-	32.1	3.52	38.7, 72.0
3	3.52 (ddd, 4.5, 4.2, 3.8)	72.0	-	32.1, 42.4
4	-	42.4	-	72.0, 140.9
5	-	140.9	-	-
6	5.35 (t, 6.0, 1H)	121.9	-	140.9, 31.8
7	-	31.8	5.35	121.9, 31.8
8	-	31.8	-	31.8, 50.3, 56.9
9	-	50.3	-	31.8, 36.6, 21.2
10	-	36.6	-	-
11	-	21.2	-	50.3, 39.8
12	-	39.8	-	21.2, 42.4
13	-	42.4	-	-
14	-	56.9	-	31.8, 42.4, 24.5
15	-	24.5	-	56.9, 29.3
16	-	29.3	-	24.5, 56.2
17	-	56.2	-	42.4, 29.3, 40.7
18	0.70 (s, 3H)	12.2	-	36.6
19	1.00 (s, 3H)	18.9	-	42.4
20		40.7	5.01	56.2, 21.4, 138.5
21	0.93 (d, 6.5, 3H)	21.4		40.7
22	5.01 (m, 1H)	138.5	5.15	40.7, 129.4
23	5.15 (m, 1H)	129.4	-	138.5, 45.9
24		46.0	5.15	129.4, 29.9, 25.6
25	-	29.9	0.82, 0.80	46.0, 20.0, 19.6
26	0.82(d, 1.5, 3H)	20.0	-	29.9
27	0.80 (d, 7.0, 3H)	19.6	-	29.9
28		25.6	0.84	46.0, 12.1

29	0.84(t, 3.7, 3H)	12.1	-	25.6

The structure of compound **2** (**Error! Reference source not found.**) was found to be identical to that of stigmasterol a 3ß sterol which is a member of phytosterols (Glastonbury, 2013). This compound has been previously isolated from *Erythrina* species like *Erythrina indica* (Nkengfack *et al*., 2001), *Erythrina stricta* (Singh *et al*., 1981), as well as *Erythrina poeppigiana* (Noudou, Nkengfack and Mbazoa, 2018). Spectral data which are similar to the one observed in

Table *9* have been reported before (Chaturvedula and Prakash, 2012). This helped with assigning the chemical shifts of compound **2.**

Table 9. ^{13}C-NMR Data of compound **2** and stigmasterol (Chaturvedula *et al.*, 2012)

Position	Compound 2 δc	Stigmasterol δc
1	38.7	37.6
2	32.1	32.1
3	72.0	72.1
4	42.4	42.4
5	140.9	141.1
6	121.9	121.8
7	31.8	31.8
8	31.8	31.8
9	50.3	50.2
10	36.6	36.6
11	21.2	21.5
12	39.8	39.9
13	42.4	42.4
14	56.9	56.8
15	24.5	24.4
16	29.3	29.3
17	56.2	56.2
18	12.2	12.2
19	18.9	18.9
20	40.7	40.6
21	21.4	21.7
22	138.5	138.7
23	129.4	129.6
24	46.0	46.1
25	29.9	29.6
26	20.0	20.2
27	19.6	19.8
28	25.6	25.4
29	12.1	12.1

Using HMBC (**Appendix 2.2.3**: HMBC) and the HSQC (**Appendix 2.2.4**: HSQC) correlations the structure of compound **2** was confirmed to be as suggested in **Error! Reference source not found..**

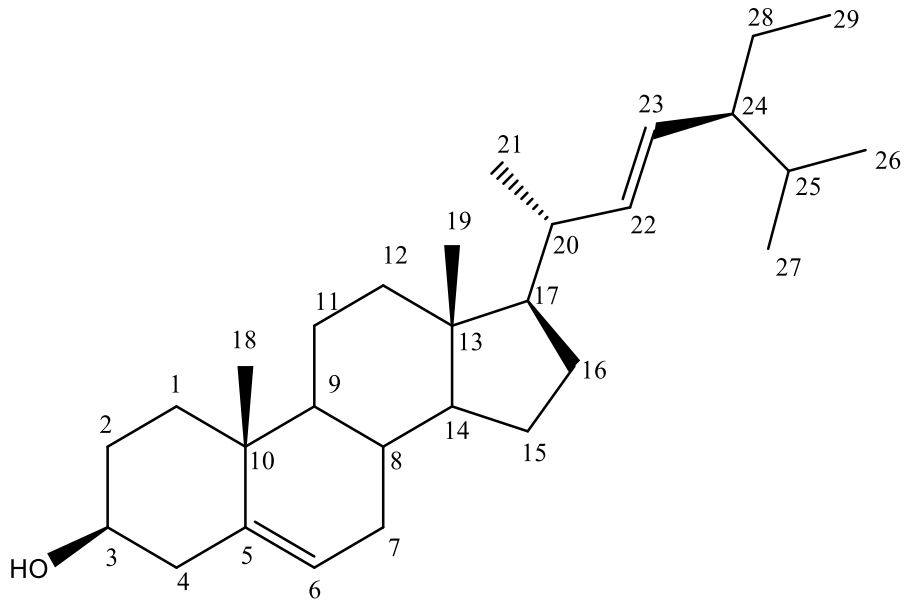

Figure 21. Structure of compound **2**

2.3.3. Structure elucidation of compound 3

This compound was isolated as a yellow amorphous solid with a melting point range of 146-149 ℃.

HR-ESI-MS of compound **3** (**Appendix 3.3:** Mass spectrum of compound **3**) detected in the positive mode at *m/z* = 423.1176 $[M+H]^+$ (calculated for $C_{26}H_{31}O_5^+$:423.2166) corresponding to the molecular formula $C_{26}H_{30}O_5$. The molecular formula depicted the presence of twelve degrees of unsaturation.

The IR spectrum of compound **3** (**Appendix 1.1.3:** Infrared for compound **3**) revealed strong absorption bands at 3266 (OH stretch), 2962 (C-H stretch) and 1726 (C=O stretch) these data corresponded with data obtained by previous investigators (Yenesew *et al.*, 1998)

The ^{13}C NMR spectrum (**Figure 22**) and DEPT spectrum () showed a total of twenty-six carbon atoms present in the structure of compound **3**. These included four methyl groups (C-4", C-5", C-4'"and C-5'"), one methoxy group OCH_3 at δ_C 60.7; three methylene groups at δ_C 42.9 (C-3), 28.2 (C-1") and δ_C 28.2 (C-1'"), seven methine groups (C-2, C-6, C-8, C-2', C-6', C-2", C-2'") and eleven quaternary carbons (C-4, C-5, C-7, C-9, C-10, C-1', C-3', C-3", C-4', C-5', C-3'") .

Amongst these signals, the carbon atom at δ_C 79.1 was identified as C-2 as it was more downfield due to the high deshielding effect caused by the oxygen atom directly bonded to C-2. In addition to this, the signal appearing at δ_C 42.9 (C-3) suggests that it is not a methyl group as it is more downfield compared to the other methyl groups and the signal at δ_C 196.0 (C-4) is characteristic of a ketone or an aldehyde. However, since there is no signal appearing far downfield in the ^1H NMR spectrum this indicates that this is a ketone, and the signal at δ_C 42.9 (C-3) is an α-carbon to the carbonyl carbon at δ_C 196.0 (C-4). This huge downfield shift is as a result of the induce electron circulation in the π bond. The signals at δ_C 28.2 (C-1"/1"'), 122.4 (C-2"/2"'), 132.6 (C-3"/3"'), 25.6 (C-4"/4"') and 17.7 (C-5"/5"'), they were indicative of isoprenyl moieties (Tsafack *et al.*, 2018).

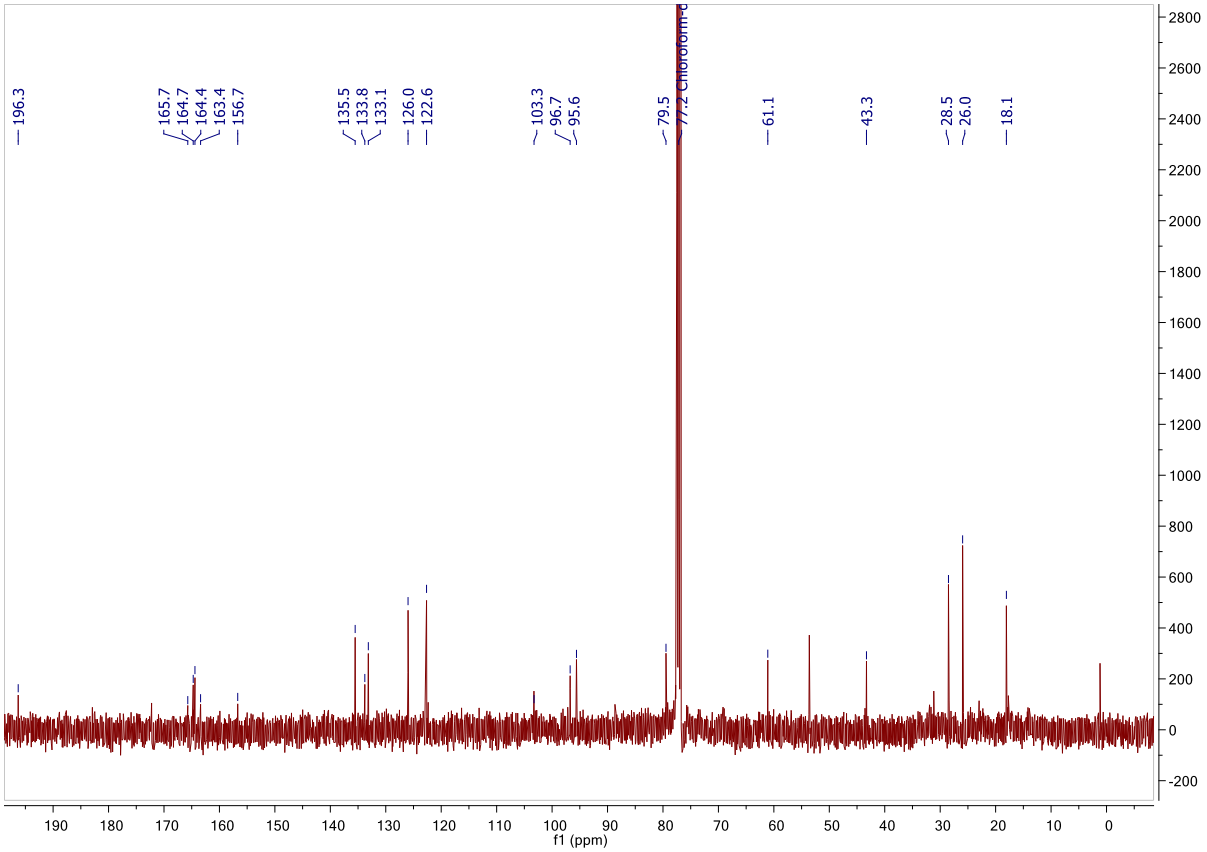

Figure 22. ^{13}C NMR spectrum (in $CDCl_3$) of compound **3**

In the ^{1}H NMR spectrum (**Error! Reference source not found.**), the signal displayed at δ_H 7.09 (s, H-2'/6') were characteristic of 3'4' and 5' substituted B cycle of flavonoids. And the two resonances at δ_H 5.96 (d, J = 2.2, H-6/8) were characteristic of protons of the ring A of flavonoids.

The HSQC spectrum (**Appendix 2.3.4:** HSQC) displayed lots of strong correlations like the proton at δ_H 2.68 (H-3eq), 3.01 (H-3ax) correlating with the carbon atom at δ_C 42.9 (C-3), the proton at δ_H 7.02 (H-2'/6') correlating with δ_C 125.7 (C-2'/6') which were in accordance with dihydroflavone-like structure. The proton at δ_H 3.38 (H-1") correlating with the carbon at δ_C 28.2 (C-1"), the proton at δ_H 5.28 (H-2") correlating with the carbon δ_C 122.4 (C-2"), the proton at δ_H 1.68 (H-4") correlating with the carbon at δ_C 25.6 (C-4") and the proton at δ_H 1.66 (H-5") with the carbon at δ_C 17.7 (C-5"), supporting the presence of the isoprenyl moiety in the structure of compound **3**.

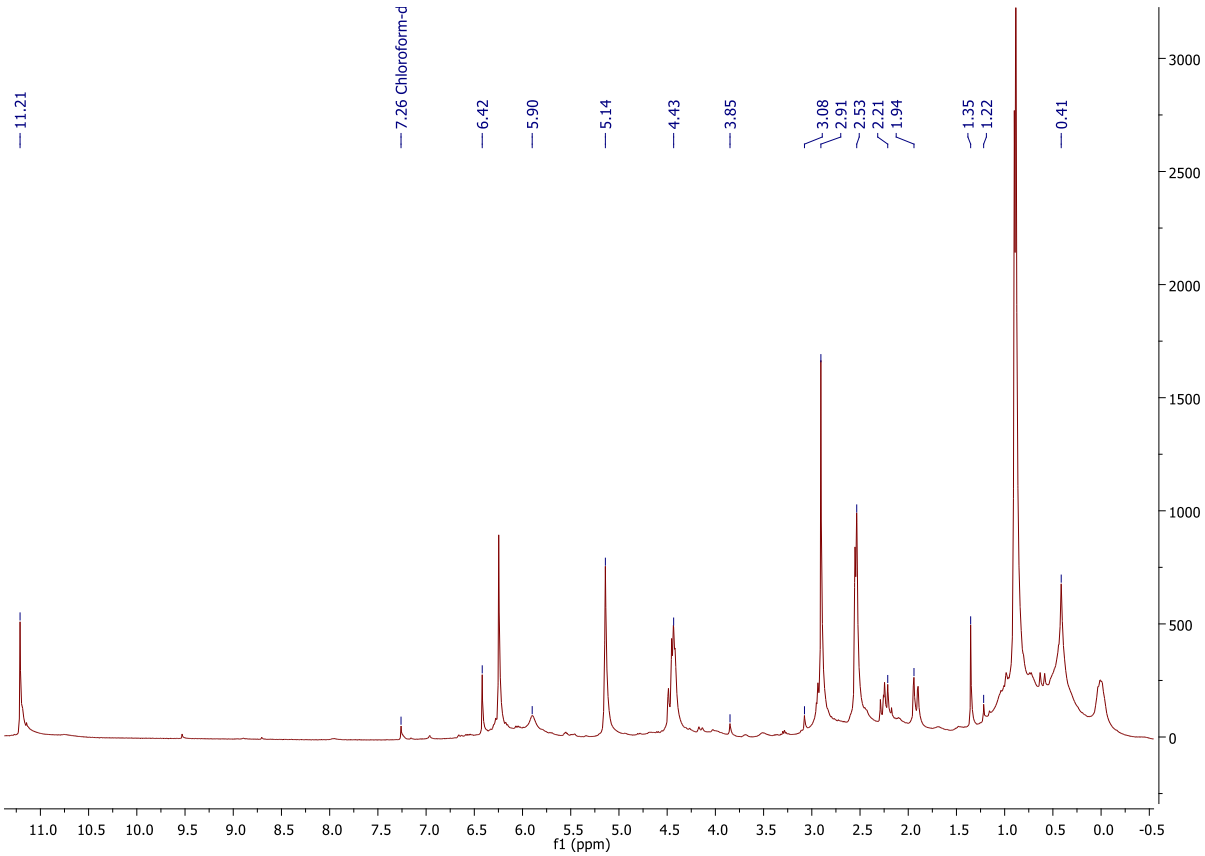

Figure 23: ^{1}H NMR spectrum (in $CDCl_3$) of compound **3**

The COSY spectrum (**Error! Reference source not found.**) revealed a considerable number of proton-proton couplings, including the coupling between the proton at δ_H 5.23 (H-2) and 2.68 (H-3) suggesting that these protons are adjacent to each other. The resonance at δ_H 5.96 (H-6/8) in the ^{1}H NMR (**Error! Reference source not found.**) did not have any correlations in the COSY spectrum (**Error! Reference source not found.**) suggesting that the corresponding proton is bonded to a carbon atom that is in between quaternary carbons.

The HMBC spectrum (**Appendix 2.3.3**: HMBC) showed that the proton at δ_H 2.68 (H-3eq) was correlating with the carbon atom at δ_C 196.3 (C-4) suggesting that the carbonyl carbon was close to C-3. It also exhibited a strong correlation between a proton at δ_H 5.96 (H-6) and a carbon atom at δ_C 164.4 (C-5). Strong correlations are also present from the proton at δ_H 5.96 (H-8) to the carbon at δ_C 163.1 (C-9). The lack of correlations to C-9, C-4, C-5, C-7 and C-10 from any proton in HSQC (**Appendix 2.3.4:** HSQC) suggest that these carbon atoms are not connected to any protons.

The HMBC spectrum (**Appendix 2.3.3**: HMBC) also revealed correlations from the proton at δ_H 5.23 (H-2) to the carbon at δ_C 133.6 (C-1'), this was indicative of a bond between C-2 and C-1'. The proton at δ_H 7.02 (H-2') was correlating with C-1' suggesting that this proton was probably close to C-1'. Another correlation from the proton at δ_H 3.38 (H-1") and the carbon at δ_C 135.5 (C-3') and was observed in the HMBC spectrum (**Appendix 2.3.3**: HMBC) suggesting that C-3' might be bonded to C-1". The correlation exhibited from the proton at 3.68 (4-OCH_3) to the carbon at 156.7 (C-4') supported the fixation of the methyl group on the hydroxyl at C-4'. This correlation was again seen between H-1"' and C-5' also between C-5' and H-6' suggesting that C-5' might be bonded to both C-1'" and C-6'. The symmetrical spot of the proton at 7.02 (H-2'/6') with the carbon at 126.0 (H-2'/6') indicated the symmetry in the ring B. More correlations observed in the HMBC spectrum are presented in **Table 10**.

Table 10. The ^1H (400MHz) and ^{13}C (400MHz) spectral data of compound **3** measured in $CDCl_3$; δ in ppm, J in Hz.

Position	δ_H (multiplicity, J in Hz)	^{13}C (δ_c)	COSY	HMBC
2	5.23 (o, 1H)	79.5	3.01	43.3 ,133.8
3	3.01 (dd, J = 17.0, 13.0 Hz, 1H) 2.68 (dd, J = 17.2, 3.1 Hz, 1H)	43.3	5.23	196.3, 79.5
4	-	196.3	-	-
5	-	164.4	-	-
6	5.96 (d, J = 2.2, 1H)	96.7	-	164.4
7	-	165.7	-	-
8	5.96 (d, J = 2.2, 1H)	95.6	-	165.7
9	-	163.4	-	-
10	-	103.3	-	-

1’	-	133.8	-	-
2’	7.02 (s, 1H)	126.0	-	43.3
3’	-	135.5	-	-
4’	-	156.7	-	-
5’	-	135.5	-	-
6’	7.02 (s, 1H)	126.0	-	133.8
1”	3.32 (d, J = 7.1, 2H)	28.5	5.23	126.0, 135.5
2”	5.23 (o, 1H)	122.6	3.32	28.5 ,132.1
3”	-	132.1	-	-
4”	1.68 (s, 3H)	26.0	-	132.1
5”	1.66 (s, 3H)	18.0	-	132.1
1’’’	3.32 (d, J = 7.1, 2H)	28.5	5.23	18.0, 122.6
2’’’	5.23 (o, 1H)	122.6	3.32	28.5
3’’’	-	133.1	-	-
4’’’	1.68 (s, 3H)	26.0	-	133.1
5’’’	1.66 (s, 3H)	18.0	-	133.1
OMe	3.68 (s, 3H)	61.1	-	-
5-OH	12.00 (s, 1H)	-	-	-

Yenesew and colleagues (Yenesew et al., 1998) have reported spectral data which are similar to the one presented in this study (**Table 11**), it was used to help assign the chemical shifts.

Table 11. ^{13}C-NMR Data of compound **3** and abyssinone V 4’-methyl ether (Yenesew *et al*., 1998)

Position	Compound **3** δc	Abyssinone V 4’-methyl ether δc
2	79.5	79.3
3	43.3	43.0
4	196.3	196.3
5	164.4	164.2
6	96.7	96.6

7	165.7	165.3
8	95.6	95.6
9	163.4	163.3
10	103.3	103.0
1’	133.8	133.7
2’	126.0	125.9
3’	135.5	135.4
4’	156.7	156.4
5’	135.5	135.4
6’	126.0	125.9
1”	28.5	28.4
2”	122.6	122.5
3”	132.1	133.0
4”	26.0	25.7
5”	18.0	17.9
1’’’	28.5	28.4
2’’’	122.6	122.5
3’’’	133.1	133.0
4’’’	26.0	25.7
5’’’	18.0	17.9
OMe	61.1	60.9

The data above suggests that the structure of compound **3** (Error! Reference source not found.) was more like that of abyssinone V 4’-methyl ether, a flavanone commonly found in *Erythrina* species (Ombito *et al.*, 2018), (Tueche *et al.*, 2018); (Yenesew *et al*., 2000).

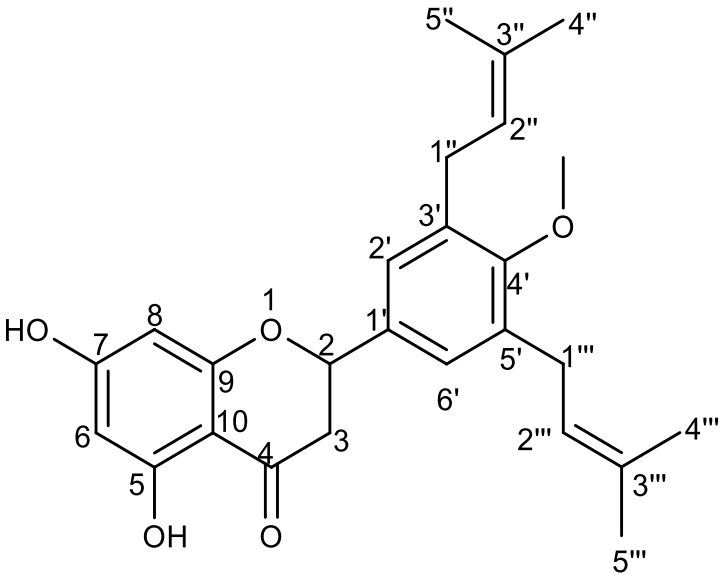

Figure 24. Structure of compound **3**

2.4. Biological assays

The biological screening of the isolated compounds, their respective extracts and fractions was conducted. The isolated compounds, extracts and fractions were evaluated for their anticancer activity using the triple-negative HCC-70 breast cancer cell line (**Error! Reference source not found.** and **Figure 26**), anti-oxidant activity (**Figure 27**). They also were assessed for their enzymatic inhibition potential (

Figure 28), antibacterial activity on *Staphylococcus aureus*, *E. coli* and cytotoxicity on HeLa cells (**Figure 29** and **Error! Reference source not found.**). Activities of isolated compounds are reported as minimal half-inhibitory concentration values (IC_{50})

2.4.1. *In vitro* Anticancer

The isolated compounds **1**, **2**, **3** and the intractable mixture SN6(compound 2 mixed with an unknown), extracts and fractions were screened for potential anticancer activity using the triple-negative HCC70 breast cancer cell line, the results of this assay are presented in **Error! Reference source not found.**. Activities of the isolated compounds are reported as minimal half-inhibitory concentration values (IC_{50}) and in all cases these values were determined in at least three independent experiments.

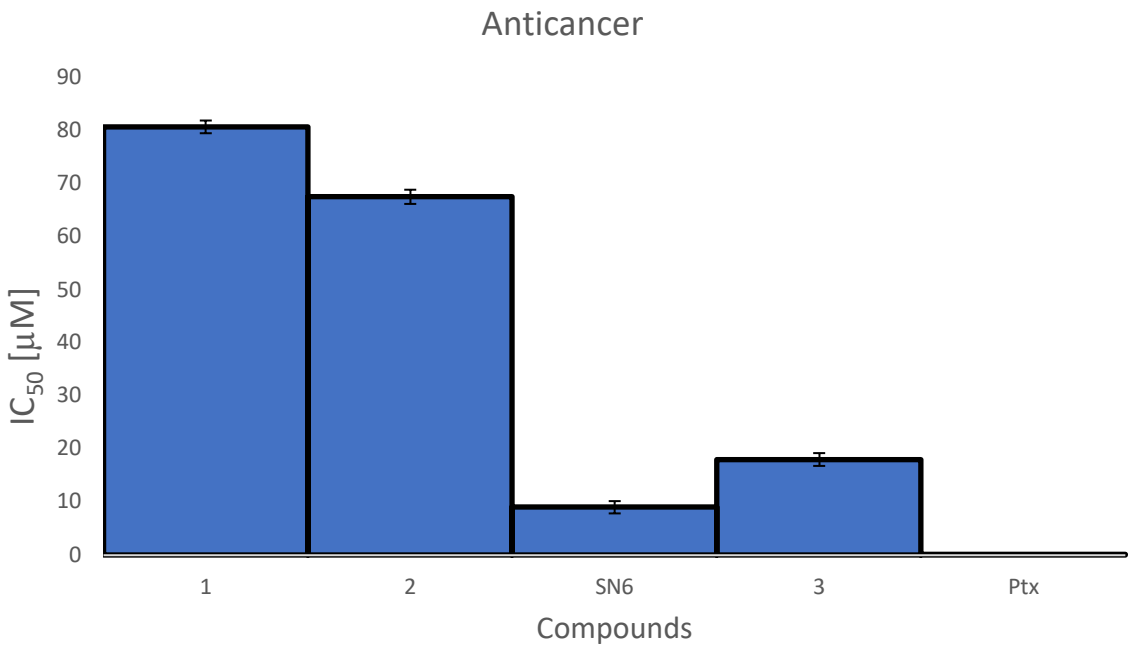

Figure 25. *In vitro* anticancer activity of isolated compounds and compound mixture. Where **1** represents lupeol (compound **1**), **2** represents stigmasterol **(**compound **2)** and **3** represents abyssinone v-4'methyl ether (compound **3**). SN6 is the unseparated mixture of compound **2** and an unknown compound and paclitaxel (Ptx) is the positive control.

The IC_{50} values were calculated based on the molecular weights of the structures of the isolated compounds. The anticancer evaluation results of the isolated compounds presented as IC_{50} in **Error! Reference source not found.** proved to be potent against the cancer cell line with the best IC_{50} values in the range of 18.05 µM and 9.045 µM. Among the isolated compounds compound **3** showed the best results inhibiting half of the cell growth with 18.05 µM. This was followed by compound **2** which inhibited half the cell growth with 67.59 µM. Compound **1** did not perform well having the highest IC_{50} (80.78µM). However, when the cancer cells were treated with the unseparated mixture of compound **2** and an unknown compound (SN6), the mixture managed to inhibit 50% of the cell growth with 9.045 µg/ml proving to be more toxic to the cancer cells compared to the individual activity of the other compounds. This may be suggestive of a synergistic effect of the two compounds, where the combination of the two compounds may affect different pathways making the treatment more effective (Cheon, 2021). A plethora of recent studies have reported the beneficial effect of the synergistic interaction of therapeutic agents, especially natural compounds as they are easily accessible and inexpensive, for treatment of multi-resistant bacterial infections or virulent malignancies like cancer (Pezzani *et al.*, 2019; Gupta, 2021; Li *et al.*, 2021; Castañeda *et al.*, 2022). This can also be

commonly found in modern medicine where cocktails of drugs are used to effectively treat multi-resistant cancer types (Gilad *et al.*, 2021).

The crude extract from the bark (B1) and fractions thereof (B2, B3 and B4) performed poorly in inhibiting the cancer cells (**Figure 26**) with the neutral fraction having effect at all on the cells. The crude extract from the bark however managed to kill over 30% of the cancer cells. It seems like there was not enough synergistic interactions within these fractions and extract to effectively inhibit the growth of cancer cells.

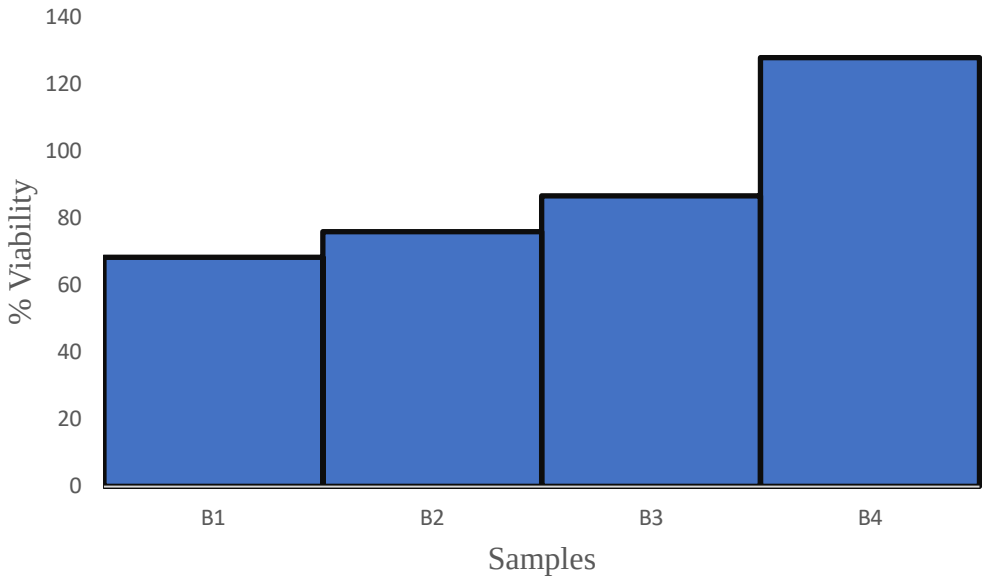

Figure 26. Anticancer activity of E. *caffra* extracts and fractions. Where B1 is the stem bark crude extract, B2 is the ethyl acetate alkaloidic fraction, B3 is the butanolic alkaloidic fraction and B4 is the neutral fraction.

2.4.2. Anti-oxidant activity

Many diseases have been linked to the overproduction of free radicals (Pham-Huy, He and Pham-Huy, 2008; Auten and Davis, 2009; Bhat *et al.*, 2015). The excessive production of free radicals and oxygen reactive species (ROS) has been found to cause oxidative stress (Lobo *et al.*, 2010; Yang *et al.*, 2011) which in consequence is linked with a variety of diseases like diabetes, Alzheimer's disease and cancer (Hussain *et al.*, 2003; Polidori *et al.*, 2007; Asmat *et*

al., 2016).Furthermore synthetic anti-oxidants have been found to be dangerous for human health and that high doses might even cause DNA damage (Lourenço, Moldão-Martins and Alves, 2019; Amarachukwu Uzombah, 2022). Consequently, the need for the use of naturally occurring anti-oxidants has greatly regarded as a safe and effective alternative to prevent ROS induced diseases.

The extracts and fractions of *E. caffra* were further evaluated for their radical-scavenging capacity and total anti-oxidant activity using DPPH; this, was done by determining the disappearance of free-radicals using a spectrophotometer. The results are presented in **Figure 27**. When conducting the anti-oxidant activity of the extracts, ascorbic acid was used as a positive control.

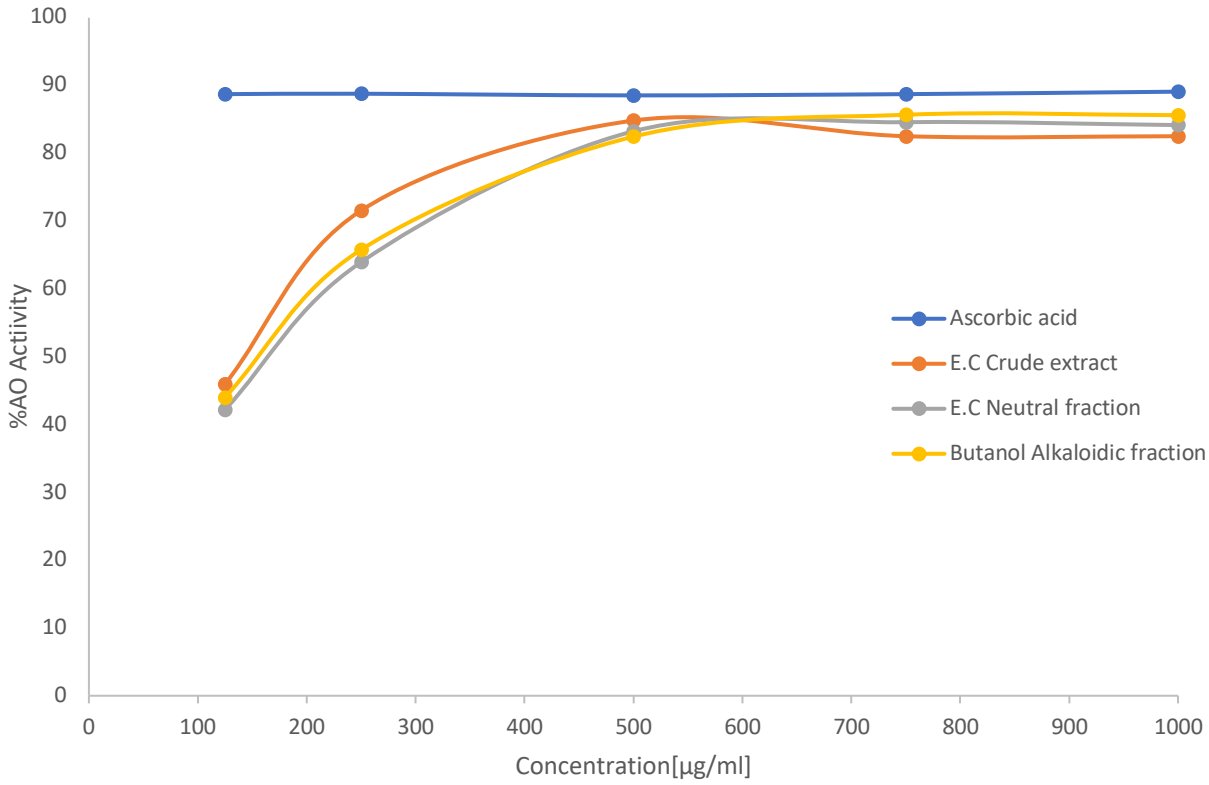

Figure 27. Anti-oxidant activity of *E.caffra* extract and fractions

The crude extract from the bark showed relatively good anti-oxidant activity as compared to the other extracts with AO_{50} (amount required to provide atleast 50% anti-oxidant activity) of 239.83 µg/mL. As the concentration of the extract and fractions increased the anti-oxidant

activity also seemed to increase. However, after the concentration at reached 500 µg/mL the activity seemed to have decreased slightly and after that it reached a plateau. This trend was observed in the extract and fractions used in the study. But this varied between extracts and fractions, for example the *n*-butanol alkaloidic fraction (B3) seemed to have a better AO_{50} of 227.05 µg/mL and had a higher plateau as compared to the other fractions and extract. It also seemed to be closer in activity to the control (ascorbic acid). This was not expected alkaloids been reported to have good anti-oxidant activity (Maiza *et al.*, 2007; Yin *et al.*, 2016; Gan *et al.*, 2017).

The same behaviour was observed in the neutral fraction which had an IC_{50} of 247.58 µg/mL and mostly consisted of flavonoids, which are also known for their anti-oxidant activity. Both these fractions display more anti-oxidant activity at high concentrations as compared to the crude extract, this might be because the fractions were highly concentrated in flavonoids and alkaloids respectively and so this causes the fractions to display more anti-oxidant activity (Kefayati *et al.*, 2017; Kiani, Arzani and Mirmohammady Maibody, 2021).

The crude extracts and fractions from *E. caffra* seem to possess promising anti-oxidant activity and might be a good alternative for preventing ROS. In addition to this, the *E.caffra* extract has displayed no cytotoxicity towards the HeLa cells (**Figure 29**) this makes it an even better alternative.

2.4.3. Anti-enzymatic: α-Amylase and α-Glucosidase

The extracts and fractions from *E. caffra* were evaluated for their enzymatic activity on *α*-amylase and *α*-glucosidase enzymes. The results of the *in vitro* experiment as percentage inhibition are presented in

Figure 28.

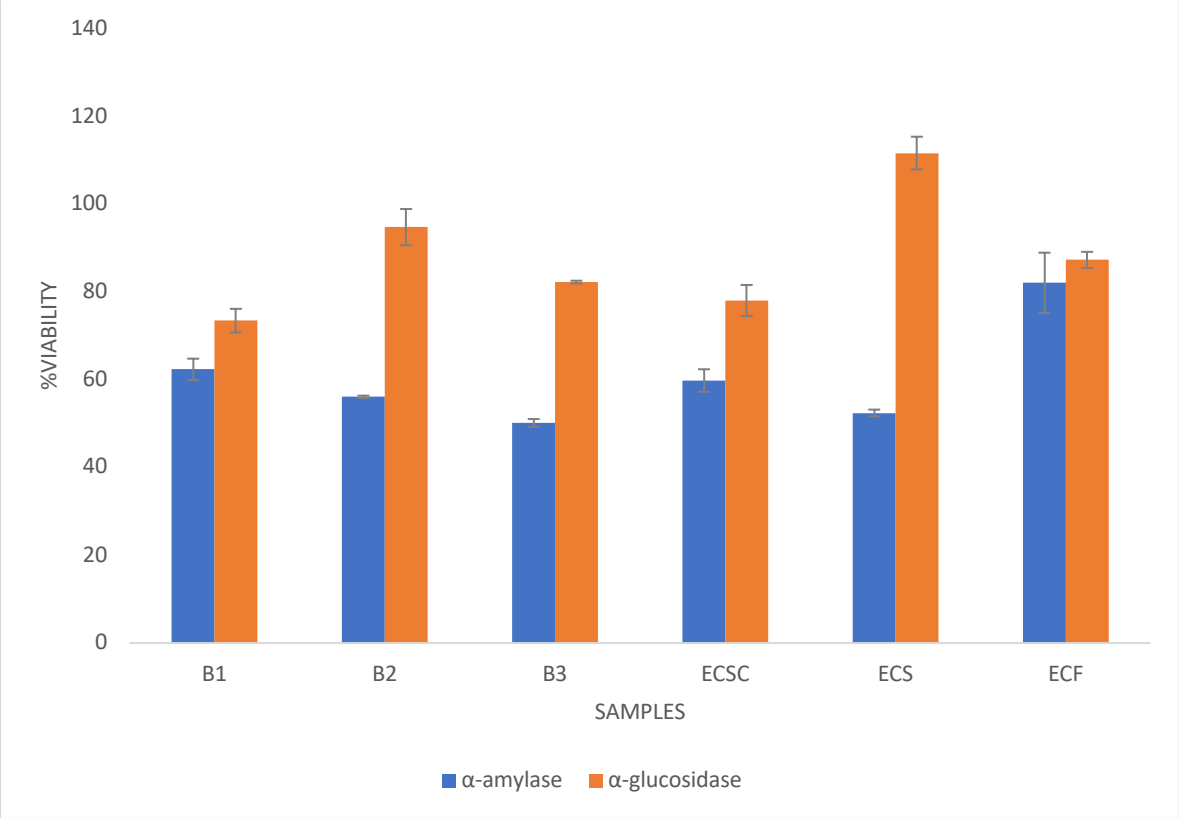

Figure 28. Enzymatic activity compound 1 and extracts from *E. caffra* on α-amylase and α-glucosidase**.** B1 represents the crude stem bark extract, B2 is the ethyl acetate alkaloidic fraction, B3 is the butanol alkaloidic fraction, ECSC is the *E. caffra* seed carp, ECS is the *E.caffra* seed and ECF is the *E. caffra* flower.

Most of the *E. caffra* extracts and fractions seemed to be good inhibitors of the *α*-amylase enzyme with the *n*-butanol alkaloidic fraction (B3) from the bark extract exhibiting promising results and inhibiting over 49% of the *α*-amylase activity. However, it showed poor results against *α*-glucosidase and only inhibited about 17% of the enzyme's activity. The crude extract from the seed (ECS) also showed promising inhibition percentage, inhibiting over 47% of the enzyme's activity, but it also showed poor results for the *α*-amylase enzyme, in fact it did not inhibit its activity at all.

This trend was observed in the extracts and fractions, they seem to inhibit the *α*-amylase enzyme relatively well but somehow, they were either not inhibiting the *α*-glucosidase or they did so to a much lesser extent. This is indicative of enzyme selectivity, in which an enzyme is more selective as to which substrate binds to it (Hedstrom, 2010).

2.4.4. Antibacterial assays and cytotoxicity

Due to the small amounts of the isolated compounds, the antibacterial assays and related cytotoxicity assay were only conducted on the *E. caffra* crude extracts and fractions. The results presented in percentage viability of the cells is reported (**Figure 29)**.

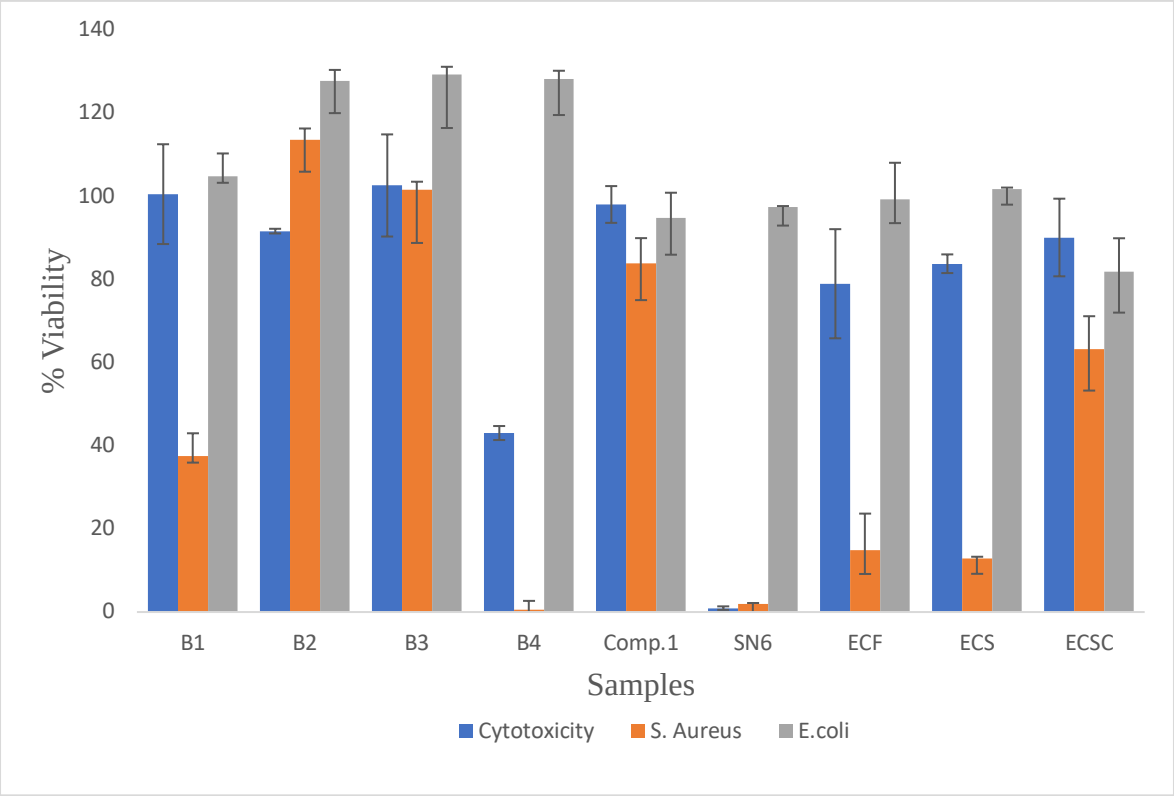

Figure 29. Effects of *E. caffra* extracts, fractions and compound **1** on *S. aureus*, *E. coli* and cytotoxicity. A 20 µM of each sample was used in each assay and viability reported in %was used to measure the activity of each sample**.** B1 represents the crude stem bark extract, B2 is the ethyl acetate alkaloidic fraction, B3 is the butanol alkaloidic fraction, B4 is the neutral fraction, compound **1** is lupeol, SN6 is an unseparated mixture, ECF is the *E. caffra* flower**,** ECS is the *E.caffra* seed, and ECSC is the *E. caffra* seed carp.

The extracts and fractions were studied for their antibacterial activity and displayed diverse degrees of inhibition activity against the tested bacteria and HeLa cells (**Figure 29**). It is evident from the results in **Figure 29** that the tested *Staphylococcus aureus* bacteria was highly susceptible to three crude extracts (B1, ECF and ECS) and two fractions from the bark extract (B4 and SN6). The percentage of viability showed that there were significant differences

between the highly active extracts and fractions. Varying degrees of cytotoxicity against the HeLa cells were displayed across all the extracts and fractions used. However, the extracts and fractions used did not show any significant activity against the bacteria *E. coli*.

Among the tested samples fraction B4 exhibited the strongest antibacterial activity against *staphylococcus aureus* (99% inhibition at 50μM). Compared to other extracts from *Erythrina* plants, this extract displayed one of the highest levels of antibacterial activity (Chitopoa *et. al.*, 2019; Sadgrove *et al.*, 2020). This fraction was the one that led to the isolation of terpenoids and flavonoids in this study, therefore the antibacterial activity displayed by this fraction can be partly attributed to the presence of terpenes and flavonoids as they have been reported to have good antibacterial activity (Chukwujekwu *et al.*, 2011; Fahmy *et al.*, 2018) . This impressive antibacterial activity however, was probably due to the synergistic effect caused by the myriad of secondary metabolites present in this fraction (Desalegn Amenu, 2014). The cytotoxicity displayed by this fraction was relatively high, reducing the viability of the HeLa cells by more than 50% at a concentration of 50 μM, this may be due to some of the flavonoids present in this fraction (Yibralign Desta *et. al.*, 2017). This fraction did not show any activity against the *E. coli* bacteria.

The results also indicated that SN6 (unseparated mixture of compound **2** and an unknown compound which was confirmed through validation via TLC) was highly bacteriostatic (a chemical agent that stops bacteria from reproducing) against *Staphylococcus aureus* inhibiting over 98% of the cell activity. This mixture displayed extremely high levels of toxicity against since HeLa cells, since this mixture is separated from the neutral fraction, the high toxicity may be due to high levels of flavonoids as it tested positive for flavonoids (**Table 4).** Researchers are highly interested in natural compound mixtures that are believed to have multiple specific targets (Aung *et al.*, 2017). This mixture also displayed extremely low inhibition for the *E. coli.* From these results, it can be seen that the further separation of the B4 fraction to obtain the SN6 mixture was detrimental to the antibacterial potential of SN6, as it did not only inhibit the bacteria cell growth very well but it also eliminated almost all of the HeLa cells. This counterproductive effect is the only factor that makes this mixture nonviable for any therapeutic consideration.

The crude extract from the seed carp (ECSC) displayed impressive antibacterial activity. It inhibited more than 80% of the *Staphylococcus aureus* cell growth at a concentration of 50 μM. It showed very little toxicity against the HeLa cells and no activity for the *E. coli* bacteria.

The crude extract from the flower (ECF) also displayed good antibacterial activity against *Staphylococcus aureus* inhibiting more than 70% of the cell growth, this extract also showed minimal damage to the HeLa cells.

The crude extract from the bark (B1) showed moderately good antibacterial activity against *Staphylococcus aureus* inhibiting over 60% of the cell growth at a concentration of 50 μM. This extract did not cause any damage to the HeLa cells. It was also not active against the *E. coli* bacteria.

The rest of the extracts either did not inhibit the bacteria cell growth or they did so poorly. They only behaved similar in the HeLa cells with some killing as many as 10% of the HeLa cells. Compound **1** also performed poorly, inhibiting less than 20% cell growth of the *Staphylococcus aureus* cells.

These results were overall satisfactory as the extracts with the best antibacterial activity were found to be ones with less cytotoxicity and relatively good antibacterial activity. These extracts were found to be potential viable candidates for therapeutic considerations (Katiyar *et al.*, 2012; Sama Fonkeng *et al.*, 2015; Elisha *et al.*, 2017; Chitopoa *et. al.*, 2019).

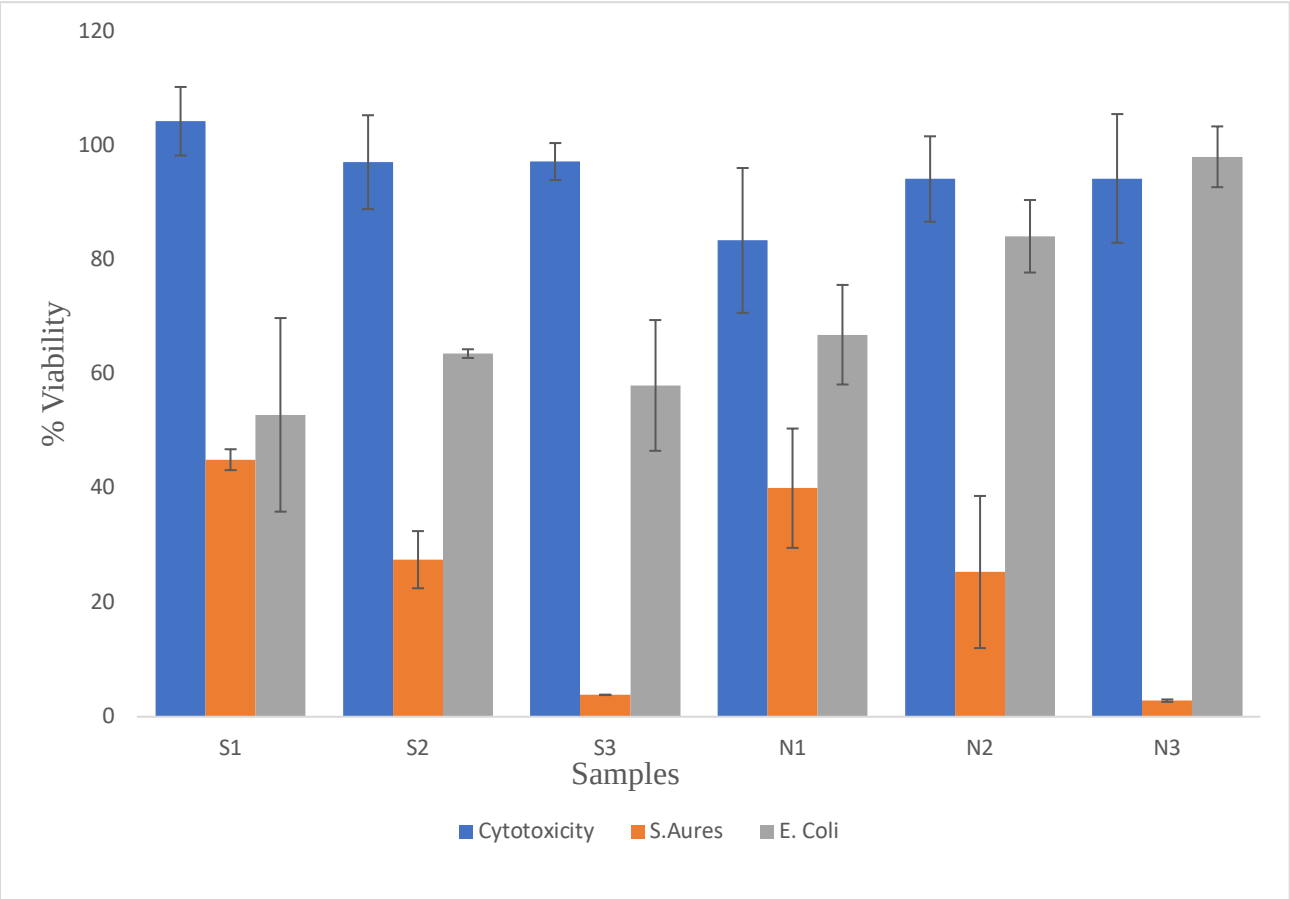

Figure 30. Effects of different concoctions from *E. caffra* extracts and fractions and on *S. aureus, E. coli* and cytotoxicity. S1 is a mixture of B4 (8 µL) and B2 (16 µL), S2 is a mixture of B4 (8 µL) and B3 (16 µL), S3 is a mixture of B4 (8 µL) and ECSC (16 µL, N1 is a mixture of B4 (50µL) and B2 (50µL), N2 is a mixture of B4 (50µL) and B3 (50µL) and N3 is a mixture of B4 (50µL) and ECSC (50µL).

The results obtained from testing antibacterial activity of the concoctions of different *E. caffra* extracts and fractions are presented in **Error! Reference source not found.**. The concoctions were prepared as outlined below. The mixtures seem to have performed exceptionally well as N3 inhibited more than 97% growth of *S. aureus* at (IC_{50} = 25µg/ml). This mixture also showed minimal damage to the HeLa cells. However, it did not show any activity against the *E. Coli*. S3 also displayed excellent activity against *S. aureus* inhibiting over 96% of the bacterial cells with reduced damage to the HeLa cells. B2, which showed no activity when tested alone against the bacterial cells, showed a remarkable change when mixed with B4 with no damage to the HeLa cells whatsoever. The same can be said about ECSC, which also had low activity against *S. aureus* but when combined with B4, displayed better activity against *S. aureus*. It is also

worth mentioning that S1 behaved remarkable better in inhibiting the *E. coli* bacterial cells inhibiting over 48% of the *E. Coli* cells, which is a feat that each fraction did not even get close to. **Figure 29** shows that both fractions B2 and B4 had no effect on *E. coli*. This trend can be observed through the mixtures in **Error! Reference source not found.**.

From the results on **Error! Reference source not found.**, it can be seen that combining the extracts and fractions from different parts of *E. caffra* is not only effective in enhancing the activity of the mixture against a specific bacterium but can also significantly decrease its cytotoxicity, increasing its likelihood for practical therapeutic uses. To the best of our knowledge, this approach has not been tried before on *E. caffra*.

2.5. Molecular networking

The *E. caffra* bark crude extract, the fractions, as well as the seed seed extract were analysed using RP-LC-ESI-MS/MS. The resulting data were processed through a feature-based molecular networking workflow providing an overview of similarity between the MS^2 spectra of all detected ion features as well as a list of library matches to public repository spectra. The finished GNPS (https://gnps.ucsd.edu/ProteoSAFe/status.jsp?task=a773a662ce054e809045b29351a829a4) was visualized in Cystoscape (Ver 3.9.1). The nodes in the molecular network were organized into seven groups (A-G) based on molecular connectivity.

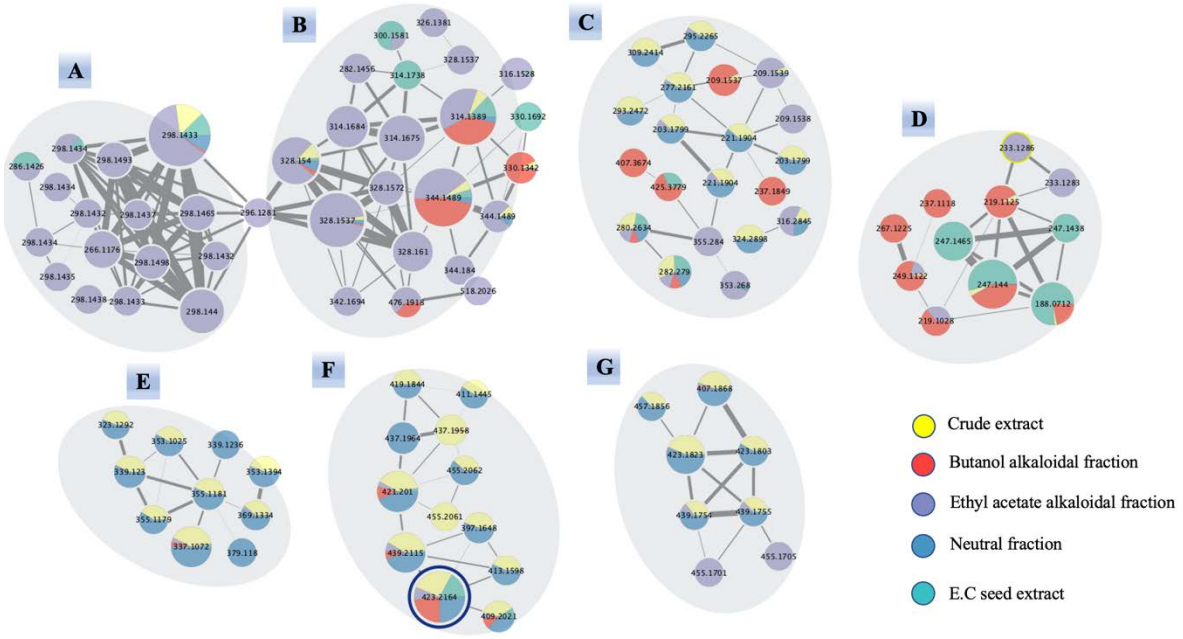

Figure 31. Clusters of interest of the feature-based molecular network of two chemically distinct extracts and fractions from *Erythrina caffra*. The putative annotations are as follows: (A) Isoquinoline alkaloids and Isoflavonoids; (B) Isoquinoline and amide derivatives; (C) Sesquiterpenes and triterpenoids; (D) Indole alkaloids; (E) Carpachromenes; (F) Isoflavonoids and flavonoids; (G) Prenylated flavanones. Node contributions correspond to peak area per sample. Increasing node size corresponds to greater peak area averaged across all extracts and fractions. Increasing edge width indicates greater spectral similarity. Isolated compounds are indicated by a blue border.

Group A: Isoquinoline alkaloids and Isoflavonoids

Group A of the molecular network in **Error! Reference source not found.** consists of features annotated as analogs of dehyrdronuciferine (*m/z* 298.1433) with the mass difference of ≈ +4 a.m.u. to the parent compound most likely being due to substitution of one carbon with an oxygen resulting in $[C_{18}H_{20}NO_3]^+$ (-3.42 ppm). Interestingly, there haven't been any prior reports on the isolation or identification of dehydronuciferine or closely related analogs from

this source. All the features in this group were dominated by contributions from the alkaloidic fraction (B2), which is consistent with the nature of the fraction. The main feature in this group had small contributions from the crude extract (B1), the seed extract (EC seed), *n*-butanol alkaloidic fraction (B3) and the neutral fraction (B4). In addition, the feature at *m/z* 266.1176 was matched to 6,7-dimethoxy-1-phenyl-3,4-dihydro-isoquinoline and annotated as a desaturated analog ($[C_{17}H_{16}NO_2]^+$, -1.89 ppm) **Error! Reference source not found.**.

Isoquinoline alkaloids from the genus *Erythrina* have been studied before (Rambo *et al.*, 2019), however there haven't been any prior reports on the isolation or identification of dehydronuciferine or closely related analogs. The nodes of group A and B are connected to each other by the feature at *m/z* 296.1281 (putatively $[C_{18}H_{18}NO_3]^+$, -1.92 ppm), however, a spectral match to library entries was not found for this feature.

Group B: Isoquinoline and amide derivatives

The features in group B are related to those of group A and appear to be distinguished by the additional presence of C and O atoms. The feature at *m/z* 314.1389 ($[C_{18}H_{20}NO_5]^+$, -1.06 ppm) was matched to 6,7-dimethoxy-1-phenyl-3,4-dihydro-isoquinoline (**Error! Reference source not found.**), similarly to the feature at *m/z* 266.1176 in group A (**Figure 39**). Furthermore, the feature at *m/z* 344.1489 (putatively $[C_{19}H_{22}NO_5]^+$, -2.61 ppm) produced an analog match to 4-epivulgarin ($[C_{15}H_{21}O_4]^+$), suggesting some shared structural motifs.

Group C: Sesquiterpenes and triterpenoids

In this cluster a feature at *m/z* 209.1539 ($[C_{13}H_{21}O_2]^+$, -2.18 ppm) was matched to costunolide ($[C_{15}H_{21}O_2]^+$, sesquiterpene lactone) with a mass difference of -24.00 amu (**Error! Reference source not found.**). Another feature at *m/z* 203.1799 ($[C_{15}H_{23}]^+$, -0.37 ppm) was annotated as a derivative of bisabolol ($[C_{15}H_{27}O\text{-}H_2O]^+$, sesquiterpene) with a mass difference of 2.02 amu to the precursor *m/z* of the library entry (in source dehydration suspected) (**Error! Reference source not found.**). The features at *m/z* 309.2414 ($[C_{19}H_{33}O_3]^+$, -5.08 ppm) and *m/z* 295.2265 ($[C_{18}H_{31}O_3]^+$, -2.78 ppm) were annotated as derivatives of linoleic acid ($[C_{18}H_{31}O_2]^+$, omega-3 fatty acid), respectively. Another feature at *m/z* 221.19 was annotated as carophyllene epoxide with an exact match ($[C_{15}H_{25}O]^+$, -2.44 ppm) (**Error! Reference source not found.**). The feature at *m/z* 425.3779 ($[C_{30}H_{49}O]^+$, -1.04 ppm) was matched to the triterpenoid allobetulinol ($[C_{29}H_{50}O_2\text{-}H_2O]^+$), while the neighbouring feature at *m/z* 407.3674 ($[C_{30}H_{47}]^+$, -

0.92 ppm) was matched to the tritepenoid uvaol ($[C_{30}H_{51}O_2]^+$) (**Error! Reference source not found.**). Both these features were most abundant in the *n*-butanol alkoidic fraction.

Group D: Indole alkaloids

This cluster is mostly dominated by features that were annotated as indole alkaloids. The feature at *m/z* 219.1125 ($[C_{12}H_{15}N_2O_2]^+$, -3.89 ppm) was annotated as abrine. This feature was an exact match and abrine and its derivatives are very common among *Erythrina* species (Harborne, 1993; Kestwal and Bhide, 2007; El-Masry *et al.*, 2010b). Contributions to this feature are exclusively from the crude extract and the alkaloidic fractions (B2 & B3), this is consistent with the nature of the fractions. This annotated tryptophan derivative had a dominant product ion at *m/z* 118.06 corresponding to the loss of the branch ($-C_3H_5NO_2$). A reference spectrum for abrine (**Figure 40**) was found to have 15 shared peaks (cosine 0.85) with the detected spectrum.

Group E: Carpachromene derivatives

This group was found to consist of carpachromene derivatives, the feature at *m/z* 337.1072 ($[C_{20}H_{17}O_5]^+$, -1.18 ppm) was matched to carpachromene with 193 shared peaks (cosine 0.87). All the features in this group had contributions only from the crude extract and the neutral fraction (**Error! Reference source not found.**).

Group F: Isoflavonoids and flavonoids

The features in this group were annotated as isoflavonoids and flavonoids. Importantly, putative flavonoids were detected in all samples. The feature at *m/z* 419.1844 ($[C_{23}H_{27}O_5]^+$, -3.46 ppm) was annotated as a derivative of kuwanon E ($[C_{25}H_{29}O_6]^+$). The reference spectrum of kuwanon E (**Error! Reference source not found.**) was found to share many peaks, but most importantly showed a dominant product ion at *m/z* 179.03 which matches the neutral loss of 5,7-dihydroxychroman-4-one. Almost half of the contributions on this feature were from the crude extract (B1) and from the neutral fraction (B4). All the other features on this cluster were annotated as isoflavonoids and flavonoid derivatives with a majority of the contributions coming from the crude extract and neutral fraction which is consistent with the previous reports (Andayi *et al.*, 2006; Kuete *et al.*, 2014).

The feature at *m/z* 423.2164 ($[C_{26}H_{31}O_5]^+$, -1.77 ppm) was identified as the isolated abyssinone V 4'-methyl ether. This annotation was corroborated by spectral matching to reference fragmentation spectra obtained from isolated compound material (**Error! Reference source not found.**). This feature was detected in all the samples with large contributions from the neutral fraction (B4) which is consistent with the nature of this fraction as this compound was isolated from the neutral fraction. The fragmentation spectrum of the *m/z* 423.2164 node was found to exhibit similar product ion distributions with major neutral loss corresponding to $C_9H_7O_4$ (*m/z* 179.03), this feature also showed a more pronounced *m/z* 153.02 fragment. Similarly, the feature at *m/z* 439.2115 ($[C_{23}H_{31}O_6]^+$, -1.28 ppm) corresponds to the isolated burttinone.

2.6. Docking studies

2.6.1. Docking results for isolated compounds

All three compounds isolated from the bark of *E. caffra* in this study were docked against different proteins including plasmodium falciparum protein, human estrogen receptor and epidermal growth receptor (Error! Reference source not found.**,** Error! Reference source not found. **and Figure 34)** and their docking scores were obtained and reported below. Their pharmacokinetic properties were accessed and reported in

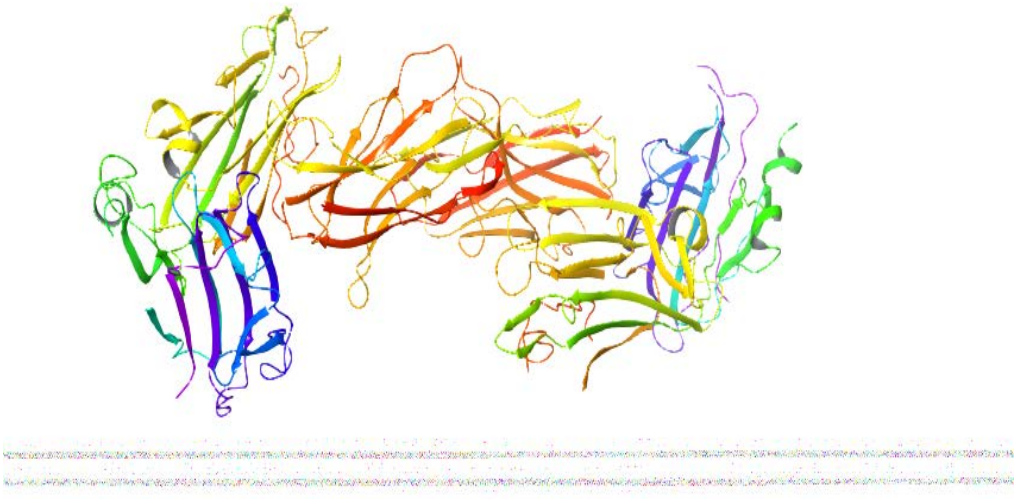

Figure 32. The 3D representation of the protein (7KJH) plasmodium falciparum protein Pf12P bound to nanobody B9

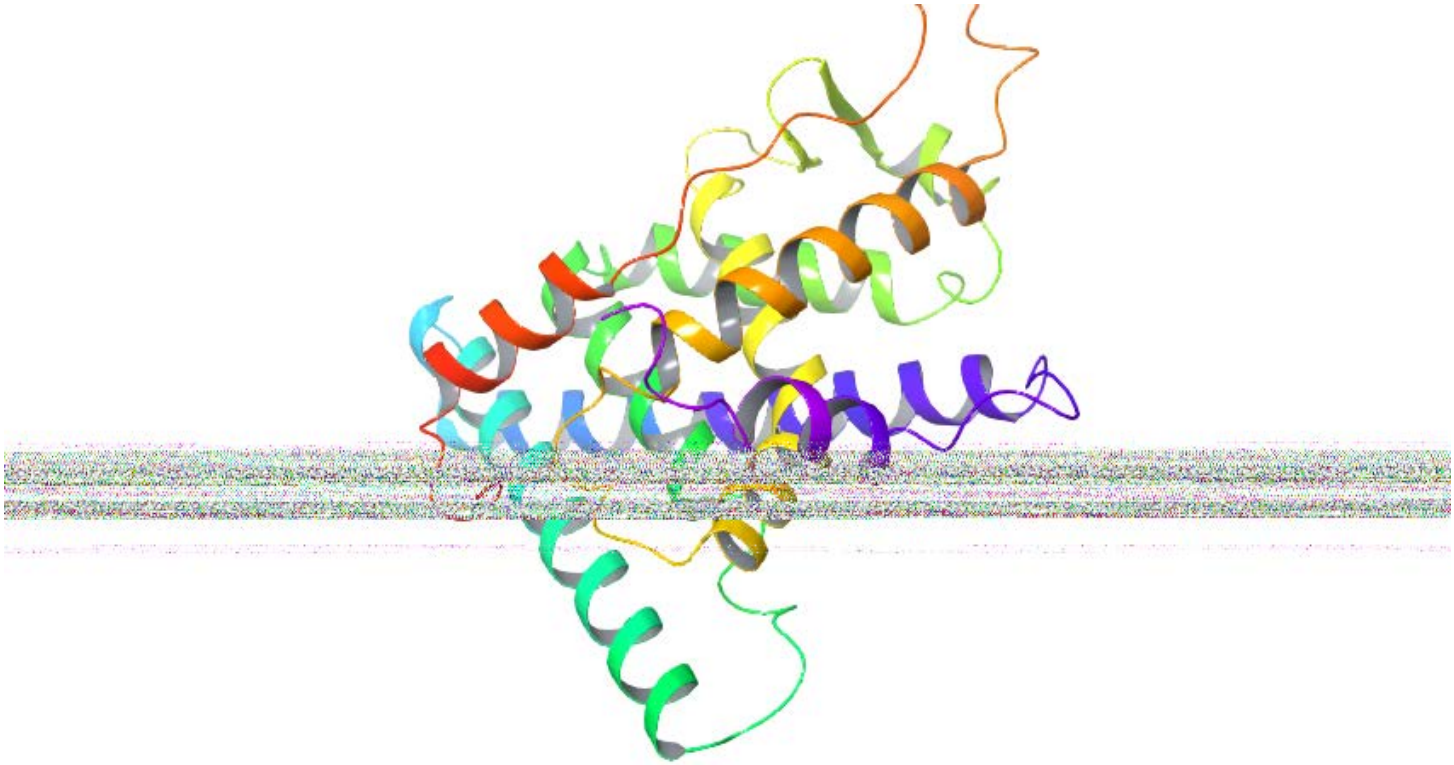

Figure 33. The 3D representation of the protein (ID:3ERT) human estrogen receptor

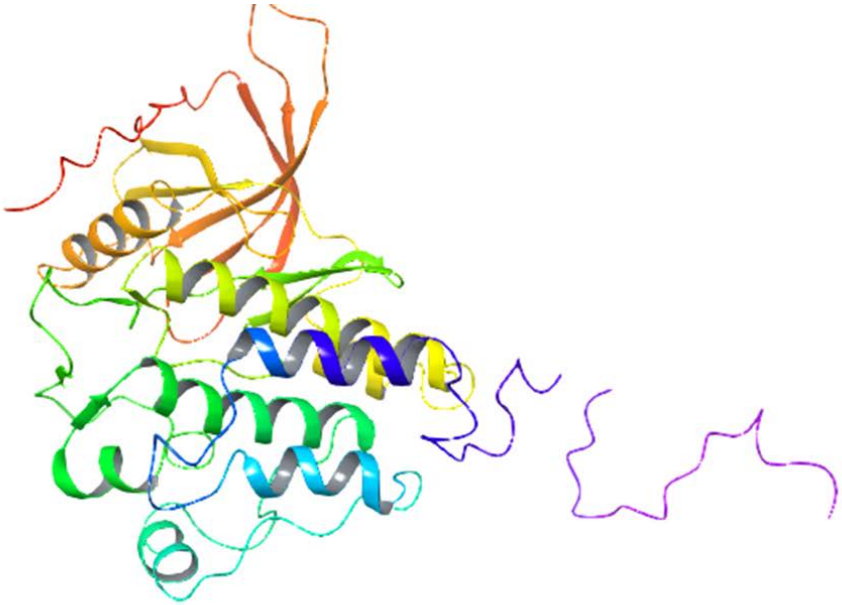

Figure 34. The 3D representation of the protein (ID:1M17) Epidermal growth factor receptor tyrosine kinase domain with 4-anilinoquinazoline inhibitor erlotinib.

Table 12. Docking results for isolated compounds docked into protein *Plasmodium falciparum* protein pf12p (PDB ID: 7kjh)

Compounds	**Docking score (Kcal/mol)**	**Glide emodel (Kcal/mol)**	**Glide energy (Kcal/mol)**
Abyssinone 4-V' methyl ether	-4.4	-56.8	-45.1
Lupeol	-3.6	-57.4	-42.8
Stigmasterol	-3.5	-45.3	-37.6

The results reported in **Table 12** were obtained from *in silico* docking of the compounds with *Plasmodium falciparum* protein (7KJH). The three compounds were individually prepared for docking using the method outlined in Docking procedures **3.7,** the Abyssinone V'4-methyl ether was found to be the best compound which had the lowest energy conformations with docking score of -4.4 kcal/mol when docked into the protein (7KJH) *Plasmodium falciparum* protein pf12p bound to nanobody b9. The binding affinity of the complexes formed between the compounds and the proteins are shown in **Table 12**. The binding affinities range from -3.5 to -4.4 kcal/mol. The more negative the docking scores, the more the ligand is favourable and forms the most stable complex, this is shown by Abyssinone V' 4-methyl ether molecule with the docking score of -4.4 kcal/mol. The least binding molecule is shown by the one which is the least negative, stigmasterol with the docking score of -3.5 kcal/mol. Abyssinone V' 4-methyl ether was found to be best compound to inhibit this protein.

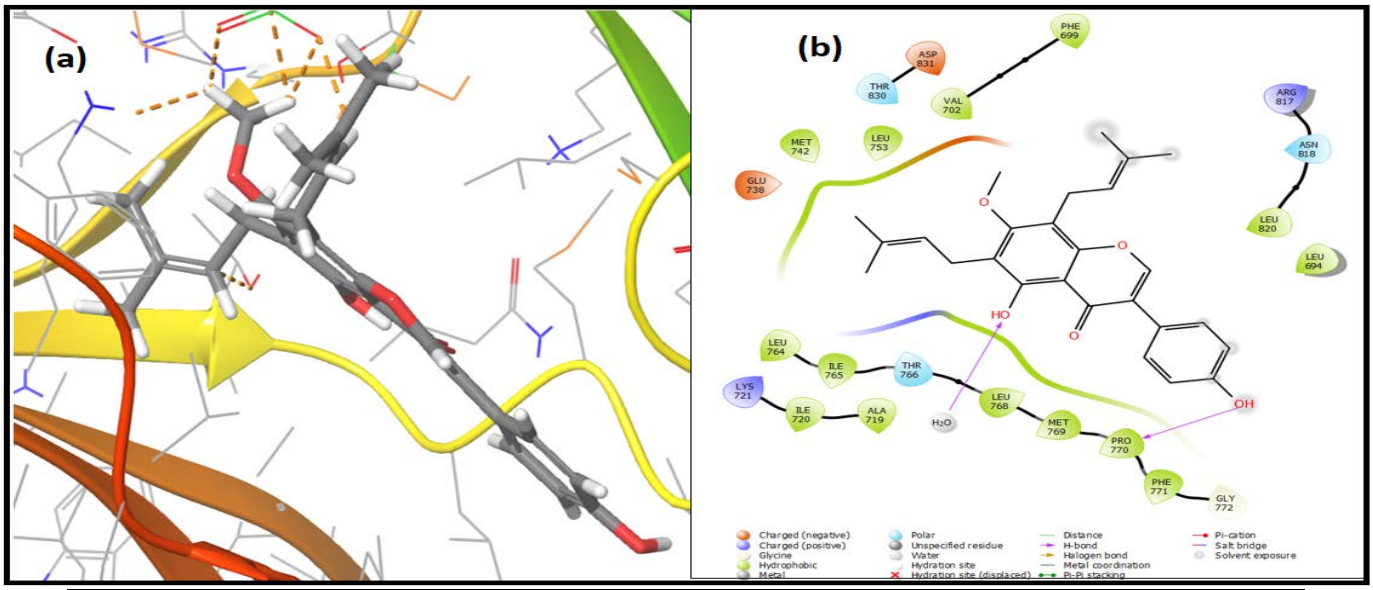

Figure 35. 2D representation of the interaction of the protein (1M17) Epidermal growth factor receptor tyrosine kinase domain with 4-anilinoquinazoline inhibitor erlotinib and the best binding inhibitor

Table 13. Docking results for compounds docked into protein (1M17) Epidermal growth factor receptor tyrosine kinase domain with 4-anilinoquinazoline inhibitor

The results reported in **Table 13** were obtained from *in silico* docking of the compounds with epidermal growth factor receptor (1M17). The four compounds were individually prepared for docking using the method outlined in Docking procedures below **3.7.** Stigmasterol was found to be the best compound as it had the low energy conformations with docking score of -3.788 kcal/mol when docked into the protein Epidermal growth factor receptor tyrosine kinase domain (1M17) which is a protein that is expressed in some types of cancers. The binding energy of the complexes formed between the compounds and the proteins are shown in **Table 13**. The binding energies range from -2.3 to -3.788 kcal/mol. The more negative the values, the

more the ligand is favourable and forms the most stable complex, this is shown by stigmasterol molecule with the docking score of -3.788 kcal/mol. The less binding molecule has the least negative docking value, lupeol with the docking score of -2.3 kcal/mol. Stigmasterol was found to be best compound to inhibit this protein.

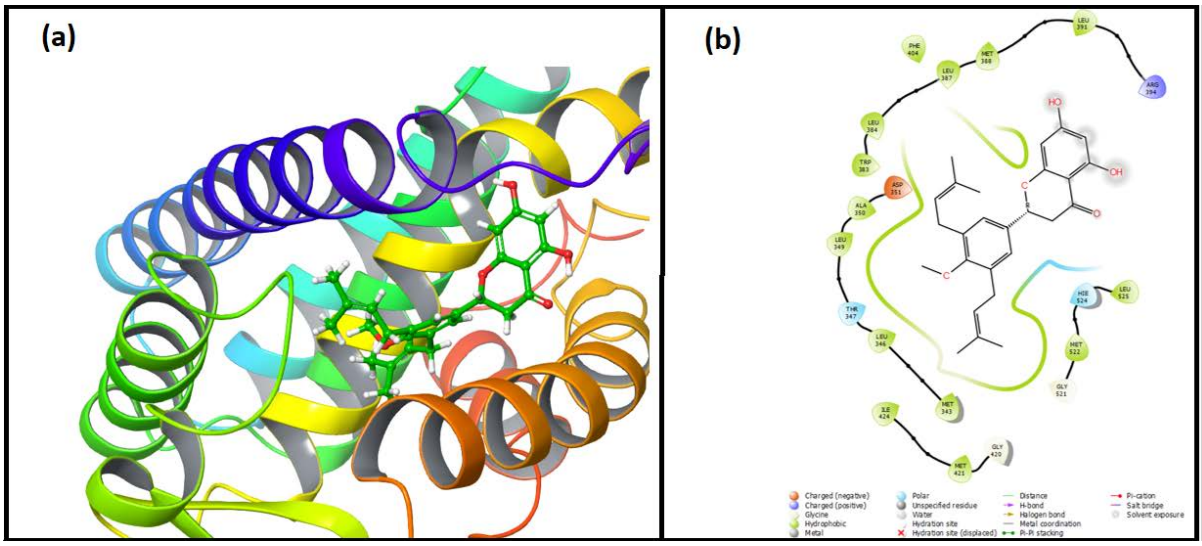

Figure 36. 2D representation of the interaction of the protein (3ERT) human estrogen receptor and the best binding inhibitor, Abyssinone 4 V'-methyl ether

Table 14. Docking results for compounds docked into protein (ID:3ERT) human estrogen receptor

Compounds	**Docking score (Kcal/mol)**	**Glide emodel (Kcal/mol)**	**Glide energy (Kcal/mol)**
Abyssinone 4 V'-methyl ether	-6.6	-28.7	**-27.5**
Lupeol	-3.4	-23.0	**-29.1**
Stigmasterol	-2.2	-31.7	**-32.0**

The results reported in **Table 14** were obtained from *in silico* docking of the compounds. The compounds were individually prepared for docking using the method outlined in **3.7** the best compound was found to have the low energy conformations with docking score of -4.027 Kcal/mol when docked into protein (ID:3ERT) human estrogen receptor which is a receptor that is expressed in some ER positive cancers. The binding energy of the complexes formed between the compounds and the proteins are shown in **Table 14**. The binding energies range from -2.2 to -6.6 Kcal/mol. The more negative the values, the more the ligand is favourable and forms the most stable complex, this is shown by Abyssinone V 4'-methyl ether molecule with the docking score of -6.6 kcal/mol. The less binding molecule has the least negative

docking value which is stigmasterol with the docking score of -2.3 kcal/mol. Abyssinone 4 V'-methyl ether was found to be best compound to inhibit this protein. These results seem to be in correlation with the *in vitro* anticancer studies in **Error! Reference source not found.** even though the type of cancer cell line used was a triple negative cancer.

2.6.2. Adsorption Distribution Metabolism Excretion Toxicity (ADMET) results

In drug design, the desired drug properties need to be checked before the compounds are taken further in the drug discovery pipeline. With this in mind, the ADMET predictions for the structures were assessed using the Qikprop module (v3.1, Schrödinger 2021-1) to predict their drug-like behaviour. The toxicity and synthetic accessibility were investigated. After the compounds were prepared by LigPrep (v3.1, Schrodinger 2021-1) they were exported to Qikprop. They were utilized for the calculations of pharmacokinetic parameters and the remarkable descriptors and pharmaceutically important properties of all the structures such as molecular weight, number of hydrogen bond donors (HBD), number of hydrogen bond acceptors (HBA), Human intestinal absorption, percent Human oral absorption, blood-brain partition coefficient (QPlogBB), Caco-2 Cell permeability (QPPCaco), Human serum albumin, MDCK(Madin Darby canine kidney cells) and the parameters of Lipinski's rule of 5 were assessed.

Table 15 shows the results of the ADMET predictions which were assessed using Qikprop v3.1. Generally, an orally active compound should not have more than three violations of the Lipinski rule. The isolated compounds presented in **Table 15** were found not to violate the rule more than three times, hence this indicates that they had good drug likeness properties. Most of the compounds seem to violate one rule except burttinone. This compound was found to be the most likely to be orally active compound. The molecular weights of the compounds were found to be less than 500 g/mol. The blood-brain partition coefficient (QPlogBB) was also low ranging from -1.837 to 0.128 suggesting that they will have less potential to cross the blood brain barrier, this indicates that any CNS-related toxicity would be reduced (Matondo *et al.*, 2022). The results obtained were within the acceptable range (< 0.90ml/g) (Thalman *et al.*, 2019) and this indicated that they are likely to be orally active compounds. The Human intestinal absorption had a value of 1 which further corroborates the remarkable oral bioavailability of the compounds.

The human oral absorption was 100% except for the Abyssinone V 4'-methyl ether. The Caco-2 cell permeability (QPPCaco), a model for gut-blood barrier which is a prediction for non-active transport was greater than 500 and this indicates outstanding results for good intestinal absorption. Commercial drugs such as dopamine and serotonin are CNS negative because they are too polar to cross the blood-brain barrier (Khan *et al.*, 2019).

For a drug to be clinically approved one of the parameters that is checked is the aqueous solubility parameter (QPlogS) and the acceptable value for this parameter is <0.5. The isolated compounds were found to be in the range of -7.8 to -7.1. The accepted range for the predicted skin permeability is -8.0 to -1.0, and the isolated compounds showed excellent predicted skin permeability values that ranged from -1.9 to -3.7. Furthermore, the prescribed range for the human serum albumin binding (QPlogKhsa) is -1.5 to 2.0, and the isolated compounds were reported to have values in the range 1.1 to 1.8. MDCK cell permeability also showed favourable results with values that fall within the prescribed range of 500 and 50 nm/sec(Irvine *et al.*, 1999; Hosey and Benet, 2015)

Chapter 3. Experimental

3.1. Materials and equipment

n-Hexane, petroleum ether (PE) supplied by Holpro analytics division, ethyl acetate (EtOAc), methanol (MeOH)) and *n*-butanol (*n*-BuOH) were supplied by MINEMA chemicals (Pty) Ltd., Dichloromethane (DCM) and deuterated chloroform ($CDCl_3$) were supplied by Sigma-Aldrich Chemie GmbH, Germany. These solvents were used in this research project for the extraction and isolation processes and as the mobile phase for thin layer chromatography (TLC) as well as in bioassay and NMR experiments. Acetone, which was supplied by Merk chemicals (Pty) Ltd, was mainly used to clean the apparatus as well as to wash samples. The hexane was further distilled in the Chemistry Department Laboratory at Rhodes University and the other solvents were used as received unless specified.

Column chromatography was used to separate compounds. Various sizes of columns ranging from 10 to 40 mm in diameter were used. Silica gel used was: technical grade, pore size 60 Å, 70-230 mesh, 63-200 μm supplied by Sigma-Aldrich Chemie GmbH, Germany. This was used as a stationary phase with a small layer of acid-washed sand supplied by Minema Chemicals (Pty) Ltd added on top to help protect the packed silica in the column. Various samples and fraction were concentrated using Büchi Rotavapor R-205.
Pre-coated TLC sheets (ALUGRAM® Xtra SIL G/UV_{254} with the layer of 0.20 mm silica gel 60 with fluorescent indicator UV_{254} (20 x 20 cm) supplied by Macherey-Nagel GmbH & Co. KG company from Germany), were used to run the TLC. An ultraviolet (UV) lamp, model CM-10A with short and long-wavelength UV of 254 and 365 nm respectively were used to visualise and observe the plate. Dragendorf's reagent was used to identify alkaloids in the alkaloidic fractions.An acid spray was used to view spots that were not visible under UV light.

NMR experiments were run on a Bruker 600 MHz and 400MHz NMR spectrometer and were referenced using the following residual protonated solvent signals: ^{1}H NMR chemical shift: 7.26 ppm for $CDCl_3$, ^{13}C NMR chemical shift: 77.00 ppm for $CDCl_3$ (Gottlieb *et. al.*, 1997). A Perkin-Elmer FT-IR Spectrum 100 spectrometer was used to run the IR spectra and Bruker Compact QToF mass spectrometer using an electrospray ionization probe (Bruker, Bremen, Germany) coupled to a Dionex Ultimate 3000 chromatogram from Rhodes University was used

to record the mass spectra. Melting points of the isolated compounds were measured using a Reicheter 281313 apparatus.

3.2. Experimental methods

3.2.1. Plant collection and extraction

The plant materials (stem bark, flower, seed and seed carp) were collected at Rhode University, behind the information technology (IT) Department building (Struben building) on the 2nd of December 2014. The plant was identified by Mr. Tony Dold a Botanist/Curator from the Selmar Schonland Herbarium (GRA), located inside the Albany Museum, where a voucher specimen of *E. caffra* (1xaviersiwenoundou/GRA) was deposited.

The plant materials were dried at ambient temperature and finely ground. Extraction was performed by maceration for 72 hours at room temperature with six different solvents (*n*-hexane, $CHCl_3$, EtOAc, MeOH, EtOH and H_2O) respectively.

3.2.2. Alkaloids extraction using acid-base method

A sample (20.795 g) of the crude extract from the bark (ECS-MeOH) which was renamed as B1, was grinded, powdered and suspended in distilled water (50 mL) and was sonicated for 30 minutes to improve the interaction between solvent and plant material and enhance mass transfer from the plant material. It was further treated with sulphuric acid (until pH = 2) and partitioned with ethyl acetate (100 mL). The organic layer was separated using a separatory funnel to afford a neutral ethyl acetate fraction (B4). The resulting aqueous layer was treated with potassium hydroxide (until pH = 9) and partitioned with ethyl acetate (100 mL) three times that yielded the basic ethyl acetate alkaloidic fraction (B2) after extraction of organic layer through a separatory funnel. The fraction was collected and concentrated under reduced pressure in a rotary evaporator to yield 154 mg of the basic ethyl acetate fraction. In addition, the remaining aqueous layer was partitioned with *n*-butanol (100 mL), repeated three times to afford the *n*-butanol alkaloidic fraction (B3). The *n*-butanol fraction (B3) obtained after being dried was 160.6 mg (**Table 3**).

3.3. Fractionation of crude extract and purification

3.3.1. Purification of the neutral fraction

A portion of fraction B4 (4 g) was purified via column chromatography and the 25 subfractions collected were combined into eight subfractions based on their retention factor. The third

fraction (S3), fourth (S4) and fifth (S5) subfractions were combined as they had the same profile (i.e., same spots). The combination of these fractions was called subfraction A (SA) with a mass of 0.9988 g. The ratio of the solvent system used to elute the column was P.E: EtOAc (9:1), the first subfractions collected (SA1 and SA2) were yellow in colour. Only 8 subfractions were collected from this column (SA1 to SA8). The TLC plates of these fractions showed various colours which are characteristic of different classes of compounds. This was achieved by spraying the developed TLC plate with a spray reagent and heating it at 105°C. Since there was a small amount of SA1 and it did not show any dominant characteristic colours, this fraction was not chosen for further purifications.

SA2 which is the second subfraction from SA was further purified by gradient elution using column chromatography. A column chromatography of SA3 was also conducted using gradient elution. This column afforded a mixture of the two spots which was combined and was given a generic name SA3-Mx with a mass of 129.5 mg.

TLC was used to check the presence of compounds throughout the extraction and isolation processes. The TLC plates of the non-alkaloidic fractions were first viewed under short wavelength UV of 254 nm and long wavelength UV of 365 nm. The spots that observed under UV were marked. To observe the spots that were not visible under UV the TLC plates of the fractions were then sprayed with an acid solution. This 1:1 solution was prepared by combining 98% of sulphuric acid with water (Arramon *et al.*, 2002). The TLC plate was heated at 105 °C after being sprayed with the acid solution. The same method was followed for the alkaloidic fractions (B2 and B3), after the TLC plates of the alkaloidic fractions were observed under UV they were subsequently sprayed with a dragendorf's reagent for the identification of alkaloids. A positive test is indicated by an orange spot and a negative test is indicated by the absence of an orange spot. The dragendorf's reagent was prepared by mixing a solution of 0.8 g bismuth nitrate pentahydrate in 40 mL of distilled water and 10 mL of glacial acetic acid and a solution of 8.0 g potassium iodide in 20 mL of distilled water (Abdul-Hameed *et al.*, 2021).

SA2 was further purified by gradient elution using column chromatography. This column was started with 195 mg of SA2, it was first eluted with 100% Petroleum ether to elute any non-polar compounds in the sample. This was followed by a series of increasing polarity until all the compounds were eluted. A total of 141 subfractions were pooled based on their TLC profiles to give 4 different compounds. This allowed the successful isolation of the target compound SA2-Prp which weighed 17.1 mg although the quantities of the other compounds isolated were too small to analyse, so more attention was placed only on one compound (i.e., SA2-Purp or compound **1**). The subfractions were collected in 6.9 mL vials and the isolated

compound was characterized. The class of compounds isolated was confirmed by spraying the TLC with an acid spray and compound 1 showed a purple colour. This is indicative of steroids. The TLC plate for the fraction SA3 had two dominant spots which showed an orange and black colour after being sprayed with an acid solution and heated at 105°C; these colours are characteristic of flavonoids and terpenoids. SA3 (286 mg) was purified via column chromatography. Elution of the non-polar/less polar compounds was accomplished by using, 100% P.E. The column was continued with increasing polarity using the solvent system P.E: EtOAc. The column also afforded 129 mg of a mixture of the orange and black spots; this mixture was named SA3-Mx.

SA3-Mx (125.2 mg) was dry loaded into a column chromatography and further purified and eluted with gradient elution using P.E: EtOAc (1:0-10:1). This column afforded SA3-Mx-Blk (compound **2**) which showed a black spot. This compound was concentrated, dried, and weighed 21.3 mg. This compound was characterized using spectroscopic techniques (NMR, IR and MS)

Preparative thin layer chromatography (PTLC) was used to conduct the rapid separation of SA4. The PTLC was prepared by mixing silica gel and a small amount of calcium sulphate with water. The mixture was spread as a thick slurry on a 20 cm x 20 cm clean glass plate. The resulting coated plate was dried and activated by heating in an oven for 30 minutes at 110°C. A line was drawn at the bottom of the PTLC plate (Sherma and Fried, 1987). The sample was carefully spotted on top of the line. To develop the PTLC a mobile phase consisting of the solvents DCM: EtOAc (9:1) was used which gave good separation between the compounds of interest. The PTLC plate was developed and then allowed to dry and observed under UV_{254}. The region of interest was marked, scrapped off, dissolved in DCM, filtered, and concentrated with a rotary evaporator and allowed to dry. The compound obtained was named SA4-Or (compound **3**) and yielded a mass of 65.2 mg.

All isolated compounds were air-dried, weighed, and IR, NMR, and MS experiments were carried out on each one of them. The melting point of each compound was also taken. The phytochemical tests were performed on all extracts, fractions and some compounds. The unsaturation index or index of hydrogen deficiency for each compound was calculated (Zhang *et al.*, 2014).

3.4. Phytochemical screening

3.4.1. Tests for alkaloids

The following methods are used to test the presence of alkaloids in an extract.

(a) Dragendorf's test

A dragendorf's reagent is prepared as follows:

A small amount of bismuth nitrate pentahydrate (0.85 g) is dissolved in 40 mL of distilled water (solution A). Solution A is mixed with 10 mL of glacial acetic acid to make solution B. To prepare solution C 8.0 g of potassium iodide is dissolved in 20 ml of distilled water. Solution B is then mixed with solution C (dragendorf's, solution D). A few drops of the dragensdorf reagent (solution D) are then added to 1 mL of extract. The formation of an orange precipitate indicates the presence of alkaloids (Pandey and Tripathi, 2014; Raal *et al.*, 2020)(Abdul-Hameed *et al.*, 2021)

3.4.2. Test for terpenes

To test for presence of terpenes in an extract 0.5 mL of chloroform is added to 1 mL of the extract followed by a few drops of concentrated sulphuric acid, a reddish brown precipitate indicates the presence of terpenoids in the extract (Rami, Sipai and Patel, 2013).

Another test for terpenes is the Liebermann-Burchard's test, this test is done by mixing 2 mg of the extract with 1 mL of acetic anhydride in a glass vial. The mixture is heated until it boils then cooled in ice. A few drops of concentrated sulphuric acid are added along the sides of the vial. A pink colour indicates the presence of terpenoids (Xiong, Wilson and Pang, 2007).

3.4.3. Tests for phenols

There are different methods that can be followed to test for aromatic compounds in an extract. Generally, the extract can be dissolved in 5 mL of distilled water followed by a few drops of neutral 5% ferric chloride solution. A dark green colour indicates the presence of aromatic compounds (Wankhar *et al.*, 2015). To test for flavonoids, 4 mL of the extract is mixed with 1.5 mL of 50% methanol solution then warmed. To the warmed solution magnesium ribbon is added followed by a few 5- drops of concentrated hydrochloric acid. A red colour indicates the

presence of flavonoids and an orange colour indicates the presence of flavones (Saikia *et al.*, 2013).

3.4.4. Test for flavonoids

About 1 g of the crude extract is dissolved with 100 ml of methanol. Then 1 ml of the stock solution is placed in a test tube and added a few drops of NaOH solution. An intense yellow colour appeared in the test tube. Upon adding a few drops of diluted acids, the solution turns colourless this indicates the presence of flavonoids (Hossain *et al.*, 2013).

3.4.5. Liquid chromatography-mass spectrometry analysis and identification methods

The analysis of the crude extracts, fractions and isolated compounds from the stem bark was carried out in LC-MS/MS mode with a Dionex UHPLC (Thermo Fisher Scientific, Sunnyvale, CA, USA) equipped with a Kinetex polar C-18 column (3.0 × 100 mm, 2.6 µm; Phenomenex, Torrance, CA, USA) at a flowrate of 0.300 mL/min using mixtures of water and acetonitrile (MeCN), both adjusted with 0.1% formic acid (FA). The water was prepared using a MilliQ filtration system (Merck Millipore, Johannesburg, South Africa) and LC-MS grade acetonitrile was purchased from Merck Millipore (Johannesburg, South Africa); formic acid was acquired from Sigma-Aldrich (Johannesburg, South Africa).

The LC-MS/MS data was recorded on a Bruker Compact QToF using an ESI-source in positive mode coupled to a Dionex Ultimate 3000 chromatograph using a gradient mobile-phase program employing water and acetonitrile (Kalinski *et al.*, 2019).

The ESI-source parameters were set as follows in positive mode: end plate offset 500 V, capillary voltage 4500 V, nebulizer pressure 3.5 bar, dry gas flow 9.0 L/min and dry temperature 200 °C). An *m*/*z* window of 100 to 2000 was analysed and MS^2 spectra were recorded in data-dependent acquisition mode, selecting the three most intense precursor ions for acquisition of MS^2 spectra at a quadrupole isolation width of 1.5 *m*/*z* and collision energy of 40.0 eV.

3.5. Bioassay methods

The anticancer, anti-oxidant, anti-enzymatic, antibacterial and cytotoxicity assays on the crude extract, fractions and pure compounds were carried out. The anticancer assay was performed by Dr. Jo-Anne de la Mare, the anti-oxidant assay was performed by the author, the anti-enzymatic assay was carried out by PhD scholar Mabate Blessing, the antibacterial and cytotoxicity were performed by Ms. Michelle Isaacs.

3.5.1. Anticancer assays

Cytotoxicity of the compounds were evaluated against the HCC70 triple negative breast cancer cell line. Paclitaxel (Ptx), a known chemotherapeutic was also tested and used as a positive control. Cytotoxicity and IC_{50} were determined by the resazurin assay according to the method described by Mbaba (Mbaba *et al.*, 2020). Breast cells (HCC70-CRL-2315-ATCC) were seeded at a density of 5000 cells/ well and allowed to attached overnight in an incubator at 37℃ and 9% CO_2. Subsequently the cells were treated with the compounds (concentration range 15.63 to 500 nM); or with a vehicle control (2% (v/v) DMSO); or positive control paclitaxel (0.16 to 500 nM) for 96 hours at 37℃ in a 9% CO_2 incubator. After 96 hours exposure, 0.54 nM of resazurin solution was added and the cells were incubated for 2-4 hours at 37℃ in a 9% CO_2 incubator. The fluorescence was then measured on a Spectramax spectrophotometer (excitation and emission wavelength set at 560 nm and 590 nm, respectively). The experiment was performed in triplicate and the data were analysed using GraphPad Prism Inc, (USA) with half-maximal inhibitory concentration (IC_{50} values) determined by non-linear regression.

3.5.2. Anti-oxidant activity

Radical-scavenging activity of plant extracts against stable DPPH (1,1-diphenyl-2-picryl hydrazyl radical) was determined spectrophotometrically. The DPPH assay was carried out as described by (Samarth *et al.*, 2008). Ascorbic acid was used as a positive control. Stock solutions of crude extracts were prepared as 1 mg/mL in methanol. Fifty microlitres of different concentration samples were added to 5 ml of 0.004% methanol solution of DPPH. After 30 minutes of incubation in the dark at room temperature, the absorbance was read against a blank at 517 nm. The assay was carried out in triplicate and percentage of inhibition was calculated using the following formula:

$$\% \text{ inhibition} = \frac{AB-AA}{AB} \times 100$$

where AB = Absorbance of blank; AA = Absorbance of test.

3.5.3. Anti-enzymatic Assay

α-Amylase Activity

The inhibition potential of the *E. caffra* extracts, isolates and the control (acarbose) were investigated and compared using the α-amylase activity assay. In brief, 2% (*w/v*) potato starch dissolved in 0.05 M of sodium phosphate buffer solution (pH~7.0) was mixed with variable concentrations of potential inhibitors ranging from 0.01–1 mg/mL. The reaction was started by adding porcine α-amylase (10 units/mL in a total reaction volume of 400 µL). The reaction mixture was incubated at 37°C for 20 min with gentle agitation at 70 rpm. The amount of reducing sugars produced was measured according to the DNS method (Miller, 1959). A control reaction was prepared using the same procedure replacing the inhibitor sample with distilled water. Extrapolation of absorbance values was performed against a glucose standard calibration curve (Mabate *et al.*, 2021). The α-amylase inhibition was expressed as a relative product (reducing sugar (RS)) percentage according to the following formula:

$$\text{Enzyme inhibition \%} = \frac{RS\ released\ by\ control - RS\ realesed\ by\ test\ reaction}{RS\ released\ by\ control} \text{ x } 100$$

α-Glucosidase Activity Assay

The inhibition of α-glucosidase activity was determined by dissolving the substrate, 10 mM *p*-nitrophenyl-α-D-glucopyranoside (*p*NPG), in 0.05 M sodium phosphate buffer (pH~7.0) in the presence of varied concentrations (0.01–1 mg/mL) of potential inhibitors. The reaction was started by adding α-glucosidase (0.1 units/mL) to a total reaction volume of 400 µL. Each concentration was tested in triplicate The reaction mixture was incubated at 37°C for 20 min and terminated by the addition of 400 µL of 2 M Na_2CO_3 solution. The reaction mixture with water instead of the inhibitors was used as a negative control. The absorbance of the released *p*-nitrophenol was measured at 405 nm. The amount of *p*-nitrophenol produced was extrapolated from a *p*-nitrophenol standard curve (Mabate *et al.*, 2021). The α-glucosidase % inhibition was calculated as relative product (*p*-nitrophenol (*p*N)) percentage as follows:

$$\text{Enzyme inhibition \%} = \frac{(pN\ released\ by\ control - pN\ released\ by\ test\ reaction)}{pN\ released\ by\ control} \text{ x } 100$$

3.5.4. Antibacterial activity

To assess the overt effect of the compounds on the growth of *S. aureus* cells, they are incubated at a fixed concentration of 50 μM or 50 μg/ml in 96-well plates containing *S. aureus* for 6 hours.

To assess the overt effect of the compounds on the growth of *E. coli* cells, they are incubated at a fixed concentration of 50 μM or 50 μg/ml for in 96-well plates containing *E. coli* for 6 hours. The numbers of cells remaining viable after exposure to the compound are determined by using the resazurin based reagent and reading resorufin fluorescence in a multiwell plate reader. These experiments were run three times.

Preparation of concoctions

All concoctions used in the study had at fixed concentration of 24μg/ml prepared as follows at concentration of:

For the S series

- S1 – 8 μL of the neutral fraction (B4) (50 μg/ml) was combined with 16 μL of the ethyl acetate fraction (B2) (50 μg/ml);
- S2 – 8 μL of the neutral fraction (B4) (50 μg/ml) was combined with 16 μL of the *n*-butanol alkaloidic fraction (B3) (50 μg/ml);
- S3 – 8 μL of the neutral fraction (B4) (50 μg/ml) was combined with 16 μL of the ECSC (50 μg/ml).

And for the N series:

- N1 – 16 μL of the neutral fraction (B4) (50 μg/ml) was combined with 16 μL of the ethyl acetate alkaloidic fraction (B2) (50 μg/ml);
- N2 – 16 μL of the neutral fraction (B4) (50 μg/ml) was combined with 16 μL of the *n*-butanol alkaloidic fraction (B3) (50 μg/ml);
- N3 – 16 μL of the neutral fraction (B4) (50 μg/ml) was combined with 16 μL of the ECSC (50 μg/ml) (Kemboi *et al.*, 2022).

3.5.5. Cytotoxicity

To assess the cytotoxicity of the extracts fractions and isolated compounds they are incubated at a fixed concentration of 50 μM or 50 μg/ml for in 96-well plates containing HeLa cells for 24 hours. The numbers of cells surviving drug exposure are determined by using the resazurin based reagent and reading resorufin fluorescence in a multiwell plate reader.

3.6. Molecular networking method parameters

The raw data collected from the LC-MS were converted to mzXML format using the Bruker Compass software (Bruker, Bremen, Germany). The converted files were processed in MZmine 2 (ver. 2.40) (Pluskal *et al.*, 2010). Mass lists were created using the mass detection module with a noise level of 1000 counts for MS^1 and 40 counts for MS^2. The chromatogram builder module was used to create peak lists with a minimum retention time of 0.05 min, a minimum peak height of 5000 counts and an *m*/*z* tolerance of 0.02. The peak lists were deconvoluted using the local minimum search algorithm with the following parameters: chromatographic threshold 0.01%, search minimum in retention time range 0.2 min, minimum relative height 0.1%, minimum absolute height 5000 counts, minimum ratio of peak top/edge 2, and peak duration range 0.02–4 min. For MS^2 scan pairing, the *m*/*z* range was set to 0.02 and the retention time range to 0.5 min. Next, the deconvoluted peak lists were aligned using the Join aligner module with an *m*/*z* tolerance of 0.05, a retention time tolerance of 1.5 min and weighting for *m*/*z* and retention time both set to 100. This 'globally' aligned peak list was then subjected to gap-filling and filtered to exclude all features present in the solvent control samples, as well as those without associated MS^2 spectra and peak IDs were reset, followed by export of a .csv table and .mgf file. The mgf file was then uploaded to GNPS (Wang *et al.*, 2016; Aron *et al.*, 2020) and a job was submitted using the feature molecular network workflow with the following parameters: Precursor and fragment ion mass tolerance = 0.02 Da, minimum cosine = 0.7, minimum matched fragment ions = 6, maximum number of edges per node = 6, minimum peak intensity = 40. The data was not filtered. The acquired data from the network was visualized using Cytoscape (ver.3.7.1) (Shannon *et al.*, 2003).

3.7. Docking procedures

The 2D structures of the compounds (ligands) were prepared using Marvin sketch (Ver. 21.10), explicit hydrogens were added and cleaned in 3D then exported subsequently to maestro (v3.1, Schrödinger 2021-1) for further examination. The molecular docking was done for the three compounds isolated from *E. caffra* stem bark.

The ribbon structure of *Plasmodium falciparum* protein Pf12p (PDB ID: 7KJH) and that of Epidermal growth factor receptor (PDB ID: 1M17) were obtained from the Protein Data Bank (PDB) (Stamos, Sliwkowski and Eigenbrot, 2002; Dietrich *et al.*, 2021). These proteins were used in this study and each protein was docked with three compounds.

The quality of the proteins was examined using Schrödinger Ramachandran plots prior to the screening. Molecular docking was performed within a program called KNIME. It includes different kinds of nodes that perform various functions and they come from a variety of software vendors together with community, native KNIME and open-source nodes. The workflow that controls the flow of data and information for molecular docking is shown below.

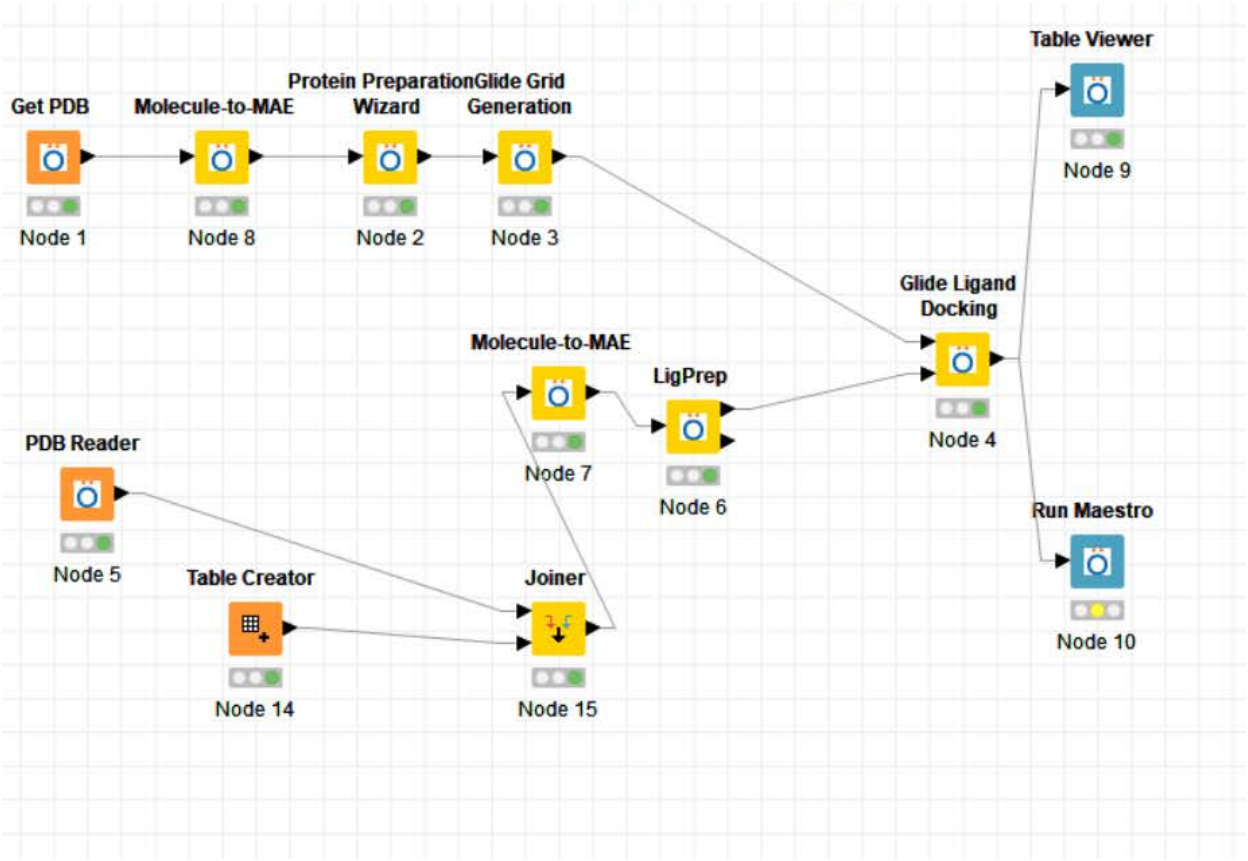

Figure 37. KNIME analytics platform flow diagram for Molecular docking.

In This workflow a protein is read by the PDB Reader node 1. Then the protein is exported to maestro (v3.1, Schrödinger 2021-1) it is then prepared using the Molecule-to-MAE node 8 and Protein Preparation Wizard note 3 which helps to prepare the protein properly (i.e., correcting the missing hydrogens, correct the charge states and bond order). Subsequently, the glide grid was prepared using the glide grid generation node 3. After protein preparation, a Glide grid is then generated from the protein receptor using the Glide Grid Generation node. The settings of the KNIME Grid Generation node were to generate the grid box at the centre of the ligand at the active site of the protein and the box allowed the ligands to fit within the active site during molecular docking. This portion was to prepare the protein for Glide docking.

The ligands were put into the workflow using the PDB reader 5 connected to a table reader node 14 which helps in naming the ligands properly after they are read. Then, the Molecule-to-MAE node 7 exported the ligands to maestro and finally, the ligands were prepared in maestro before the glide grid docking. The ligand preparation is a necessary tool in the

Schrödinger software because it minimizes the energy, improves the incorrect valences and the protonation of the ligands. Finally, the molecular docking was done by the glide ligand node 4. The results and the 3D structure of the protein-ligand docking were then viewed using Table viewer node 9. Results and the protein interaction 2D diagram were view by maestro using the run maestro node 10.

Chapter 4. Conclusion

The main goal of this study was to conduct a thorough investigation for the anticancer, anti-oxidant, anti-enzymatic, antibacterial activity and cytotoxicity of the crude extracts, fractions, concoctions and isolated compounds of *E. caffra* as well as to characterize and identify the isolated compounds.

In the course of this work, three compounds were isolated from the bark extract of *E. caffra* and characterized using spectroscopic techniques of FT-IR, NMR (^{1}H, ^{13}C, DEPT-135, HMBC, HSQC, COSY, NOESY) and LC-ESI-MS. These compounds were identified as lupeol (**1**) (a terpenoid), stigmasterol (**2**) (a terpenoid), and a flavanone namely 5,7-dihydroxy-4'-methoxy-3',5'-diprenylflavanone (**3**) (Abyssinone V' 4-methyl-ether, a flavanone)

The crude extract, fractions and isolated compounds were evaluated for their anticancer activity. The extract and fractions performed poorly and inhibited up to 30% of the cancer cells lines (HCC-70) at a concentration ranging from 15.63 to 50.0 nM. However, the isolated compounds displayed good activities against the cancer cell line (HCC-70) with the best compound (abyssinone V'4-methyl ether) having IC_{50} of 18.05 μM. However, when the cell line was tested against a mixture of compound **2** and an unknown compound (SN6), the anticancer activity of the mixture was more potent than that of the individual compounds with an IC_{50} of 9.045 μg/ml. Furthermore, this showed the power of the synergistic effect of the two compounds which increased the potency significantly. The extracts did not perform well probably because of the lower concentration of active compounds in the whole extract.

Inspired by the results above concoctions of extracts and fractions were formed and evaluated for their antibacterial activity. Most of these concoctions had activities that were significantly increased with minimal to no damage to the HeLa cells. However, when they were tested against the same bacteria individually, some of them performed poorly. The crude extract from the bark and its fractions were tested for their anti-oxidant activity, the crude from the bark displayed high anti-oxidant activity at lower concentration but less activity at higher concentrations. However, the *n*-butanol alkaloidic fraction had a steady increase in activity

with increasing concentration. These two samples were the showed good anti-oxidant activities.

The crude extracts and fractions were also tested for their enzymatic activity on α-Amylase and α-glucosidase. They performed moderately good with the *n*-butanol alkaloidic fraction displaying promising results and inhibiting over 49% of the α-Amylase activity

Molecular docking simulations of the isolated compounds were carried out and performed on the three different proteins (*Plasmodium falciparum*, human estrogen receptor and epidermal growth receptor) to assess the binding abilities of the isolated compounds against the proteins of receptor positive cancer and against a protein for a malaria strain. Abyssinone 4 V'-methyl ether proved to be the best inhibitor for the human estrogen receptor out of all the isolated compounds with a docking score of -6.6 kcal/mol. The molecular docking led to speculations that the isolated compounds (specifically those with the best docking scores) could be useful as alternative drugs for other types of cancer (receptor positive). The pharmacokinetic properties (ADMET), obtained through *in silico* modelling, of these compounds confirmed these speculations by proving that these compounds could be potentially good candidates for different kinds of therapies.

Through the data obtained from molecular networking, over 20 secondary metabolites were putatively identified, using their fragmentation spectra, including one isolated in this study. Some of these secondary metabolites like abrine have already been isolated from this plant and from many other *Erythrina* species. The data also showed the approximate contributions of each extract and fraction in a node corresponding to a specific precursor mass showing the approximate amount that might be present in a specific extract or fraction. In conjunction with molecular networking, future work could be done in identifying those extracts with potentially new compounds and isolating them for the evaluation of their biological activities. Based on their activities they could be used as frameworks for designing a library of bioactive compounds which could be evaluated both *in silico* and *in vivo* for their pharmacokinetic properties. Alternatively, the structure-activity relationships could be examined for these compounds.

Chapter 5. References

Abbas, M., Saeed, F., Anjum, F. M., Afzaal, M., Tufail, T., Bashir, M. S., Ishtiaq, A., Hussain, S., & Suleria, H. A. R., 2017. Natural polyphenols: An overview. In *International Journal of Food Properties*. 20(8), pp.1689-1699

Abdul-Hameed, Z. H., Alarif, W. M., Sobhi, T. R., Abdel-Lateff, A., Ayyad, S. E. N., Badria, F. A., & Saber, J., 2021. New cytotoxic indole-type alkaloids obtained from Rhazya stricta leaves. *South African Journal of Botany*, *137*, pp.298–302.

Abel, S.A., 2020. Synthetic approaches to naturally occurring strigolactones and selected analogues (Doctoral dissertation, University of Tasmania).

Aerts, R., 2009. *Erythrina abyssinica* Lam. ex DC.

Ahmed, Z., Aziz, S., Alauddin, S., Mohiuddin, S.G., Javed, A., Ahmed, R., Bitar, A.N. and Ghadzi, S.M.S., 2020. In vitro cytotoxic and antimicrobial activities of *Erythrina suberosa* (Roxb) bark. *Journal of pharmacy & Bioallied sciences*, *12*(2), p.210-216.

Akram, S. M., & Prakash, V. (2018). Rickettsia Prowazekii (Epidemic Typhus).

Al-Mahmood, S., Sapiezynski, J., Garbuzenko, O.B. and Minko, T., 2018. Metastatic and triple-negative breast cancer: challenges and treatment options. *Drug Delivery and Translational Research*, *8*(5), pp.1483-1507.

Aldbass, A., Amina, M., Al Musayeib, N.M., Bhat, R.S., Al-Rashed, S., Marraiki, N., Fahmy, R. and El-Ansary, A., 2021. Cytotoxic and anti-excitotoxic effects of selected plant andalgal extracts using COMET and cell viability assays. *Scientific reports*, *11*(1), pp.1-11.

Amenu, D., 2014. Antimicrobial activity of medicinal plant extracts and their synergistic effect on some selected pathogens. *American Journal of Ethnomedicine*, *1*(1), pp.18-29.

Andayi, A.W., Yenesew, A., Derese, S., Midiwo, J.O., Gitu, P.M., Jondiko, O.J., Akala, H.,

Liyala, P., Wangui, J., Waters, N.C. and Heydenreich, M., 2006. Antiplasmodialflavonoids from Erythrina sacleuxii. *Planta Medica*, *72*(02), pp.187-189.

Aron, A.T., Gentry, E.C., McPhail, K.L., Nothias, L.F., Nothias-Esposito, M., Bouslimani, A., Petras, D., Gauglitz, J.M., Sikora, N., Vargas, F. and van Der Hooft, J.J., 2020. Reproducible molecular networking of untargeted mass spectrometry data using GNPS. *Nature protocols*, *15*(6), pp.1954-1991.

Arramon, G., Saucier, C., Colombani, D. and Glories, Y., 2002. Identification of triterpene saponins in Quercus robur L. and Q. petraea Liebl. heartwood by LC-ESI/MS and NMR. *Phytochemical Analysis: An International Journal of Plant Chemical and Biochemical Techniques*, *13*(6), pp.305-310.

Atanassova, M., Georgieva, S. and Ivancheva, K., 2011. Total phenolic and total flavonoid contents, antioxidant capacity and biological contaminants in medicinal herbs. *Journal of the University of Chemical Technology & Metallurgy*, *46*(1), pp. 81-88

Aung, T.N., Qu, Z., Kortschak, R.D. and Adelson, D.L., 2017. Understanding the effectiveness of natural compound mixtures in cancer through their molecular mode of action. *International Journal of Molecular Sciences*, *18*(3), p.656.

Auten, R.L. and Davis, J.M., 2009. Oxygen toxicity and reactive oxygen species: the devil is in the details. *Pediatric Research*, *66*(2), pp.121-127.

Avhad, M.S., Tiwari, M.K. and Ushir, Y.V., 2019. Ethnobotanical studies of *Erythrina indica* Plants. *Indian Journal of Pathology and Oncology, pp.* 67-70

Bai, A.D., Lo, C.K., Komorowski, A.S., Suresh, M., Guo, K., Garg, A., Tandon, P., Senecal, J., Del Corpo, O., Stefanova, I. and Fogarty, C., 2022. *Staphylococcus aureus* bacteremia mortality: a systematic review and meta-analysis. *Clinical Microbiology and Infection.*

Bergman, M.E., Davis, B. and Phillips, M.A., 2019. Medically useful plant terpenoids: biosynthesis, occurrence, and mechanism of action. *Molecules*, *24*(21), p.3961.

Burstein, H.J., Polyak, K., Wong, J.S., Lester, S.C. and Kaelin, C.M., 2004. Ductal carcinoma *in situ* of the breast. *New England Journal of Medicine*, *350*(14), pp.1430-1441.

Bhat, A.H., Dar, K.B., Anees, S., Zargar, M.A., Masood, A., Sofi, M.A. and Ganie, S.A., 2015. Oxidative stress, mitochondrial dysfunction and neurodegenerative diseases; a mechanistic insight. *Biomedicine & Pharmacotherapy*, *74*, pp.101-110.

Brito-Arias, M., 2022. N-glycosides in synthesis and characterization of glycosides. *Cham: Springer, Cham*. pp. 229-284.

Bruschi, P., Mancini, M., Mattioli, E., Morganti, M. and Signorini, M.A., 2014. Traditional uses of plants in a rural community of Mozambique and possible links with Miombodegradation and harvesting sustainability. *Journal of Ethnobiology and Ethnomedicine*, *10*(1), pp.1-22.

Castañeda, A.M., Meléndez, C.M., Uribe, D. and Pedroza-Díaz, J., 2022. Synergistic effects of natural compounds and conventional chemotherapeutic agents: recent insights for the development of cancer treatment strategies. *Heliyon*, p.e09519.

Chen, T.C., Da Fonseca, C.O. and Schönthal, A.H., 2015. Preclinical development and clinical use of perillyl alcohol for chemoprevention and cancer therapy. *American Journal of Cancer Research*, *5*(5), p.1580.

Cheon, C., 2021. Synergistic effects of herbal medicines and anticancer drugs: A protocol for systematic review and meta-analysis. *Medicine*, *100*(46). pp. 1-3

Chitopoa, W., Muchachaa, I. and Mangoyi, R., 2019. Evaluation of the antimicrobial activity of *Erythrina abyssinica* leaf extract. *Jornal of Microbial and Biochemical Technology*, *11*(2). pp. 413

Chukwujekwu, J.C., de Kock, C.A., Smith, P.J., Van Heerden, F.R. and Van Staden, J., 2016. Antiplasmodial activity of compounds isolated from *Erythrina caffra*. *South African Journal of Botany*, *106*, pp.101-103.

Chukwujekwu, J.C., Van Heerden, F.R. and Van Staden, J., 2011. Antibacterial activity of

flavonoids from the stem bark of *Erythrina caffra* thunb. *Phytotherapy Research*, *25*(1), pp.46-48.

Chukwujekwu, J.C., Van Heerden, F.R. and Van Staden, J., 2011. Antibacterial activity of flavonoids from the stem bark of *Erythrina caffr*a thunb. *Phytotherapy Research*, *25*(1), pp.46-48.

Cowan, M.M., 1999. Plant products as antimicrobial agents. *Clinical microbiology reviews*, *12*(4), pp.564-582.

D'Angelo, A., Orlandi, A., Bufi, E., Mercogliano, S., Belli, P. and Manfredi, R., 2021. Automated breast volume scanner (ABVS) compared to handheld ultrasound (HHUS) and contrast-enhanced magnetic resonance imaging (CE-MRI) in the early assessment of breast cancer during neoadjuvant chemotherapy: an emerging role to monitoring tumor response?. *La Radiologia Medica*, *126*(4), pp.517-526.

Daglia, M., 2012. Polyphenols as antimicrobial agents. *Current Opinion in Biotechnology*, *23*(2), pp.174-181.

De Ávila, J.M., Dalcol, I.I., Pereira, A.O., Santos, E.W., Ferraz, A., Santos, M.Z., Mostardeiro, M.A. and Morel, A.F., 2018. Antimicrobial Evaluation of *Erythrinan* Alkaloids from *Erythrina crista-galli L. Medicinal Chemistry*, *14*(8), pp.784-790.

DeSantis, C.E., Bray, F., Ferlay, J., Lortet-Tieulent, J., Anderson, B.O. and Jemal, A., 2015. International Variation in Female Breast Cancer Incidence and Mortality RatesInternational Variation in Female Breast Cancer Rates. *Cancer Epidemiology, Biomarkers & Prevention*, *24*(10), pp.1495-1506.

Desta, Z.Y., Sewald, N. and Majinda, R.R., 2016. Cytotoxic flavonoids from *Erythrina caffra* Thunb. *Bulletin of the Chemical Society of Ethiopia*, *30*(3), pp.427-435.

Dietrich, M.H., Chan, L.J., Adair, A., Keremane, S., Pymm, P., Lo, A.W., Cao, Y.C. and Tham, W.H., 2021. Nanobody generation and structural characterization of *Plasmodium falciparum* 6-cysteine protein Pf12p. *Biochemical Journal*, *478*(3), pp.579-595.

Donlan, R.M., 2002. Biofilms: microbial life on surfaces. *Emerging Infectious Diseases*, *8*(9), p.881.

Dragovic-Uzelac, V., Levaj, B., Mrkic, V., Bursac, D. and Boras, M., 2007. The content of polyphenols and carotenoids in three apricot cultivars depending on stage of maturity and geographical region. *Food Chemistry*, *102*(3), pp.966-975.

Eisenstein, M. (2020). The skin microbiome. In *Nature*, *588*(7838), pp. S209. https://doi.org/10.1038/d41586-020-03523-7 [Accessed June 2022]

El-Masry, S., Hammoda, H.M., Zaatout, H.H., Alqasoumi, S.I. and Abdel-Kader, M.S., 2010. Constituents of *Erythrina caffra* stem bark grown in Egypt. *Natural Product Sciences*, *16*(4), pp.211-216.

Elisha, I.L., Botha, F.S., McGaw, L.J. and Eloff, J.N., 2017. The antibacterial activity of extracts of nine plant species with good activity against *Escherichia coli* against five other bacteria and cytotoxicity of extracts. *BMC Complementary and Alternative Medicine*, *17*(1), pp.1-10.

Eliston, C. W., & Ellis, I. O., 1991. Pathological prognostic factors in breast cancer. I. The value of histological grade in breast cancer: experience from a large study with long-term follow-up. *Histopathology, 19*(5), pp. 403–410.

Eliyatkın, N., Yalçın, E., Zengel, B., Aktaş, S. and Vardar, E., 2015. Molecular classification of breast carcinoma: from traditional, old-fashioned way to a new age, and a new way. *The Journal of Breast Health*, *11*(2), p.59.

Ellis, I.O., Galea, M., Broughton, N., Locker, A., Blamey, R.W. and Elston, C.W., 1992. Pathological prognostic factors in breast cancer. II. Histological type. Relationship with survival in a large study with long-term follow-up. *Histopathology*, *20*(6), pp.479-489.

Elzagheid, M.I., 2018. Laboratory activities to introduce carbohydrates qualitative analysis to college students. *World Jornal of Chemical Education*, *6*(2), pp.82-86.

Emaikwu, V., Ndukwe, I.G., Mohammed, R., Iyun, O.R.A. and Anyam, J.V., 2020. Isolation and Characterization of Lupeol from the Stem of *Tapinanthus globiferus* (A Rich.) and its Antimicrobial Assay. *Journal of Applied Sciences and Environmental Management*, *24*(6), pp.1015-1020.

Esquivel, C.M., Garcia, M., Armando, L., Ortiz, G., Lascano, F.M. and Foscarini, J.M., 2018. Laparoscopic sleeve gastrectomy resolves NAFLD: another formal indication for bariatric

surgery?. *Obesity Surgery*, *28*(12), pp.4022-4033.

Etkin, N.L., 2005. Fundamentals of Pharmacognosy and Phytotherapy. *Economic Botany*, *59*(4), pp.414-414.

Fabricant, D.S. and Farnsworth, N.R., 2001. The value of plants used in traditional medicine for drug discovery. *Environmental Health Perspectives*, *109*(1), pp.69-75.

Faguet, G.B., 2015. A brief history of cancer: age-old milestones underlying our current knowledge database. *International Journal of Cancer*, *136*(9), pp.2022-2036.

Fahmy, N.M., Al-Sayed, E., El-Shazly, M. and Singab, A.N., 2018. Comprehensive review on flavonoids biological activities of *Erythrina* plant species. *Industrial Crops and Products*, *123*, pp.500-538.

Fahmy, N.M., Al-Sayed, E., El-Shazly, M. and Singab, A.N., 2018. Comprehensive review on flavonoids biological activities of Erythrina plant species. *Industrial Crops and Products*, *123*, pp.500-538.

Fatima, H., Shahid, M., Jamil, A. and Naveed, M., 2021. Therapeutic Potential of Selected Medicinal Plants Against Carrageenan Induced Inflammation in Rats. *Dose-Response*, *19*(4), pp.1-14

Fredriksson, M., 2021. India's Traditional Knowledge Digital Library and the Politics of Patent Classifications. *Law and Critique*, pp.1-19.

Gajdács, M., 2019. The continuing threat of methicillin-resistant *Staphylococcus aureus*. *Antibiotics*, *8*(2), p.52.

Gan, J., Feng, Y., He, Z., Li, X. and Zhang, H., 2017. Correlations between antioxidant activity and alkaloids and phenols of maca (Lepidium meyenii). *Journal of Food Quality*, *2017*.

Gebre-Medhin, M., Kindblom, L.G., Wennbo, H., Törnell, J. and Meis-Kindblom, J.M., 2001. Growth hormone receptor is expressed in human breast cancer. *The American Journal of Pathology*, *158*(4), pp.1217-1222.

Gilad, Y., Gellerman, G., Lonard, D. M., & O'malley, B. W.,2021. Drug Combination in Cancer Treatment—From Cocktails to Conjugated Combinations. *Cancers*, *13*(4), 1–26. pp. 669

Gimza, B.D. and Cassat, J.E., 2021. Mechanisms of antibiotic failure during *Staphylococcus aureus* osteomyelitis. *Frontiers in Immunology, 12*, pp. 1-5

Ginsburg, O., Yip, C.H., Brooks, A., Cabanes, A., Caleffi, M., Dunstan Yataco, J.A., Gyawali, B., McCormack, V., McLaughlin de Anderson, M., Mehrotra, R. and Mohar, A., 2020. Breast cancer early detection: A phased approach to implementation. *Cancer*, *126*, pp.2379-2393.

Glastonbury, S., 2013. Principles and Practice of Phytotherapy. Modern Herbal Medicine. *Australian Journal of Herbal Medicine*, *25*(2), pp.95-96.

Gogoi, J., Nakhuru, K.S., Policegoudra, R.S., Chattopadhyay, P., Rai, A.K. and Veer, V., 2016. Isolation and characterization of bioactive components from Mirabilis jalapa L. radix. *Journal of Traditional and Complementary Medicine*, *6*(1), pp.41-47.

Gottlieb, H.E., Kotlyar, V. and Nudelman, A., 1997. NMR chemical shifts of common laboratory solvents as trace impurities. *Journal of Organic Chemistry*, *62*(21), pp.7512-7515.

Guerrant, R.L., Steiner, T.S., Lima, A.A. and Bobak, D.A., 1999. How intestinal bacteria cause disease. *The Journal of Infectious Diseases*, *179*(Supplement_2), pp.S331-S337.

Gupta, M., 2021. Synergistic anti-cancer effects of natural products and their mode of action. *Asian Journal of Pharmaceutical and Clinical Research*, *14*(2), pp. 5-21

Grice, E.A. and Segre, J.A., 2011. The skin microbiome. *Nature Reviews Microbiology*, *9*(4), pp.244-253.

Haas, A., 2007. The phagosome: compartment with a license to kill. *Traffic*, *8*(4), pp.311-330.

Habtemariam, S., 2019. Chapter 6—Introduction to plant secondary metabolites—From biosynthesis to chemistry and antidiabetic action. *Medicinal Foods as Potential Therapies for Type-2 Diabetes and Associated Diseases*, pp.109-132.

Harborne, J.B., 1993. The alkaloids: Vol. 41: edited by A. Brossi and GA Cordell, Academic Press, San Diego.

Hartmann, L.C., Radisky, D.C., Frost, M.H., Santen, R.J., Vierkant, R.A., Benetti, L.L., Tarabishy, Y., Ghosh, K., Visscher, D.W. and Degnim, A.C., 2014. Understanding the Premalignant Potential of Atypical Hyperplasia through Its Natural History: A Longitudinal Cohort Study Breast Cancers after Atypical Hyperplasia. *Cancer Prevention Research*, *7*(2), pp.211-217.

Hartmann, L.C., Degnim, A.C., Santen, R.J., Dupont, W.D. and Ghosh, K., 2015. Atypical hyperplasia of the breast—risk assessment and management options. *New England Journal of Medicine*, *372*(1), pp.78-89.

Hedstrom, L., 2001. Enzyme specificity and selectivity. Wiley Online Library.

Hoda, S.A. and Hoda, R.S., 2005. Robbins and cotran pathologic basis of disease. *Advances in Anatomic Pathology 12(2)*; p 10*3*

Hosey, C.M. and Benet, L.Z., 2015. Predicting the extent of metabolism using in vitro permeability rate measurements and in silico permeability rate predictions. *Molecular pharmaceutics*, *12*(5), pp.1456-1466.

Hsu, Y.M., Lai, W.C., Li, C.Y., Lan, Y.H., Tsai, Y.C., Hunyadi, A., Hou, M.F., Yuan, S.S., Wu, Y.C. and Chang, F.R., 2016. Estrogenic and Anti-estrogenic Constituents of *Erythrina caffra*. *Natural product communications*, *11*(8), pp.1099-1102

Huo, D., Ikpatt, F., Khramtsov, A., Dangou, J.M., Nanda, R., Dignam, J., Zhang, B., Grushko, T., Zhang, C., Oluwasola, O. and Malaka, D., 2009. Population differences in breast cancer: survey in indigenous African women reveals over-representation of triple-negative breast cancer. *Journal of Clinical Oncology*, *27*(27), p.4515.

Hutchings, A., 1996. *Zulu medicinal plants: An inventory*. University of Natal press. pp 464

Idrees, M., Mohammad, A.R., Karodia, N. and Rahman, A., 2020. Multimodal role of amino acids in microbial control and drug development. *Antibiotics*, *9*(6), p.330.

Irshad, H., 2014. Automated mitosis detection in color and multi-spectral high-content images in histopathology: application to breast cancer grading in digital pathology (Doctoral dissertation, Grenoble)

Irvin Jr, W., Muss, H.B. and Mayer, D.K., 2011. Symptom management in metastatic breast cancer. *The Oncologist*, *16*(9), pp.1203-1214.

Irvine, J.D., Takahashi, L., Lockhart, K., Cheong, J., Tolan, J.W., Selick, H.E. and Grove, J.R., 1999. MDCK (Madin–Darby canine kidney) cells: a tool for membrane permeability screening. *Journal of Pharmaceutical Sciences*, *88*(1), pp.28-33.

Ivshina, A.V., George, J., Senko, O., Mow, B., Putti, T.C., Smeds, J., Lindahl, T., Pawitan, Y., Hall, P., Nordgren, H. and Wong, J.E., 2006. Genetic reclassification of histologic grade delineates new clinical subtypes of breast cancer. *Cancer Research*, *66*(21), pp.10292-10301.

Iyer, R. and Chaichana, K.L., 2018. Minimally invasive resection of deep-seated high-grade gliomas using tubular retractors and exoscopic visualization. *Journal of Neurological Surgery Part A: Central European Neurosurgery*, *79*(04), pp.330-336.

Jhan, J.R. and Andrechek, E.R., 2017. Triple-negative breast cancer and the potential for targeted therapy. *Pharmacogenomics*, *18*(17), pp.1595-1609.

Kainsa, S., Kumar, P. and Rani, P., 2012. Medicinal plants of Asian origin having anticancer potential: short review. *Asian Journal of Biomedical and Pharmaceutical Sciences*, *2*(10), pp.1-11.

Kalinski, J.C.J., Waterworth, S.C., Siwe Noundou, X., Jiwaji, M., Parker-Nance, S., Krause, R.W., McPhail, K.L. and Dorrington, R.A., 2019. Molecular networking reveals two distinct chemotypes in pyrroloiminoquinone-producing Tsitsikamma favus sponges. *Marine Drugs*, *17*(1), p.60.

Kaplan, J.B., Mlynek, K.D., Hettiarachchi, H., Alamneh, Y.A., Biggemann, L., Zurawski, D.V., Black, C.C., Bane, C.E., Kim, R.K. and Granick, M.S., 2018. Extracellular polymeric substance (EPS)-degrading enzymes reduce *staphylococcal* surface attachment

and biocide resistance on pig skin in vivo. *PLoS One*, *13*(10), pp. 1-13

Katiyar, C., Gupta, A., Kanjilal, S. and Katiyar, S., 2012. Drug discovery from plant sources: An integrated approach. *An International Quarterly Journal of Research in Ayurved*, *33*(1), p.10.

Kaur, R.A.J.B.I.R. and Arora, S.A.R.O.J., 2015. Alkaloids-important therapeutic secondary metabolites of plant origin. *Journal of Critical Reviews*, *2*(3), pp.1-8.

Kefayati, Z., Motamed, S.M., Shojaii, A., Noori, M. and Ghods, R., 2017. Antioxidant activity and phenolic and flavonoid contents of the extract and subfractions of Euphorbia splendida Mobayen. *Pharmacognosy Research*, *9*(4), p.362.

Kemboi, D., Langat, M.K., Siwe-Noundou, X., Krause, R.W., Isaacs, M.L. and Tembu, V.J., 2022. In vitro antibacterial and cytotoxic effects of Euphorbia grandicornis Blanc chemical constituents. *BMC Complementary Medicine and Therapies*, *22*(1), pp.1-10.

Kestwal, R.M. and Bhide, S.V., 2007. Purification of β-galactosidase from *Erythrina indica:* involvement of tryptophan in active site. *Biochimica et Biophysica Acta (BBA)-General Subjects*, *1770*(10), pp.1506-1512.

Khan, M.F., Verma, G., Akhtar, W., Shaquiquzzaman, M., Akhter, M., Rizvi, M.A. and Alam, M.M., 2019. Pharmacophore modeling, 3D-QSAR, docking study and ADME prediction of acyl 1, 3, 4-thiadiazole amides and sulfonamides as antitubulin agents. *Arabian Journal of Chemistry*, *12*(8), pp.5000-5018.

Klevens, R.M., 2007. Active bacterial core surveillance (ABCs) MRSA investigators. Invasive methicillin-resistant *Staphylococcus aureus* infections in the United States. *Journal of American Medical Association, 298*, pp.1763-1771.

Kojima, Y., Acar, A., Eaton, E.N., Mellody, K.T., Scheel, C., Ben-Porath, I., Onder, T.T.,

Wang, Z.C., Richardson, A.L., Weinberg, R.A. and Orimo, A., 2010. Autocrine TGF-β and stromal cell-derived factor-1 (SDF-1) signaling drives the evolution of tumor-promoting mammary stromal myofibroblasts. *Proceedings of the National Academy of Sciences*, *107*(46), pp.20009-20014.

Kone, W.M., Solange, K.N. and Dosso, M., 2011. Assessing sub-Saharan Erythrina for efficacy: traditional uses, biological activities and phytochemistry. *Pakistan Journal of Biological Sciences*, *14*(10), pp.560-571.

Kuete, V., Sandjo, L.P., Kwamou, G.M., Wiench, B., Nkengfack, A.E. and Efferth, T., 2014. Activity of three cytotoxic isoflavonoids from *Erythrina excelsa* and *Erythrina senegalensis* (neobavaisoflavone, sigmoidin H and isoneorautenol) toward multi-factorial drug resistant cancer cells. *Phytomedicine*, *21*(5), pp.682-688.

Kurtz, J.R., Goggins, J.A. and McLachlan, J.B., 2017. Salmonella infection: Interplay between the bacteria and host immune system. *Immunology Letters*, *190*, pp.42-50.

Kwamou, G.M., Sandjo, L.P., Kuete, V., Wandja, A.A., Tankeo, S.B., Efferth, T. and Nkengfack, A.E., 2015. Unprecedented new nonadecyl para-hydroperoxycinnamate isolated from *Erythrina excelsa* and its cytotoxic activity. *Natural Product Research*, *29*(10), pp.921-925.

Laing, K. (2019). *Immune responses to bacteria | British Society for Immunology*. British

Society for Immunology. https://www.immunology.org/public-information/bitesized-immunology/pathogens-and-disease/immune-responses-bacteria,[retrieved 20 June 2022]

Lee, J.S., Oh, W.K., Ahn, J.S., Kim, Y.H., Mbafor, J.T., Wandji, J. and Fomum, Z.T., 2009. Prenylisoflavonoids from *Erythrina senegalensis* as novel HIV-1 protease inhibitors.

Planta Medica, *75*(03), pp.268-270.

Li, C.I., Uribe, D.J. and Daling, J.R., 2005. Clinical characteristics of different histologic types of breast cancer. *British Journal of Cancer*, *93*(9), pp.1046-1052.

Li, S., Zhang, F., Xiao, X., Guo, Y., Wen, Z., Li, M. and Pu, X., 2021. Prediction of Synergistic Drug Combinations for Prostate Cancer by Transcriptomic and Network Characteristics. *Frontiers in Pharmacology*, *12*, p.634097.

Li, X., Yang, J., Peng, L., Sahin, A.A., Huo, L., Ward, K.C., O'Regan, R., Torres, M.A. and Meisel, J.L., 2017. Triple-negative breast cancer has worse overall survival and cause-specific survival than non-triple-negative breast cancer. *Breast Cancer Research and Treatment*, *161*(2), pp.279-287.

Limmathurotsakul, D., Dunachie, S., Fukuda, K., Feasey, N.A., Okeke, I.N., Holmes, A.H., Moore, C.E., Dolecek, C., van Doorn, H.R., Shetty, N. and Lopez, A.D., 2019. Improving the estimation of the global burden of antimicrobial resistant infections. *The Lancet Infectious Diseases*, *19*(11), pp. e392-e398.

Lin, J., Elkon, J., Ricart, B., Palmer, E., Zevallos-Delgado, C., Noonepalle, S., Burgess, B., Siegel, R., Ma, Y. and Villagra, A., 2021. Phase I Study of Entinostat in Combination with Enzalutamide for Treatment of Patients with Metastatic Castration-Resistant Prostate Cancer. *The Oncologist*, *26*(12), pp.e2136-e2142.

Linares, D.M., Ross, P. and Stanton, C., 2016. Beneficial Microbes: the pharmacy in the gut. *Bioengineered* 7(1), pp. 11–20.

Lobo, V., Patil, A., Phatak, A. and Chandra, N., 2010. Free radicals, antioxidants and functional foods: Impact on human health. *Pharmacognosy Reviews*, *4*(8), p.118.

Lourenço, S.C., Moldão-Martins, M. and Alves, V.D., 2019. Antioxidants of natural plant origins: From sources to food industry applications. *Molecules*, *24*(22), p.4132.

Mabate, B., Daub, C.D., Malgas, S., Edkins, A.L. and Pletschke, B.I., 2021. A Combination Approach in Inhibiting Type 2 Diabetes-Related Enzymes Using Ecklonia radiata Fucoidan and Acarbose. *Pharmaceutics*, *13*(11), p.1979.

Macintyre, M., 2020. Indigenous healing: An introduction to complementary medicine (pp. 33-47). Routledge.

Maennling, A.E., Tur, M.K., Niebert, M., Klockenbring, T., Zeppernick, F., Gattenlöhner, S., Meinhold-Heerlein, I. and Hussain, A.F., 2019. Molecular targeting therapy against EGFR family in breast cancer: progress and future potentials. *Cancers*, *11*(12), p.1826.

Mahady, G.B., 2005. Medicinal plants for the prevention and treatment of bacterial infections. *Current Pharmaceutical Design*, *11*(19), pp.2405-2427.

Maiza-Benabdesselam, F., Khentache, S., Bougoffa, K., Chibane, M., Adach, S., Chapeleur, Y., Henry, M. and Laurain-Mattar, D., 2007. Antioxidant activities of alkaloid extracts of two Algerian species of Fumaria: Fumaria capreolata and Fumaria bastardii. *Records of Natural Products*, *1*(2-3), p.28.

Matondo, A., Dendera, W., Isamura, B.K., Mambo, H.V., Muzomwe, M. and Mudogo, V., 2022. In silico drug repurposing of anticancer drug 5-FU and analogues against SARS-CoV-2 main protease: molecular docking, pharmacokinetics and chemical reactivity.

Matondo, A., Dendera, W., Isamura, B.K., Mambo, H.V., Muzomwe, M. and Mudogo, V., 2022. In silico drug repurposing of anticancer drug 5-FU and analogues against SARS-CoV-2 main protease: molecular docking, pharmacokinetics and chemical reactivity studies. Advances and Applications in Bioinformatics and Chemistr,*15* (2022) pp. 59-77

Mbaba, M., Dingle, L.M., Cash, D., de la Mare, J.A., Laming, D., Taylor, D., Hoppe, H.C., Edkins, A.L. and Khanye, S.D., 2020. Repurposing a polymer precursor: Synthesis and in vitro medicinal potential of ferrocenyl 1, 3-benzoxazine derivatives. *European Journal of Medicinal Chemistry*, *187*, p.111924.

McCormack, V., McKenzie, F., Foerster, M., Zietsman, A., Galukande, M., Adisa, C., Anele, A., Parham, G., Pinder, L.F., Cubasch, H. and Joffe, M., 2020. Breast cancer survival and survival gap apportionment in sub-Saharan Africa (ABC-DO): a prospective cohort study. *The Lancet Global health*, *8*(9), pp.e1203-e1212.

McLaughlin, J.S. and Shafritz, A.B., 2011. Cutaneous warts. *Journal of Hand Surgery*, *36*(2), pp.343-344.

Miller, G.L., 1959. Use of dinitrosalicylic acid reagent for determination of reducing sugar.*Analytical Chemistry*, *31*(3), pp.426-428.

Miller, L.S. and Cho, J.S., 2011. Immunity against Staphylococcus aureus cutaneous infections. *Nature Reviews Immunology*, *11*(8), pp.505-518.

Mishra, G., Singh, P., Verma, R., Kumar, S., Srivastav, S., Jha, K.K. and Khosa, R.L., 2011. Traditional uses, phytochemistry and pharmacological properties of Moringa oleifera plant: An overview. *Der Pharmacia Lettre*, *3*(2), pp.141-164.

Missiakas, D. and Winstel, V., 2022. Selective Host Cell Death by. Fighting an Elusive Enemy*: Staphylococcus aureus* and its Antibiotic Resistance, Immune-Evasion and Toxic Mechanisms*. Frantiers in Immunology.,11*(1). pp 60-61

Mook, S., Schmidt, M.K., Rutgers, E.J., van de Velde, A.O., Visser, O., Rutgers, S.M., Armstrong, N., van't Veer, L.J. and Ravdin, P.M., 2009. Calibration and discriminatory

accuracy of prognosis calculation for breast cancer with the online Adjuvant! program: a hospital-based retrospective cohort study. *The Lancet Oncology*, *10*(11), pp.1070-1076.

Musau, J.K., Mbaria, J.M. and Gakuya, D.W., 2011. The antibacterial activity of some medicinal plants used in Meru Central District, Kenya. *A Journal of Kenya Veterinary Association.,1*(1) pp. 18-24

Mukandiwa, L., Naidoo, V. and Eloff, J.N., 2012. In vitro antibacterial activity of seven plants used traditionally to treat wound myiasis in animals in Southern Africa. *Journal of medicinal plants research*, *6*(27), pp. 4379-4388

Nayak, P.S., Kar, D.M. and Nayak, S.P., 2015. Isolation and characterization of stigmasterol from chloroform fraction of aerial part of Argemone mexicana L. *International Journal of Pharmarcy and Pharmaceutical Science.,7*, pp.25-29.

Nguyen, H.T., Nguyen, T.H. and Otto, M., 2020. The staphylococcal exopolysaccharide PIA–Biosynthesis and role in biofilm formation, colonization, and infection. *Computational and Structural Biotechnology Journal*, *18*, pp.3324-3334.

Ningthoujam, S.S., Talukdar, A.D., Potsangbam, K.S. and Choudhury, M.D., 2012. Challenges in developing medicinal plant databases for sharing ethnopharmacological knowledge. *Journal of Ethnopharmacology*, *141*(1), pp.9-32.

Nkengfack, A.E., Vouffo, T.W., Vardamides, J.C., Kouam, J., Fomum, Z.T., Meyer, M. and Sterner, O., 1997. Phenolic metabolites from *Erythrina* species. *Phytochemistry*, *46*(3), pp.573-578.

Noudou, B.S., Nkengfack, A.E. and Djama C.M., 2018. Characterisation of indole alkaloids from seeds of *Erythrina Poeppigiana* (Fabaceae). *International Journal of Medical Research and Pharmaceutical Sciences*, *5*(2). pp. 33-38

Nowicka, D. and Grywalska, E., 2019. *Staphylococcus aureus* and host immunity in recurrent furunculosis. *Dermatology*, *235*(4), pp.295-305.

Olajuyigbe, O.O. and Afolayan, A.J., 2012. In vitro pharmacological activity of the crude acetone extract of *Erythrina caffra* Thunb: antibacterial and antifungal assessment. *Journal of Medicinal Plants Research*, *6*(9), pp.1713-1720.

Olajuyigbe, O.O. and Afolayan, A.J., 2012. In vitro antibacterial and time-kill evaluation of the *Erythrina caffra* Thunb. extract against bacteria associated with diarrhoea. *The Scientific World Journal*, *2012*., pp. 1-8

Ombito, J.O., Majinda, R.R., Masesane, I.B., Bojase, G., Schüffler, A. and Opatz, T., 2018. Prenylated isoflavones from the stem bark of *Erythrina sacleuxii*. *Phytochemistry Letters*, *26*, pp.110-114.

Östman, A. and Augsten, M., 2009. Cancer-associated fibroblasts and tumor growth–bystanders turning into key players. *Current Opinion in Genetics & Development*, *19*(1), pp.67-73.

Oturanel, C. E, Kıran, İ., Ciftci, A. and Atlı, O., 2017. Cytotoxic, antiproliferative and apoptotic effects of perillyl alcohol and its biotransformation metabolite on A549 and HepG2 cancer cell lines. *Anti-Cancer Agents in Medicinal Chemistry (Formerly Current Medicinal Chemistry-Anti-Cancer Agents)*, *17*(9), pp.1243-1250.

Paludan, Pradeu, T., Masters, S.L. and Mogensen, T.H., 2021. Constitutive immune mechanisms: Mediators of Host Defence and Immune Regulation. *Nature Reviews Immunology*, *21*(3)., pp. 137-150).

Pandey, A. and Tripathi, S., 2014. Concept of standardization, extraction and pre phytochemical screening strategies for herbal drug. *Journal of Pharmacognosy and Phytochemistry*, *2*(5). pp. 115-119

Pavia, D. L., Lampman, G. M., Kriz, G. S., & Vyvyan, J. R., 2000. Chapter 6 Furans and benzo[b]furans. In *Tetrahedron Organic Chemistry Series*, *20*(C)

Pateh, U.U., Haruna, A.K., Garba, M., Iliya, I., Sule, I.M., Abubakar, M.S. and Ambi, A.A., 2009. Isolation of stigmasterol, β-sitosterol and 2-hydroxyhexadecanoic acid methyl ester from the rhizomes of Stylochiton lancifolius Pyer and Kotchy (Araceae).*Nigerian Journal of Pharmaceutical Sciences*, *8*(1), pp.19-25.

Pérez, M.A., Raimondi, A.R. and Itoiz, M.E., 2005. An experimental model to demonstrate the carcinogenic action of oral chronic traumatic ulcer. *Journal of Oral Pathology & Medicine*, *34*(1), pp.17-22.

Perwez Hussain, S., Hofseth, L.J. and Harris, C.C., 2003. Radical causes of cancer. *Nature Reviews Cancer*, *3*, pp.276-285.

Pezzani, R., Salehi, B., Vitalini, S., Iriti, M., Zuñiga, F.A., Sharifi-Rad, J., Martorell, M. and Martins, N., 2019. Synergistic effects of plant derivatives and conventional chemotherapeutic agents: an update on the cancer perspective. *Medicina*, *55*(4), p.110.Pham-Huy, L.A., He, H. and Pham-Huy, C., 2008. Free radicals, antioxidants in disease and health. *International journal of biomedical science*, *4*(2), p.89.

Pillay, C.C., Jäger, A.K., Mulholland, D.A. and Van Staden, J., 2001. Cyclooxygenase inhibiting and anti-bacterial activities of South African Erythrina species. *Journal of Ethnopharmacology*, *74*(3), pp.231-237.

Pimentel de Araujo, F., Monaco, M., Del Grosso, M., Pirolo, M., Visca, P. and Pantosti, A., 2021. Staphylococcus aureus clones causing osteomyelitis: a literature review (2000–2020). *Journal of Global Antimicrobial Resistance*, *26*, pp.29-36.

Pluskal, T., Castillo, S., Villar-Briones, A. and Orešič, M., 2010. MZmine 2: modular

framework for processing, visualizing, and analyzing mass spectrometry-based molecular profile data. *BMC Bioinformatics*, *11*(1), pp.1-11.

Polidori, M.C., Griffiths, H.R., Mariani, E. and Mecocci, P., 2007. Hallmarks of protein oxidative damage in neurodegenerative diseases: focus on Alzheimer's disease. *Amino Acids*, *32*(4), pp.553-559.

Quideau, S., 2009. Why bother with polyphenols. *Groupe Polyphenols: The International Society Dedicated to the Promotion of Research on Polyphenols*. 24. pp. 10-14.

Raal, A., Meos, A., Hinrikus, T., Heinämäki, J., Romāne, E., Gudienė, V., Koshovyi, O., Kovaleva, A., Fursenco, C., Chiru, T. and Nguyen, H.T., 2020. Dragendorff's reagent: Historical perspectives and current status of a versatile reagent introduced over 150 years ago at the University of Dorpat, Tartu, Estonia. *Die Pharmazie-An International Journal of Pharmaceutical Sciences*, *75*(7), pp.299-306.

Rambo, D.F., Biegelmeyer, R., Toson, N.S., Dresch, R.R., Moreno, P.R.H. and Henriques, A.T., 2019. The genus Erythrina L.: A review on its alkaloids, preclinical, and clinical studies. *Phytotherapy Research*, *33*(5), pp.1258-1276.

Rami, E., Sipai, S. and Patel, I., 2013. Studies on qualitative and quantitative phytochemical analysis of Piper longum Linn. *International Journal of Pharma Bio Sciences*, *4*(3), pp.1381-1388.

Rao, S., Linke, L., Magnuson, R., Jauch, L. and Hyatt, D.R., 2022. Antimicrobial resistance and genetic diversity of Staphylococcus aureus collected from livestock, poultry and humans. *One Health*, *15*, p.100407.

Rasigade, J.P., Dumitrescu, O. and Lina, G., 2014. New epidemiology of Staphylococcus aureus infections. *Clinical Microbiology and Infection*, *20*(7), pp.587-588.

Raven, P.H., 1974. Erythrina (Fabaceae): achievements and opportunities., *Lloydia-A Quarterly Journal of Biological Science.* pp. 321-331

Reffuveille, F., Josse, J., Vallé, Q., Gangloff, C.M. and Gangloff, S.C., 2017. Staphylococcus aureus Biofilms and their Impact on the Medical Field. *The rise of virulence and antibiotic resistance in Staphylococcus aureus*, *11*, p.187.

Regev-Yochay, G., Dagan, R., Raz, M., Carmeli, Y., Shainberg, B., Derazne, E., Rahav, G. and Rubinstein, E., 2004. Association between carriage of Streptococcus pneumoniae and Staphylococcus aureus in children. *Jama*, *292*(6), pp.716-720.

Reynolds, T., Kuska, B., & Curtis, L. (2012). *NIH Human Microbiome Project defines normal bacterial makeup of the body | National Institutes of Health (NIH).* National Institutes of Health. https://www.nih.gov/news-events/news-releases/nih-human-microbiome-project-defines-normal-bacterial-makeup-body, [retrieved 18 June 2022]

Ribet, D. and Cossart, P., 2015. How bacterial pathogens colonize their hosts and invade deeper tissues. *Microbes and infection*, *17*(3), pp.173-183.

Rosai, J., 1991. Borderline epithelial breast lesions. *The American Journal of Surgical Pathology*, *15*, pp.209-221.

Sadgrove, N.J., Oliveira, T.B., Khumalo, G.P., van Vuuren, S.F. and van Wyk, B.E., 2020. Antimicrobial isoflavones and derivatives from *Erythrina* (Fabaceae): structure activity perspective (Sar & Qsar) on experimental and mined values against *Staphylococcus aureus*. *Antibiotics*, *9*(5), p.223.

Saidu, K., Onah, J., Orisadipe, A., Olusola, A., Wambebe, C. and Gamaniel, K., 2000. Antiplasmodial, analgesic, and anti-inflammatory activities of the aqueous extract of the stem bark of Erythrina senegalensis. *Journal of ethnopharmacology*, *71*(1-2), pp.275-280.

Saikia, R., Talukdar, A.D. and Chetia, P., Preliminary phytochemical investigation and TLC profiling of ethnomedicinally important plant, Scoparia dulcis Linnaeus.

Sama Fonkeng, L., Mouokeu, R.S., Tume, C., Njateng, G.S.S., Kamcthueng, M.O., Ndonkou, N.J. and Kuiate, J.R., 2015. Anti-Staphylococcus aureus activity of methanol extracts of12 plants used in Cameroonian folk medicine. *BMC Research Notes*, *8*(1), pp.1-6.

Samarth, R.M., Panwar, M., Kumar, M., Soni, A., Kumar, M. and Kumar, A., 2008. Evaluation of antioxidant and radical-scavenging activities of certain radioprotective plant extracts. *Food chemistry*, *106*(2), pp.868-873.

Samura, M., Kitahiro, Y., Tashiro, S., Moriyama, H., Hamamura, Y., Takahata, I., Kawabe, R., Enoki, Y., Taguchi, K., Takesue, Y. and Matsumoto, K., 2022. Efficacy and Safety of Daptomycin versus Vancomycin for Bacteremia Caused by Methicillin-Resistant Staphylococcus aureus with Vancomycin Minimum Inhibitory Concentration> 1 μg/mL: A Systematic Review and Meta-Analysis. *Pharmaceutics*, *14*(4), p.714.

Schäfer, M., 2008. Werner S. *Cancer as an overhealing wound: an old hypothesis revisited. Nat Rev Mol Cell Biol*, *9*, pp.628-638.

Schaumburg, F., Pauly, M., Anoh, E., Mossoun, A., Wiersma, L., Schubert, G., Flammen, A., Alabi, A.S., Muyembe-Tamfum, J.J., Grobusch, M.P. and Karhemere, S., 2015. Staphylococcus aureus complex from animals and humans in three remote African regions. *Clinical Microbiology and Infection*, *21*(4), pp.345-e1.

Schausberger, P., 2018. Herbivore-associated bacteria as potential mediators and modifiers of induced plant defense against spider mites and thrips. *Frontiers in plant science*, *9*, p.1107.

Schilcher, K. and Horswill, A.R., 2020. Staphylococcal biofilm development: structure, regulation, and treatment strategies. *Microbiology and Molecular Biology Reviews*, *84*(3), pp.e00026-19.

Sebei, K., Sakouhi, F., Herchi, W., Khouja, M.L. and Boukhchina, S., 2015. Chemical composition and antibacterial activities of seven Eucalyptus species essential oils leaves. *Biological Research*, *48*(1), pp.1-5.

Sender, R., Fuchs, S. and Milo, R., 2016. Revised estimates for the number of human and bacteria cells in the body. *PLoS biology*, *14*(8), p.e1002533.

Shahbazi, Y., 2015. Chemical composition and in vitro antibacterial activity of Mentha spicata essential oil against common food-borne pathogenic bacteria. *Journal of pathogens*, *2015*.

Shannon, P., Markiel, A., Ozier, O., Baliga, N.S., Wang, J.T., Ramage, D., Amin, N., Schwikowski, B. and Ideker, T., 2003. Cytoscape: a software environment for integrated models of biomolecular interaction networks. *Genome research*, *13*(11), pp.2498-2504.

Sherma, J. and Fried, B., 1987. Preparative thin layer chromatography. In *Journal of Chromatography Library* (Vol. 38, pp. 105-127). Elsevier.

Shwe, H.H., Win, K.K., Moe, T.T., Myint, A.A. and Win, T., 2019. Isolation and structural characterization of lupeol from the stem bark of Diospyros ehretioides Wall. *IEEE-SEM*, *7*, pp.140-144.

Siddharth, S. and Sharma, D., 2018. Racial disparity and triple-negative breast cancer in African-American women: a multifaceted affair between obesity, biology, and

socioeconomic determinants. *Cancers*, *10*(12), p.514.

Singh, H., Chawla, A.S., Kapoor, V.K., Kumar, N., Piatak, D.M. and Nowicki, W., 1981. Investigation of Erythrina spp. IX. Chemical constituents of Erythrina stricta bark.*Journal of Natural Products*, *44*(5), pp.526-529.

Sloane, J.P., Amendoeira, I., Apostolikas, N., Bellocq, J.P., Bianchi, S., Boecker, W., Bussolati, G., Coleman, D., Connolly, C.E., Eusebi, V. and De Miguel, C., 1999.

Consistency achieved by 23 European pathologists from 12 countries in diagnosing breast disease and reporting prognostic features of carcinomas. *Virchows Archiv*, *434*(1), pp.3-10.

Smolarczyk, K., Mlynarczyk-Bonikowska, B., Rudnicka, E., Szukiewicz, D., Meczekalski, B., Smolarczyk, R. and Pieta, W., 2021. The impact of selected bacterial sexually transmitted diseases on pregnancy and female fertility. *International Journal of Molecular Sciences*, *22*(4), p.2170.

Sobral, M. V, Xavier, A. L and Lima, T.D.C, 2014. de Sousa P. Antitumor activity of monoterpenes found in essential oils. *The Scientific World Journal*, *953451*, pp.1-35.

Sotiriou, C. and Pusztai, L., 2009. Gene-expression signatures in breast cancer. *New England Journal of Medicine*, *360*(8), pp.790-800.

Sotiriou, C., Wirapati, P., Loi, S., Harris, A., Fox, S., Smeds, J., Nordgren, H., Farmer, P., Praz, V., Haibe-Kains, B. and Desmedt, C., 2006. Gene expression profiling in breast cancer: understanding the molecular basis of histologic grade to improve prognosis. *Journal of the National Cancer Institute*, *98*(4), pp.262-272.

Stamos, J., Sliwkowski, M.X. and Eigenbrot, C., 2002. Structure of the epidermal growth factor

receptor kinase domain alone and in complex with a 4-anilinoquinazoline inhibitor. *Journal of biological chemistry*, *277*(48), pp.46265-46272.

Stead, L.A., Lash, T.L., Sobieraj, J.E., Chi, D.D., Westrup, J.L., Charlot, M., Blanchard, R.A., Lee, J.C., King, T.C. and Rosenberg, C.L., 2009. Triple-negative breast cancers are increased in black women regardless of age or body mass index. *Breast Cancer Research*, *11*(2), pp.1-10.

Stoltenberg, M., Spence, D., Daubman, B.R., Greaves, N., Edwards, R., Bromfield, B., Perez-Cruz, P.E., Krakauer, E.L., Argentieri, M.A. and Shields, A.E., 2020. The central role of provider training in implementing resource-stratified guidelines for palliative care in low-income and middle-income countries: Lessons from the Jamaica Cancer Care and Research Institute in the Caribbean and Universidad Católica in Latin America. *Cancer,126*, pp.2448-2457.

Taffurelli, M. (2018). Ductal carcinoma in situ of the breast. In *Ductal Carcinoma in Situ of the Breast* (Vol. 350, Issue 14). Massachusetts Medical Society. https://doi.org/10.1007/9783319574516

Tavassoli, F.A., 1998. Ductal carcinoma in situ: introduction of the concept of ductal intraepithelial neoplasia. *Modern pathology: an official journal of the United States and Canadian Academy of Pathology, Inc*, *11*(2), pp.140-154.

Tchuente Djoko, C., Gade, I.S., Atchade, A.D.T., Tamfu, A.N., Mihaela Dinica, R., Sangu, E., Tchoffo Djankou, M., Henoumont, C., Laurent, S. and Talla, E., 2021. An α-Sophoradiol Glycoside from the Root Wood of Erythrina senegalensis DC.(Fabaceae) with α-Amylase and α-Glucosidase Inhibitory Potential. *Natural Product Communications*, *16*(9), p.1934578X211044564.

Temkin, E., Fallach, N., Almagor, J., Gladstone, B.P., Tacconelli, E., Carmeli, Y. and DRIVE-AB Consortium, 2018. Estimating the number of infections caused by antibiotic-resistant

Escherichia coli and Klebsiella pneumoniae in 2014: a modelling study. *The Lancet Global Health*, *6*(9), pp.e969-e979.

Tjahjandarie, T.S., Pudjiastuti, P., Saputri, R.D. and Tanjung, M., 2014. Antimalarial and antioxidant activity of phenolic compounds isolated from Erythrina crista-galli L. *J Chem Pharm Res*, *6*(4), pp.786-790.

Tong, W., 2013. Biotransformation of terpenoids and steroids. *Natural Products, Springer*, pp.2733-2759.

Tueche, A.B., Zingue, S., Tchoupang, E.N., Gueyo, T.N., Gbaweng Yaya, A.J., Njuh, A.N., Ntsa, D.M. and Njamen, D., 2018. Abyssinone V-4'Methyl Ether isolated from erythrina droogmansiana (Leguminosae) inhibits cell growth and mammary glands hyperplasia induced in swiss mice by the 7, 12-Dimethylbenz (a) anthracene. *Evidence-Based Complementary and Alternative Medicine, 2018*.

Tugume, P., Kakudidi, E.K., Buyinza, M., Namaalwa, J., Kamatenesi, M., Mucunguzi, P. and Kalema, J., 2016. Ethnobotanical survey of medicinal plant species used by communities around Mabira Central Forest Reserve, Uganda. *Journal of ethnobiology and ethnomedicine, 12*(1), pp.1-28.

Turco, J. and Winkler, H.H., 2021. Interactions between Rickettsia prowazekii and cultured host cells: alterations induced by gamma interferon. In *Interferon and nonviral pathogens* (pp. 95-115). CRC Press.

Tyagi, A.K., Singh, R.P., Agarwal, C., Chan, D.C. and Agarwal, R., 2002. Silibinin strongly synergizes human prostate carcinoma DU145 cells to doxorubicin-induced growth Inhibition, G2-M arrest, and apoptosis. *Clinical cancer research*, *8*(11), pp.3512-3519.

Tyagi, R., Sharma, G., Jasuja, N.D. and Menghani, E., 2016. Indian medicinal plants as an effective antimicrobial agent. *J Crit Rev*, *3*(2), pp.69-71.

Ullah, K., K.(2016). Diabetes mellitus and oxidative stress—A concise review. *Saudi Pharmaceutical Journal*, *24*(5), pp.547-553.

Uribe-Querol, E. and Rosales, C., 2020. Phagocytosis: our current understanding of a universal biological process. *Frontiers in Immunology*, *11*, p.1066.

Utami, D.T., 2019. Antimicrobial activity of dadap serep (Erythrina subumbrans (Hassk.) Merr.) leaves extract. *Journal of Chemical Natural Resources*, *1*(1), pp.45-49.

Uzombah, T.A., 2022. The Implications of Replacing Synthetic Antioxidants with Natural Ones in the Food Systems.

Van Hal, S.J., Jensen, S.O., Vaska, V.L., Espedido, B.A., Paterson, D.L. and Gosbell, I.B., 2012. Predictors of mortality in Staphylococcus aureus bacteremia. *Clinical microbiology reviews*, *25*(2), pp.362-386.

Veeresham, C., 2012. Natural products derived from plants as a source of drugs. *Journal of advanced pharmaceutical technology & research*, *3*(4), p.200.

Verpoorte, R., 2000. Pharmacognosy in the new millennium: leadfinding and biotechnology.*Journal of pharmacy and pharmacology*, *52*(3), pp.253-262.

Verschaeve, L. and Van Staden, J., 2008. Mutagenic and antimutagenic properties of extracts from South African traditional medicinal plants. *Journal of Ethnopharmacology*, *119*(3), pp.575-587.

Venkata, S.P.C. and Indra, P., 2012. Isolation of stigmasterol and β-sitosterol from the dichloromethane extract of Rubus suavissimus. *Int Curr Pharm J*, *1*, pp.239-42.

Wang, M., Carver, J.J., Phelan, V.V., Sanchez, L.M., Garg, N., Peng, Y., Nguyen, D.D., Watrous, J., Kapono, C.A., Luzzatto-Knaan, T. and Porto, C., 2016. Sharing and community curation of mass spectrometry data with Global Natural Products Social Molecular Networking. *Nature biotechnology*, *34*(8), pp.828-837.

Wang, T.H., Hsia, S.M., Wu, C.H., Ko, S.Y., Chen, M.Y., Shih, Y.H., Shieh, T.M., Chuang, L.C. and Wu, C.Y., 2016. Evaluation of the antibacterial potential of liquid and vapor phase phenolic essential oil compounds against oral microorganisms. *PLoS One*, *11*(9), p.e0163147.

Wanjala, C.C., Juma, B.F., Bojase, G., Gashe, B.A. and Majinda, R.R., 2002. Erythrinaline alkaloids and antimicrobial flavonoids from Erythrina latissima. *Planta Medica*, *68*(07), pp.640-642.

Wankhar, W., Srinivasan, S., Rajan, R. and Rathinasamy, S., 2015. Phytochemicals screening and antimicrobial efficacy of Scoparia dulcis Linn (Scrophulariaceae) against clinical isolates. *Journal of Pharmacognosy and Phytochemistry*, *3*(6).

Weigelt, B., Baehner, F.L. and Reis-Filho, J.S., 2010. The contribution of gene expression profiling to breast cancer classification, prognostication and prediction: a retrospective of the last decade. *The Journal of Pathology: A Journal of the Pathological Society of Great Britain and Ireland*, *220*(2), pp.263-280.

Weigelt, B., Geyer, F.C. and Reis-Filho, J.S., 2010. Histological types of breast cancer: how special are they?. *Molecular oncology*, *4*(3), pp.192-208.

Wen, H.Y. and Brogi, E., 2018. Lobular carcinoma in situ. *Surgical pathology clinics*, *11*(1), pp.123-145.

WHO. (2019). WHO Global Report on Traditional and Complementary Medicine 2019. https://www.who.int/publications/i/item/978924151536, [retrieved 19 June 2022]

WHO. (2020). *Antibiotic resistance*. https://doi.org/10.1017/S0195941700058215, [retrieved 19 June 2022]

WHO. (2022). *Cancer*. https://www.who.int/news-room/fact-sheets/detail/cancer [retrieved 19 June 2022]

Xiong, Q., Wilson, W.K. and Pang, J., 2007. The Liebermann–Burchard reaction: sulfonation, desaturation, and rearrangment of cholesterol in acid. *Lipids*, *42*(1), pp.87-96.

Yang, H., Jin, X., Lam, C.W.K. and Yan, S.K., 2011. Oxidative stress and diabetes mellitus.*Clinical chemistry and laboratory medicine*, *49*(11), pp.1773-1782.

Yates, T.A., Khan, P.Y., Knight, G.M., Taylor, J.G., McHugh, T.D., Lipman, M., White, R.G., Cohen, T., Cobelens, F.G., Wood, R. and Moore, D.A., 2016. The transmission of Mycobacterium tuberculosis in high burden settings. *The Lancet infectious diseases*, *16*(2), pp.227-238.

Yenesew, A., Midiwo, J.O., Miessner, M., Heydenreich, M. and Peter, M.G., 1998. Two prenylated flavanones from stem bark of *Erythrina burttii*. *Phytochemistry*, *48*(8), pp.1439-1443.

Yin, T.P., Cai, L., Xing, Y., Yu, J., Li, X.J., Mei, R.F. and Ding, Z.T., 2016. Alkaloids with antioxidant activities from Aconitum handelianum. *Journal of Asian Natural Products Research*, *18*(6), pp.603-610.

Yuan, L., Wang, B., Zha, D., Liu, C., Li, M., Xie, Y., Yang, H., Cao, Y., Xu, H. and Li, R.W., 2022. Origin of magnetic field-induced magnetic anisotropy in amorphous CoFeB thin films. AIP Advances, 12(4), p.045203.

Zhang, H.X., Lunga, P.K., Li, Z.J., Dai, Q. and Du, Z.Z., 2014. Flavonoids and stilbenoids from Derris eriocarpa. Fitoterapia, 95, pp.147-153.

Ziegler, J., Et Facchini, Pj (2008). Biosynthèse des alcaloïdes: Métabolisme et trafic. Revue Annuelle de la biologie végétale, 59(1), pp.735-769.

Chapter 6. Appendices

Appendix 1: Infrared

Appendix 1.1.1: Infrared for compound **1**

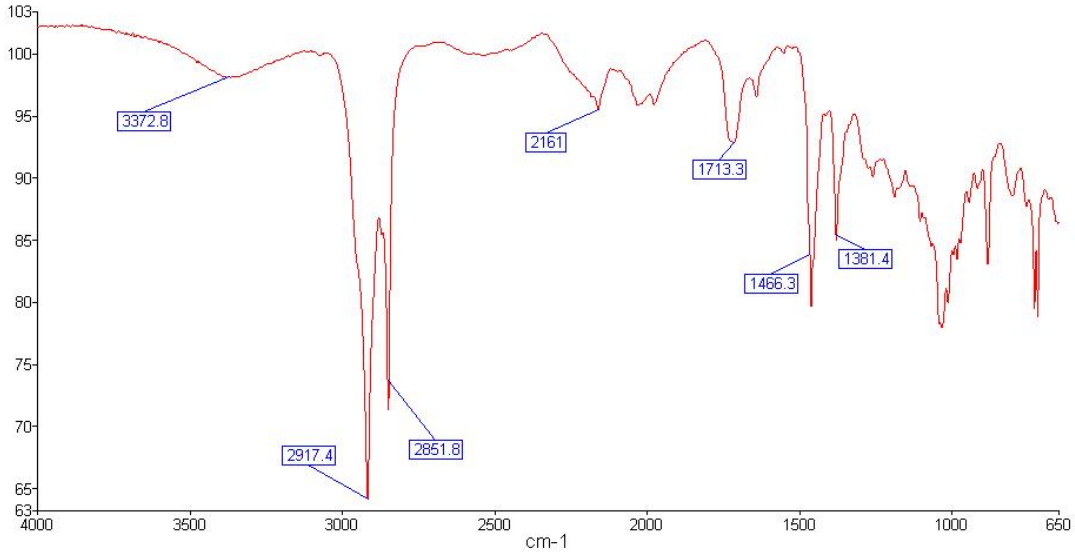

Appendix 1.1.2: Infrared for compound **2**

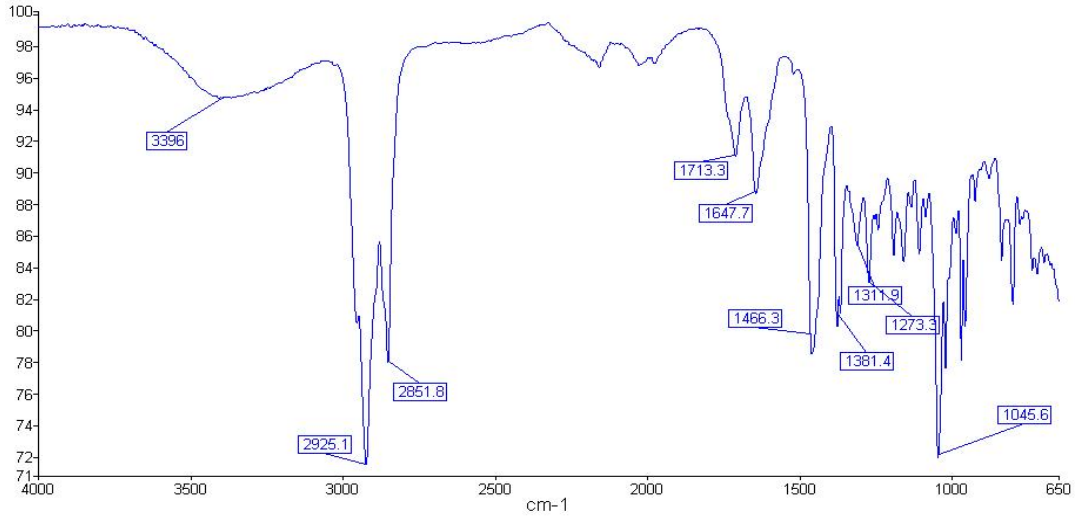

Appendix 1.1.3: Infrared for compound **3**

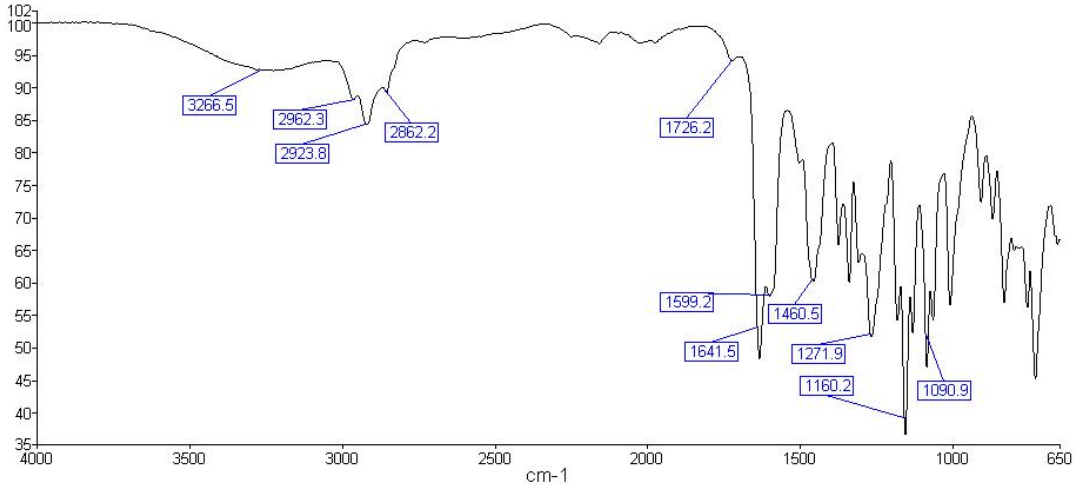

Appendix 2: Nuclear Magnetic resonance spectra Spectroscopy

Appendix 2.1: NMR for compound **1**

Appendix 2.1.1: DEPT-135

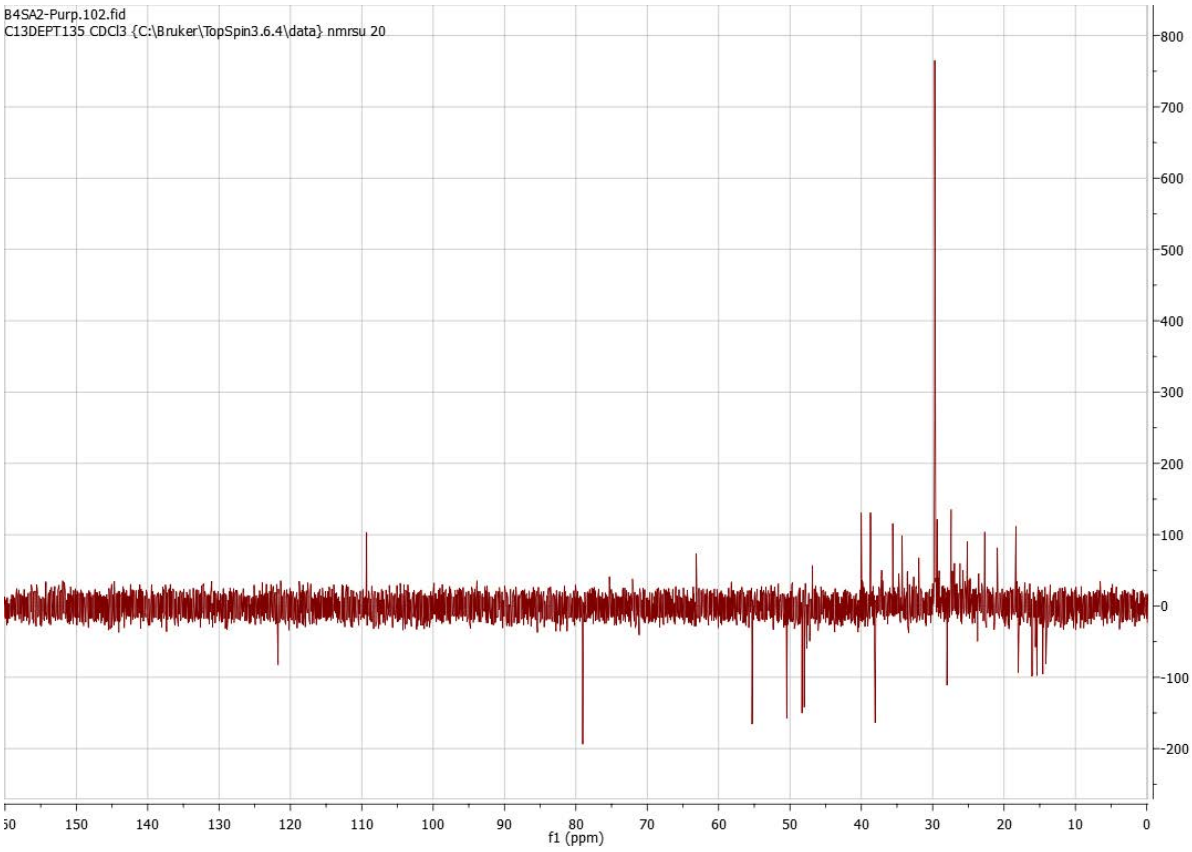

Appendix 2.2.2: COSY

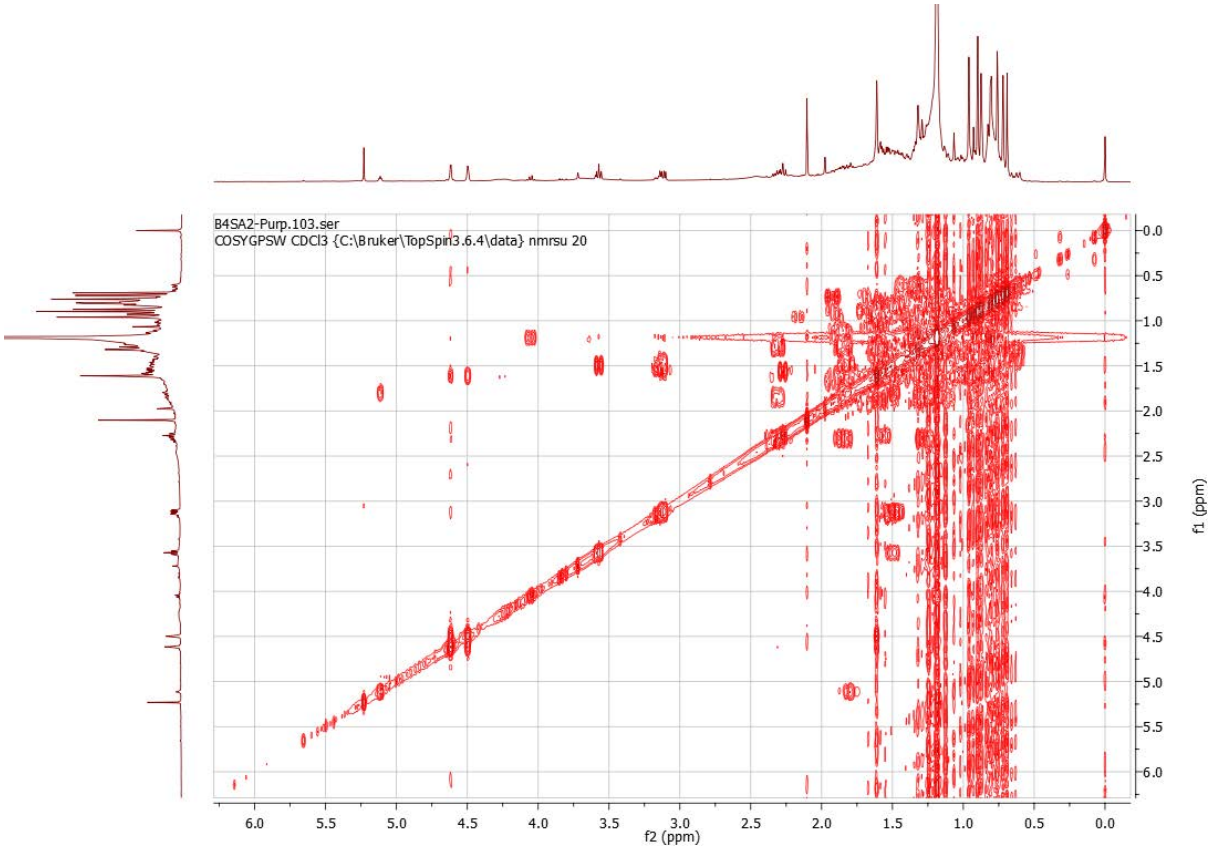

Appendix 2.2.3: HMBC

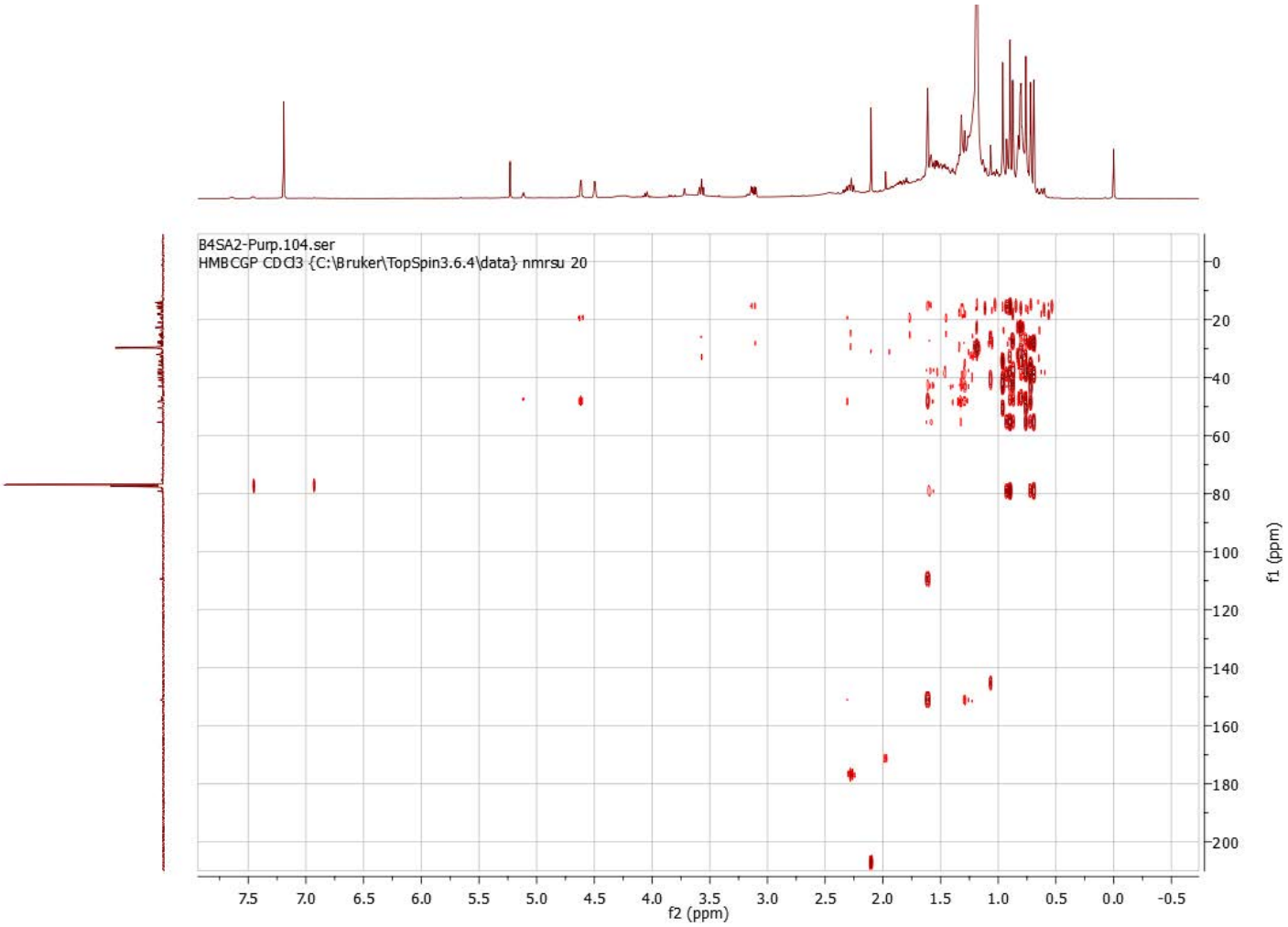

Appendix 2.2.4: HSQC

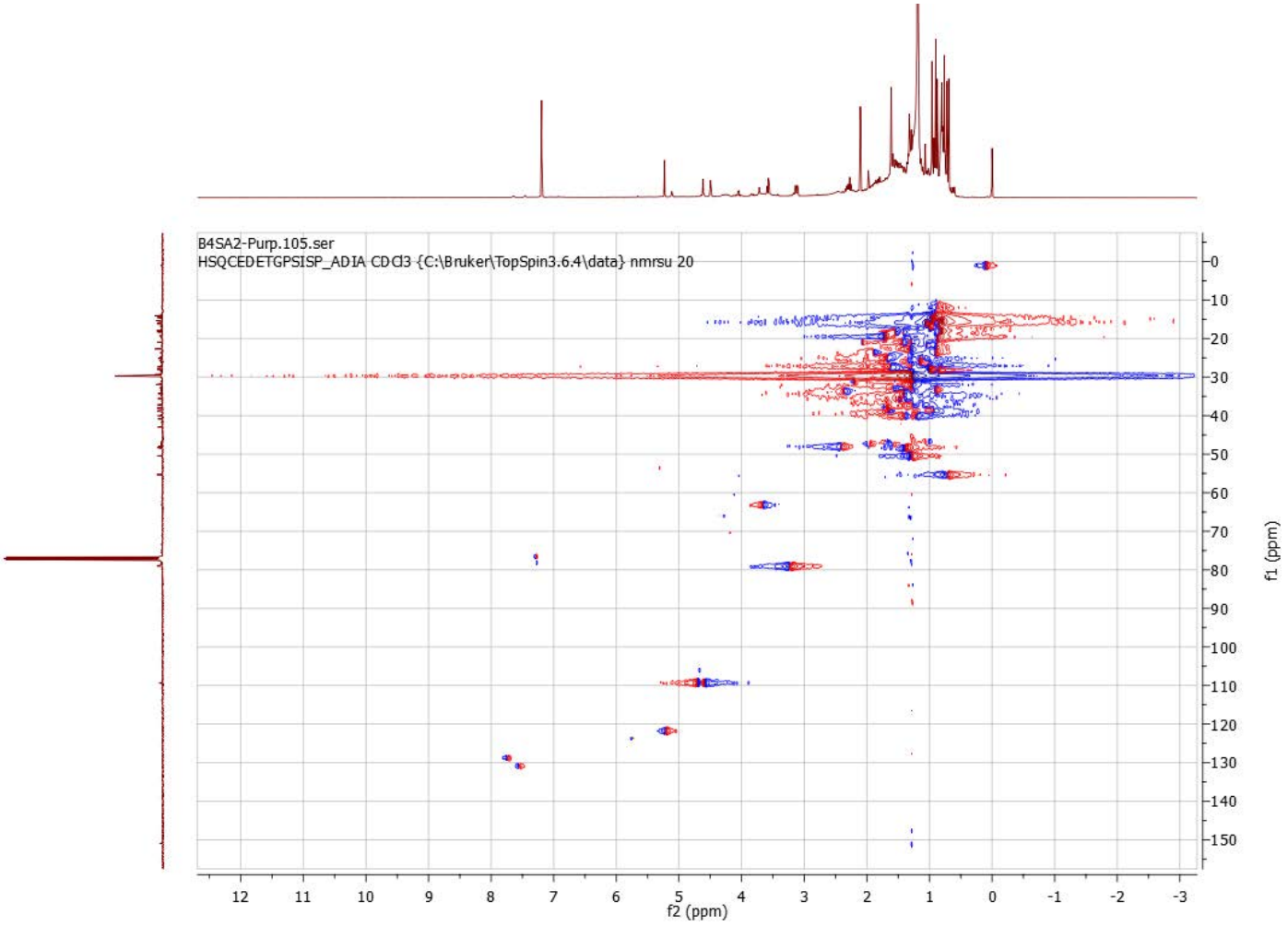

Appendix 2.2: NMR spectra for Compound **2**

Appendix 2.2.1: DEPT-135

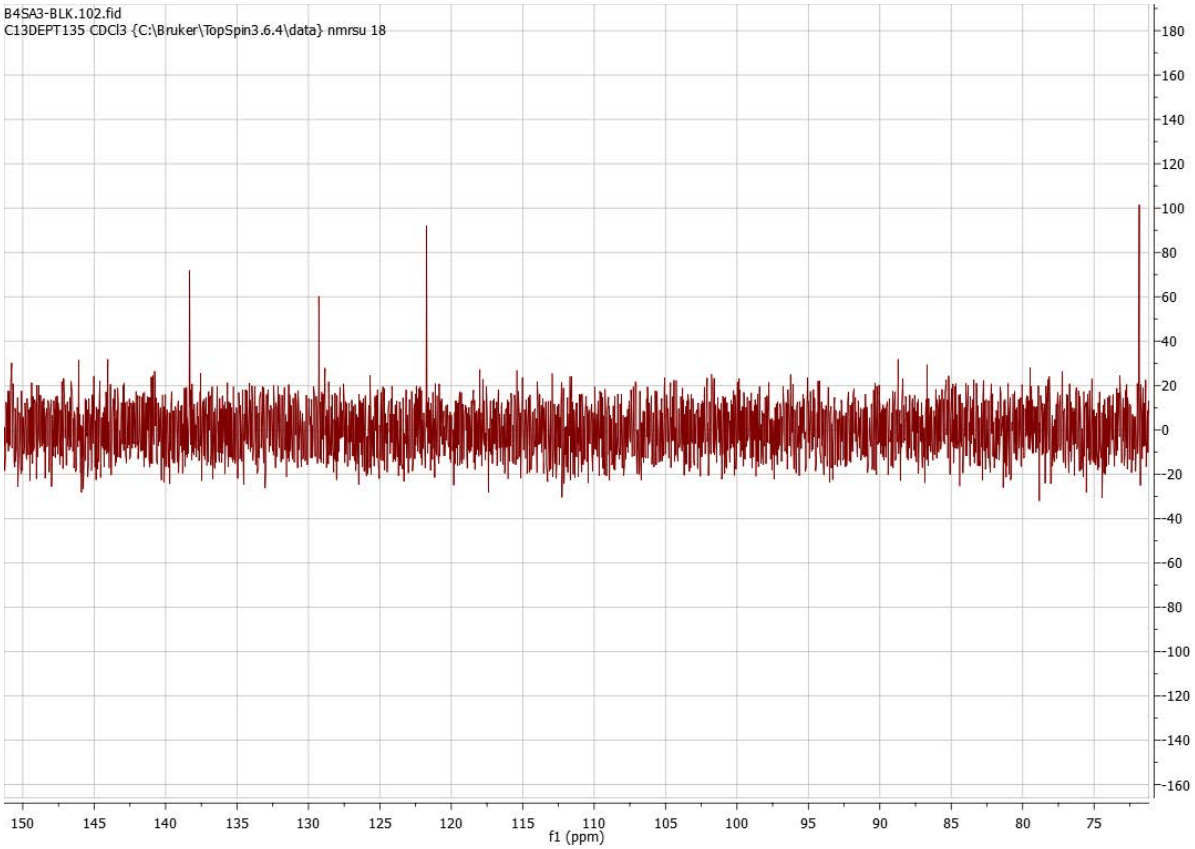

Appendix 2.2.2: COSY

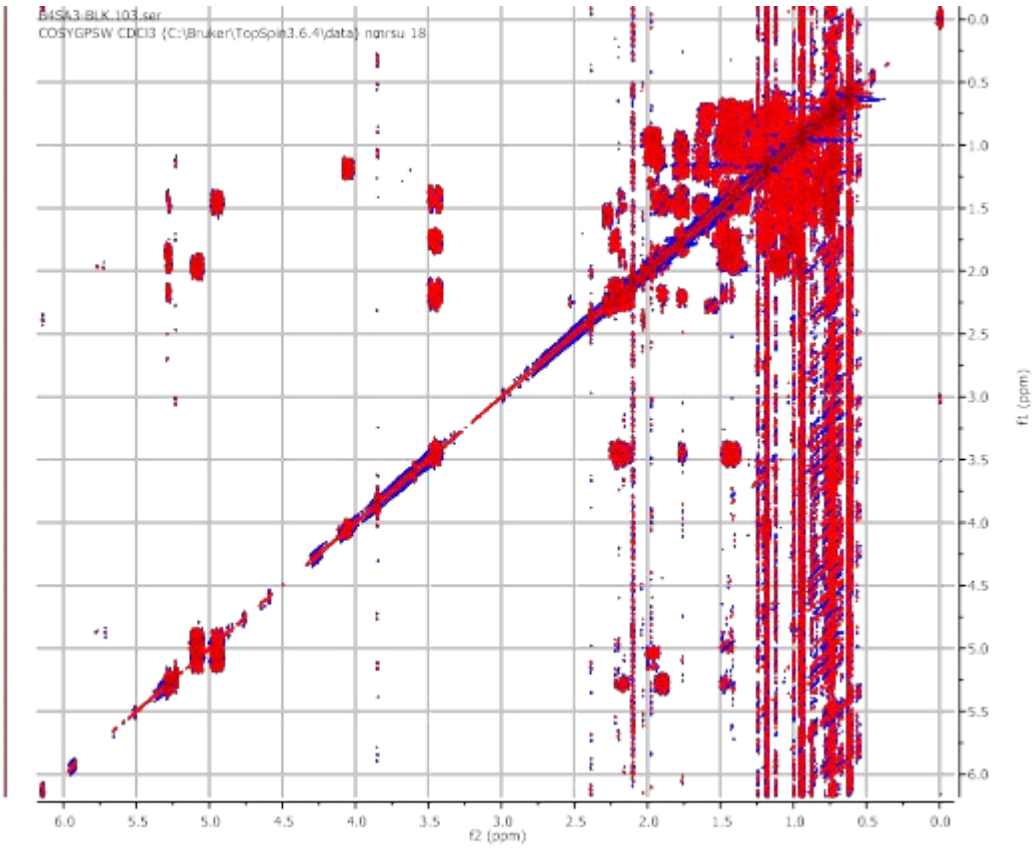

Appendix 2.2.3: HMBC

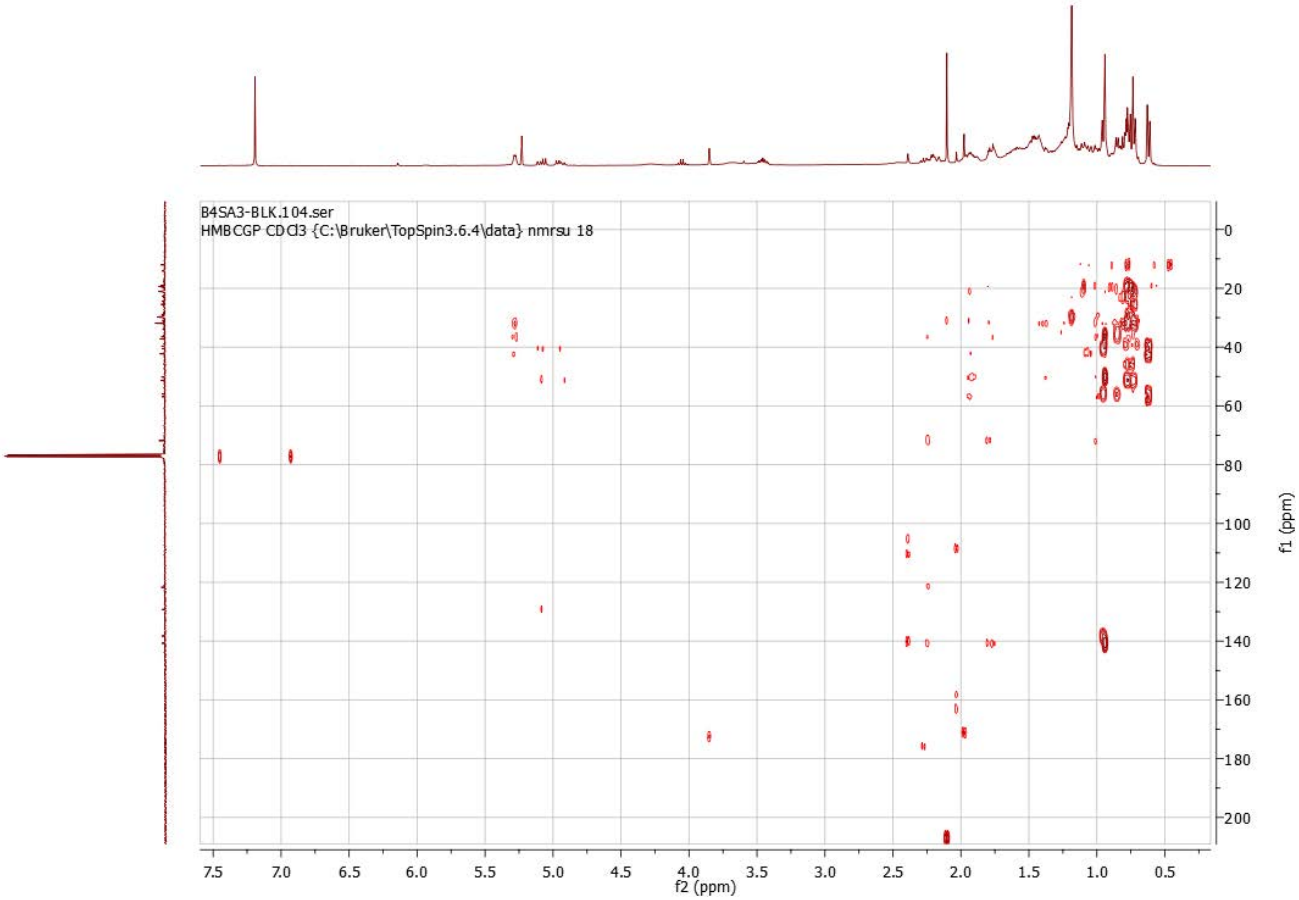

Appendix 2.2.4: HSQC

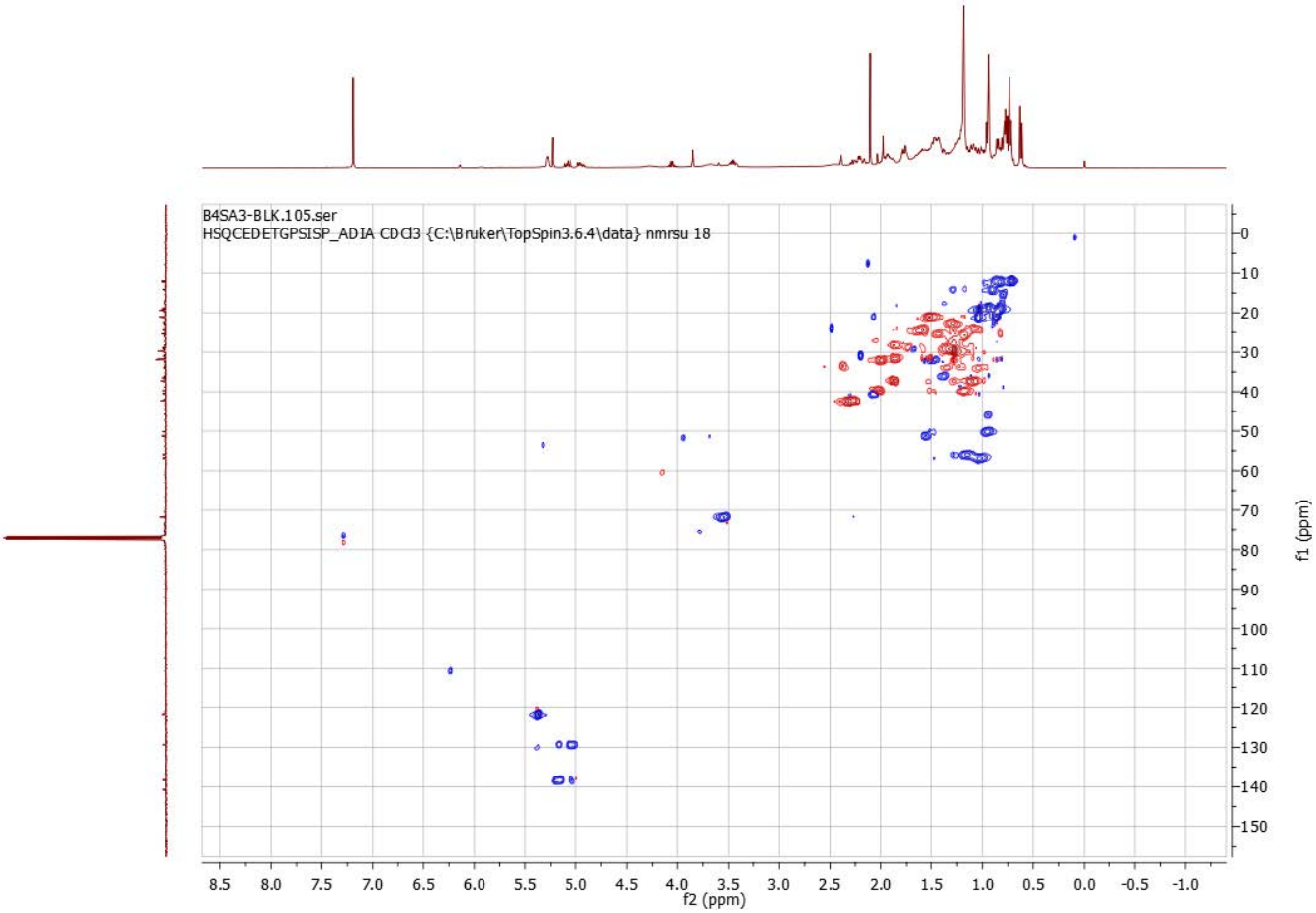

Appendix 2.3: NMR spectra for compound **3**

Appendix 2.3.1: DEPT-135

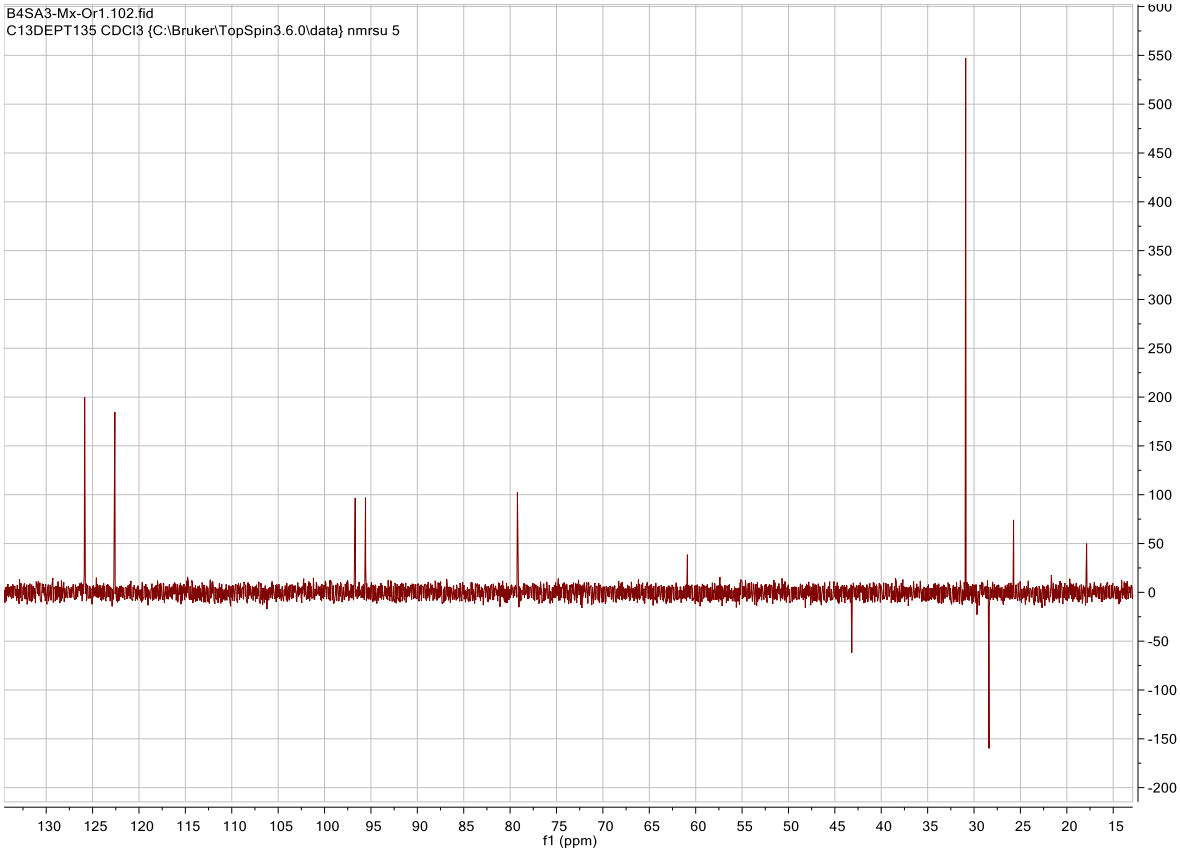

Appendix 2.3.2: COSY

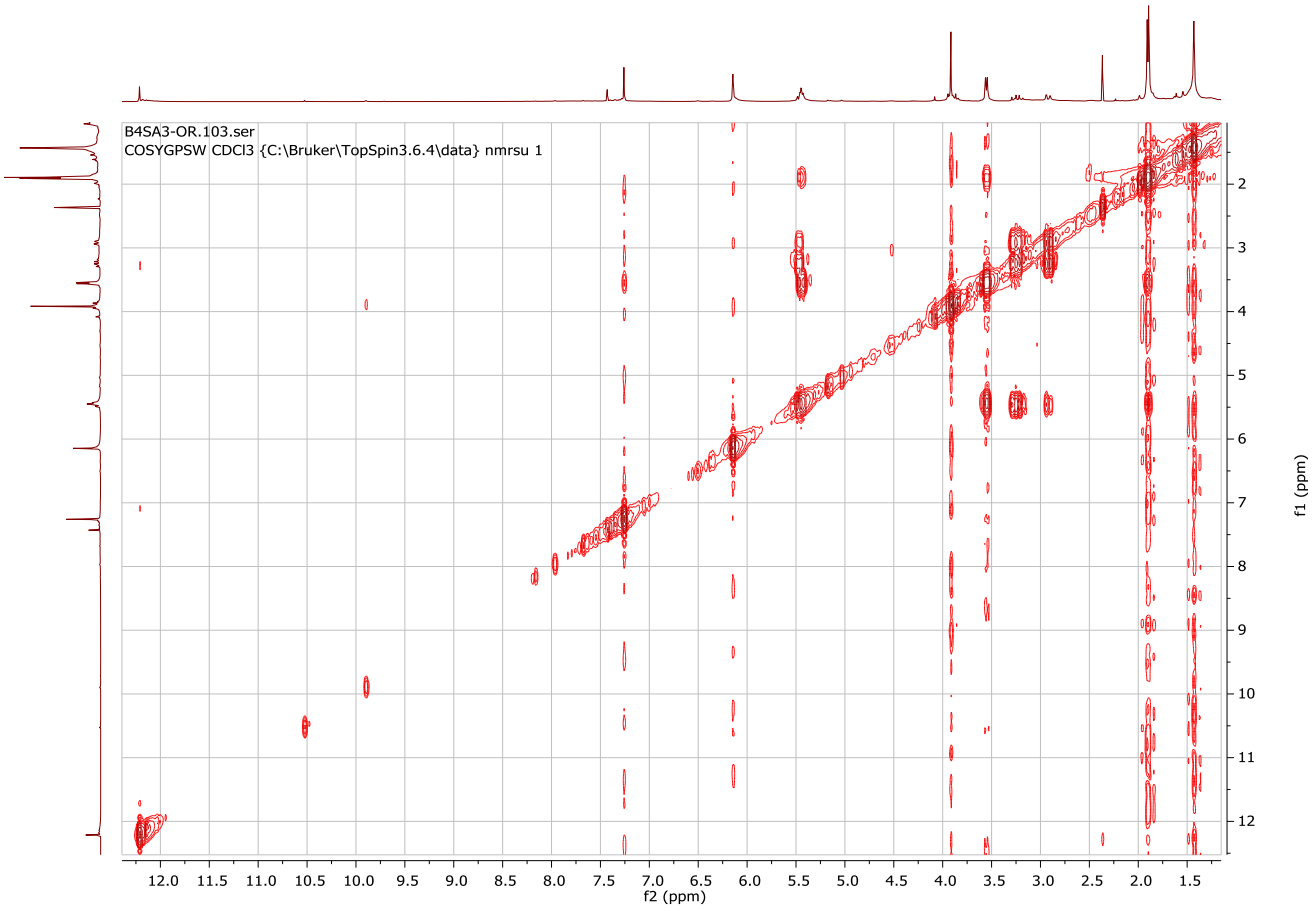

Appendix 2.3.3: HMBC

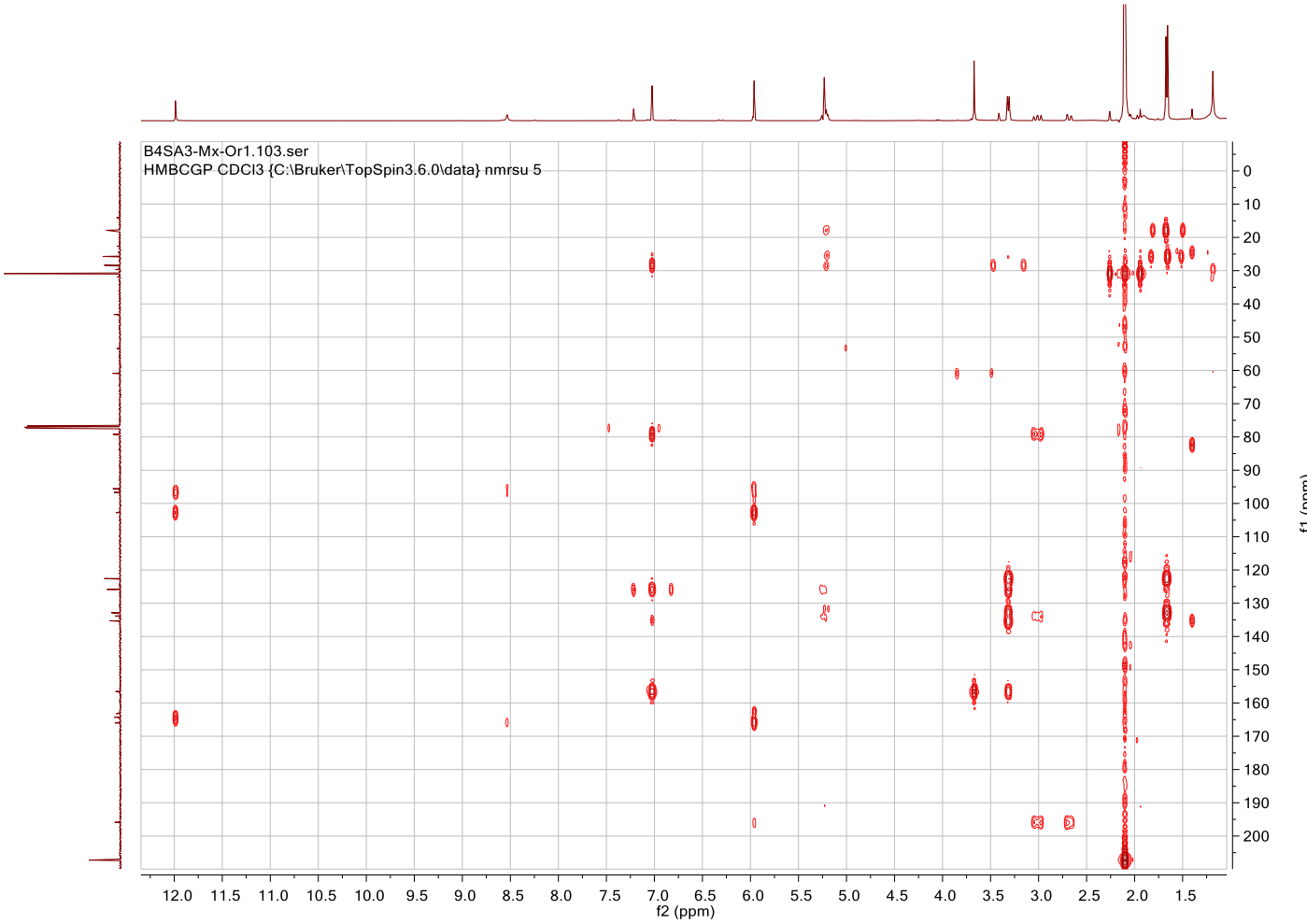

Appendix 2.3.4: HSQC

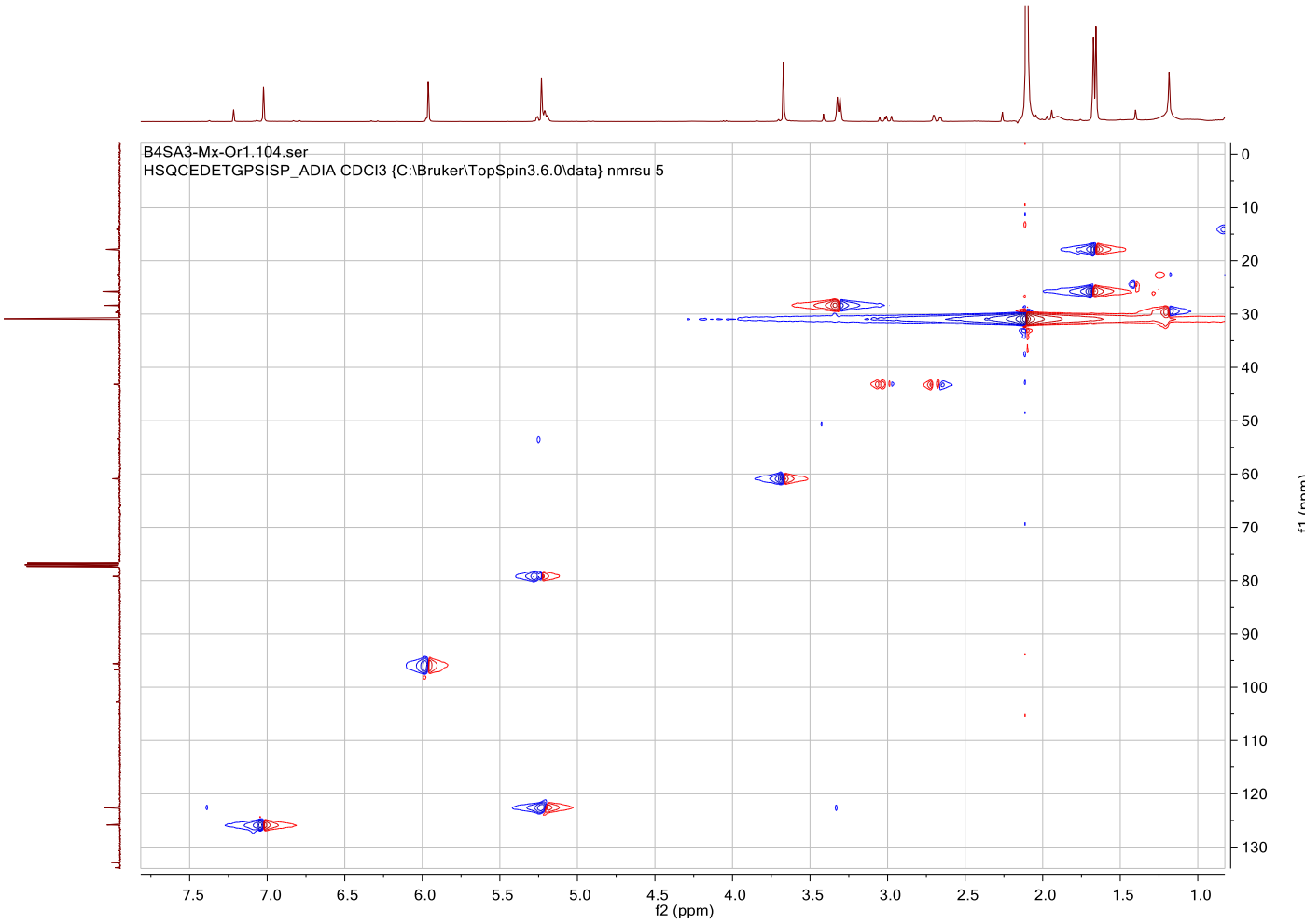

Appendix 3: Mass spectra

Appendix 3.1: Mass spectrum for compound **1**

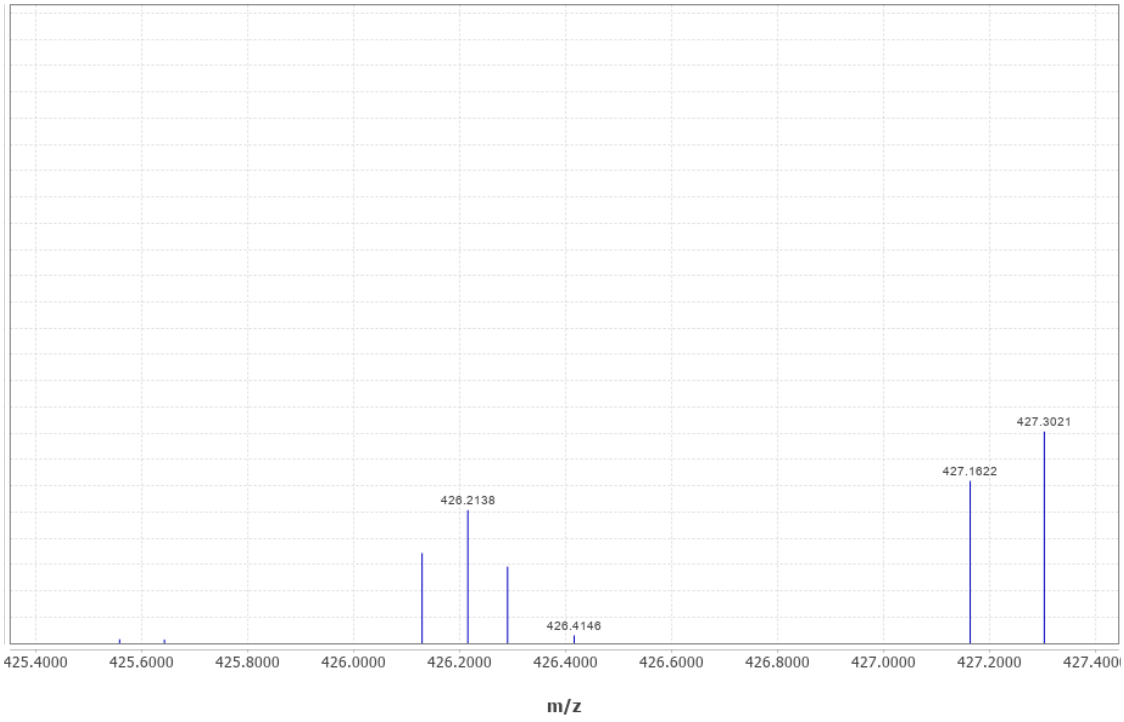

Appendix 3.2: Mass spectrum for compound **2**

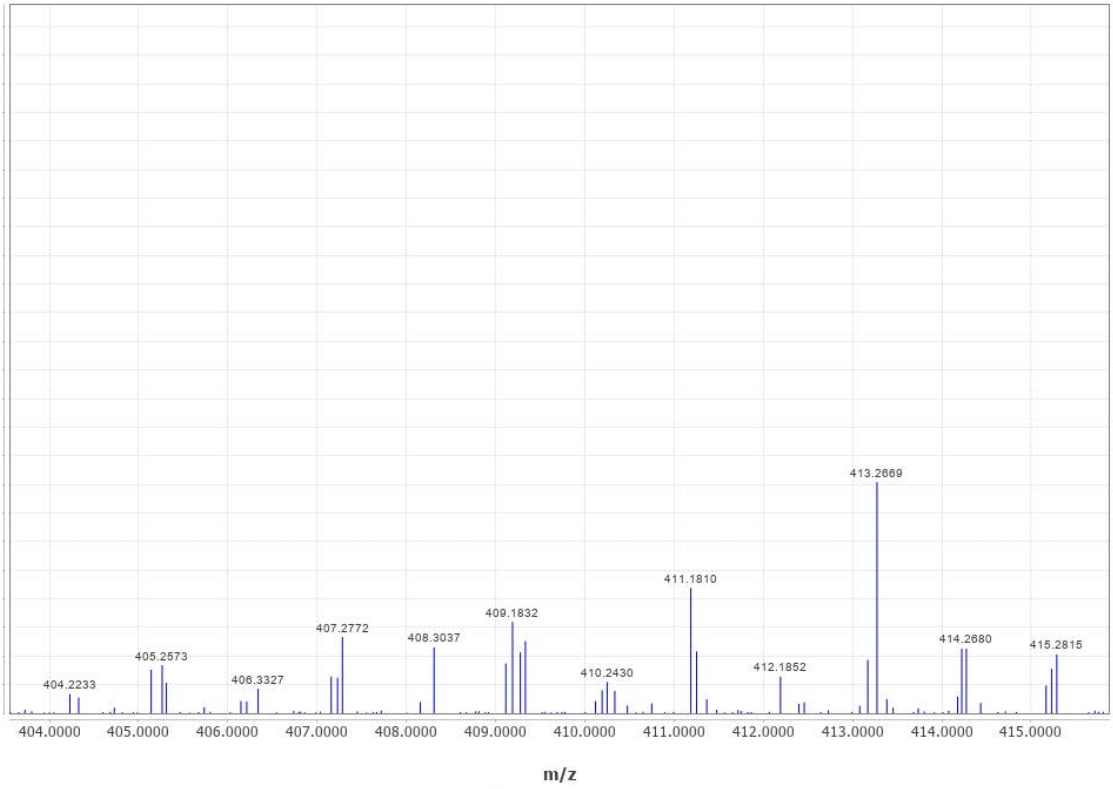

Appendix 3.3: Mass spectrum of compound **3**

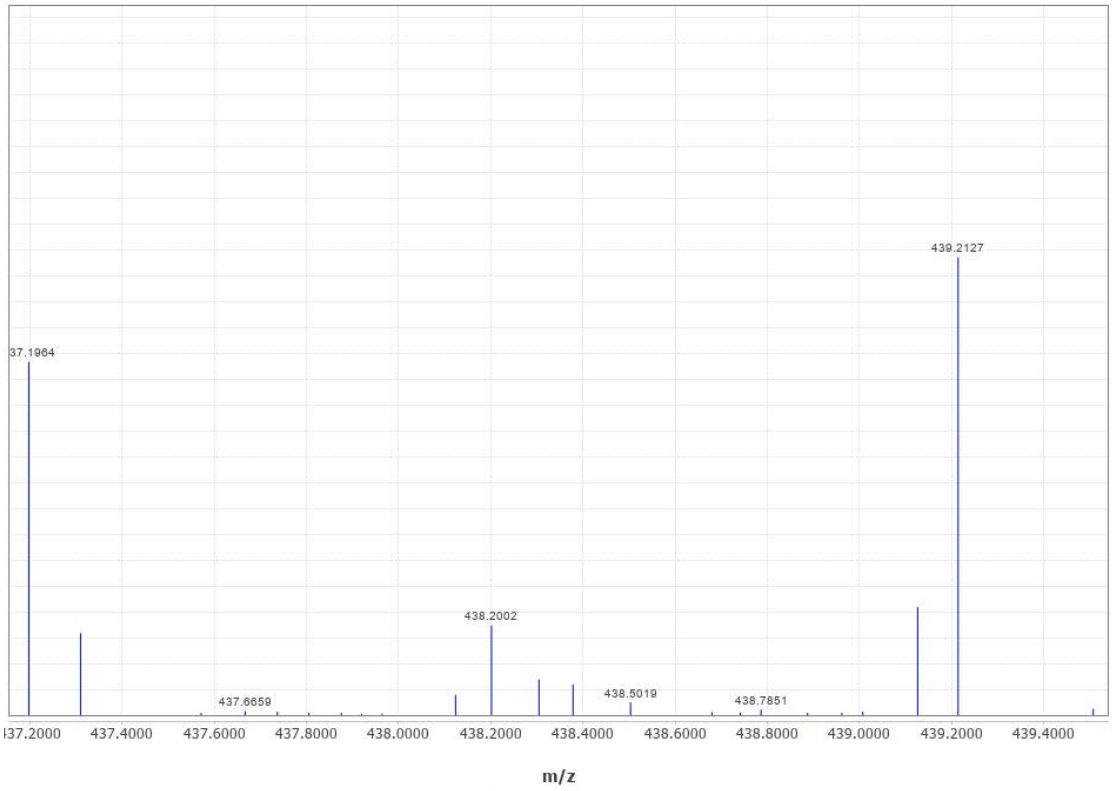

Appendix 4: Fragmentation spectra

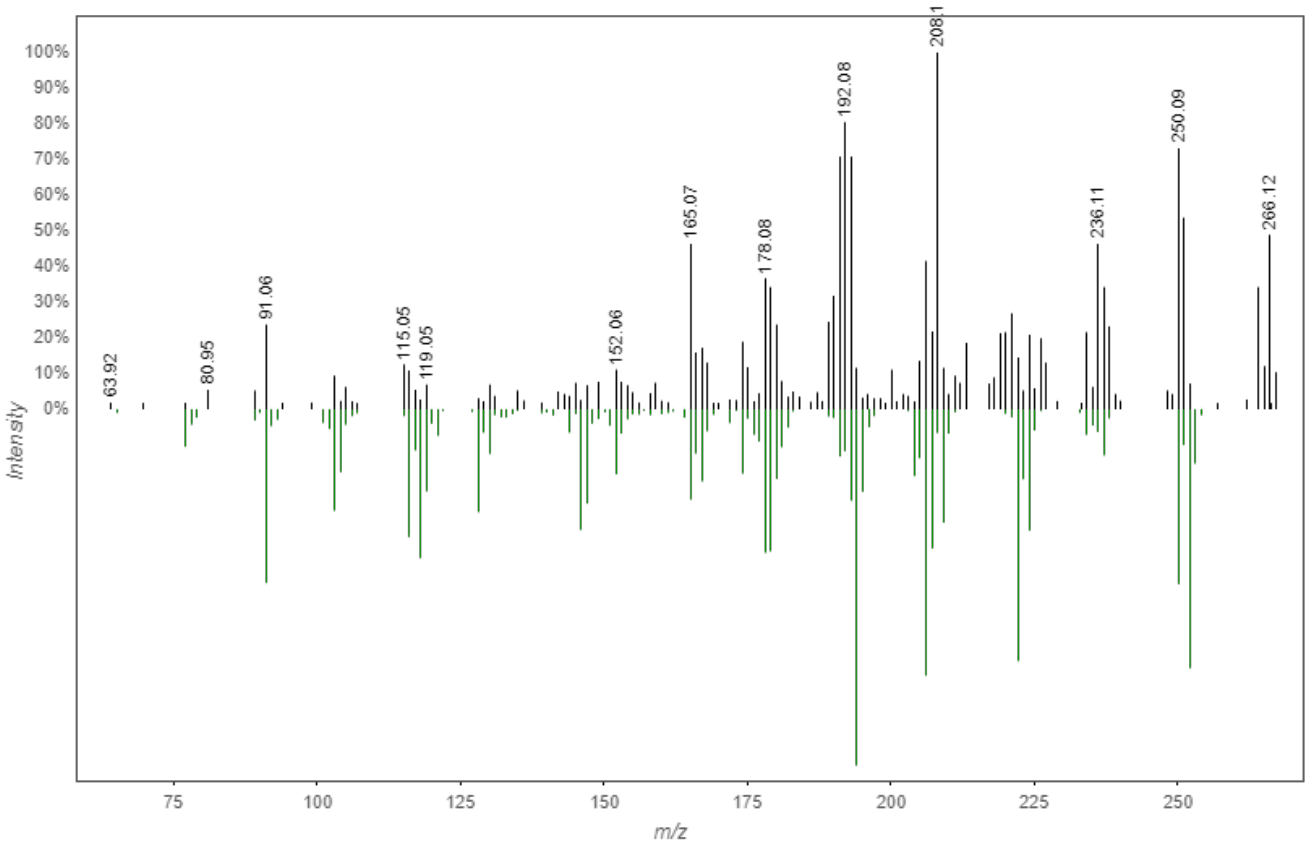

Figure 38. MS2 spectra of the feature 266.1176 annotated as a derivative of 6,7-dimethoxy-1-phenyl-3,4-dihydro-isoquinoline

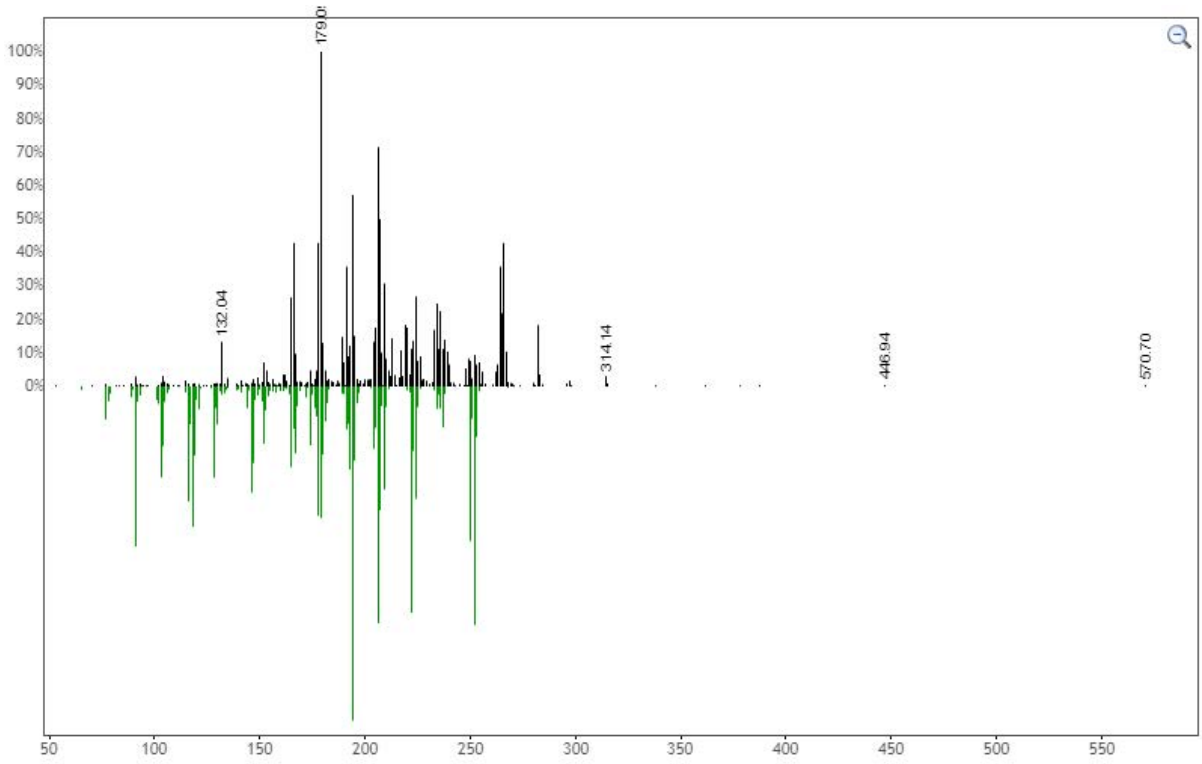

Figure 39. MS2 spectra of the feature 314.1389 annotated as a derivative of 6,7-dimethoxy-1-phenyl-3,4-dihydro-isoquinoline

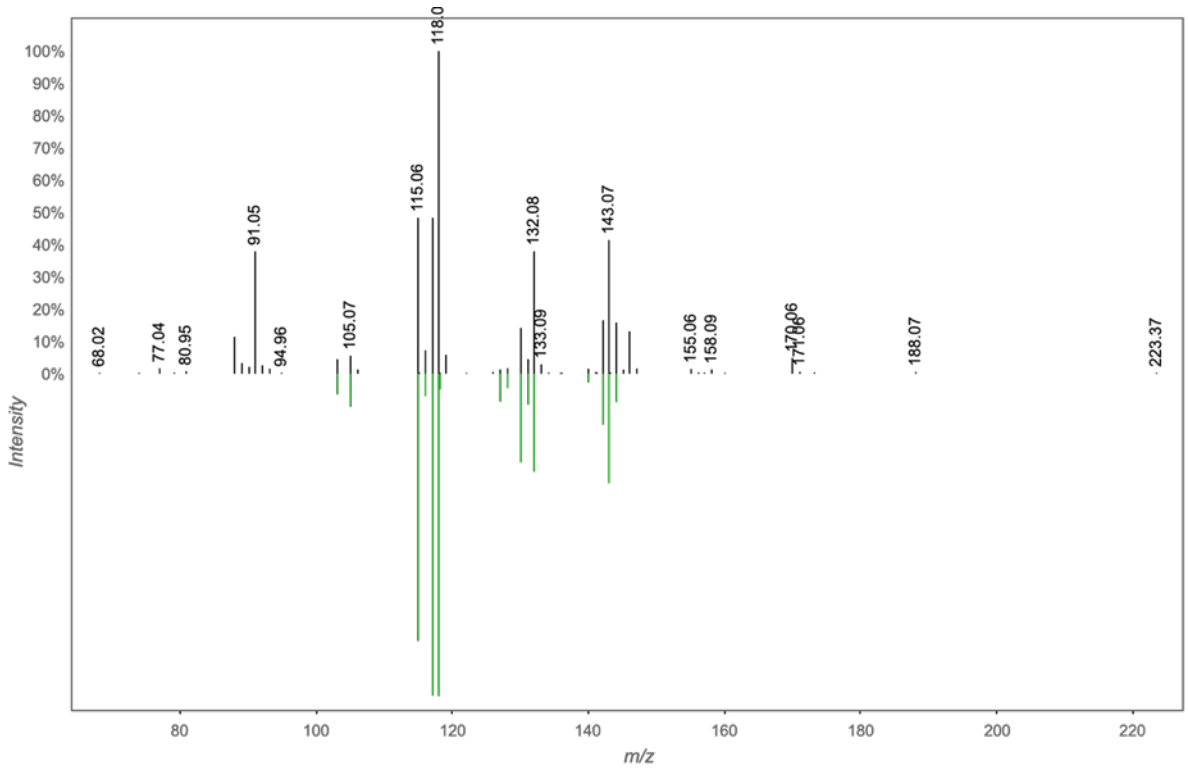

Figure 40. MS2 spectra of the feature 219.1125 annotated as abrine.

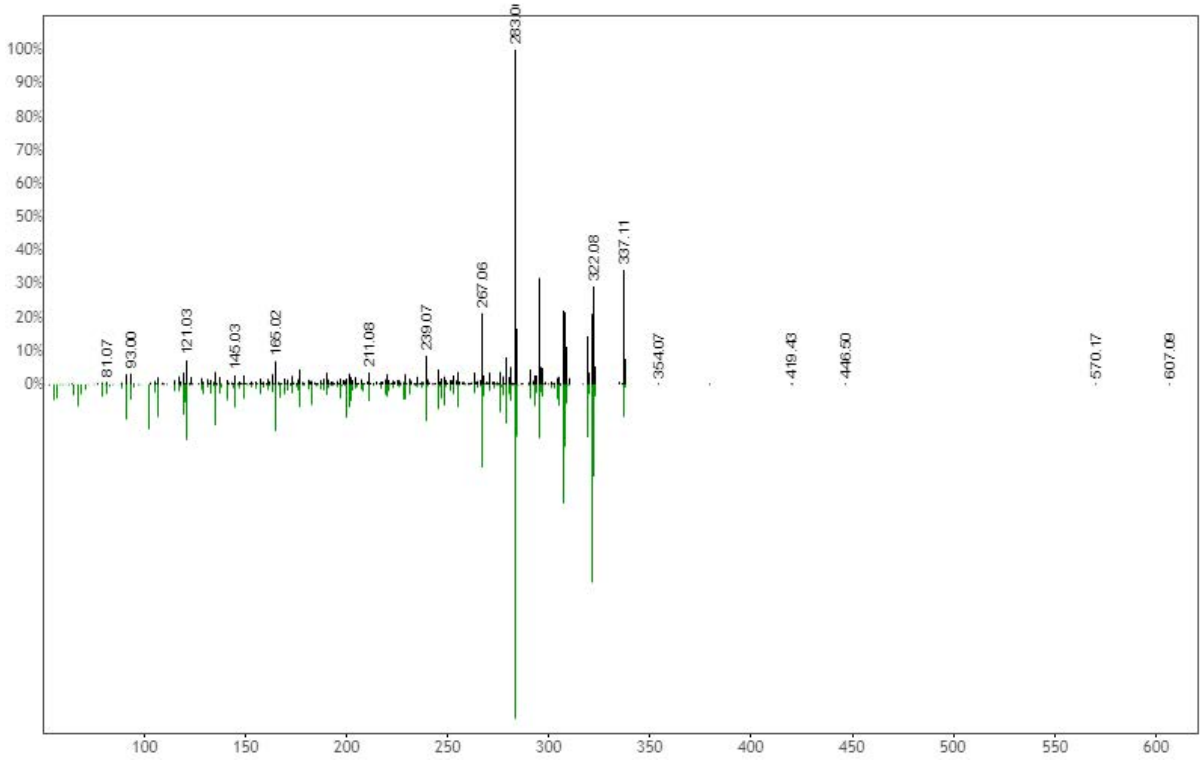

Figure 41. MS2 spectra of the feature 337.1072 annotated as carpachromene derivative.

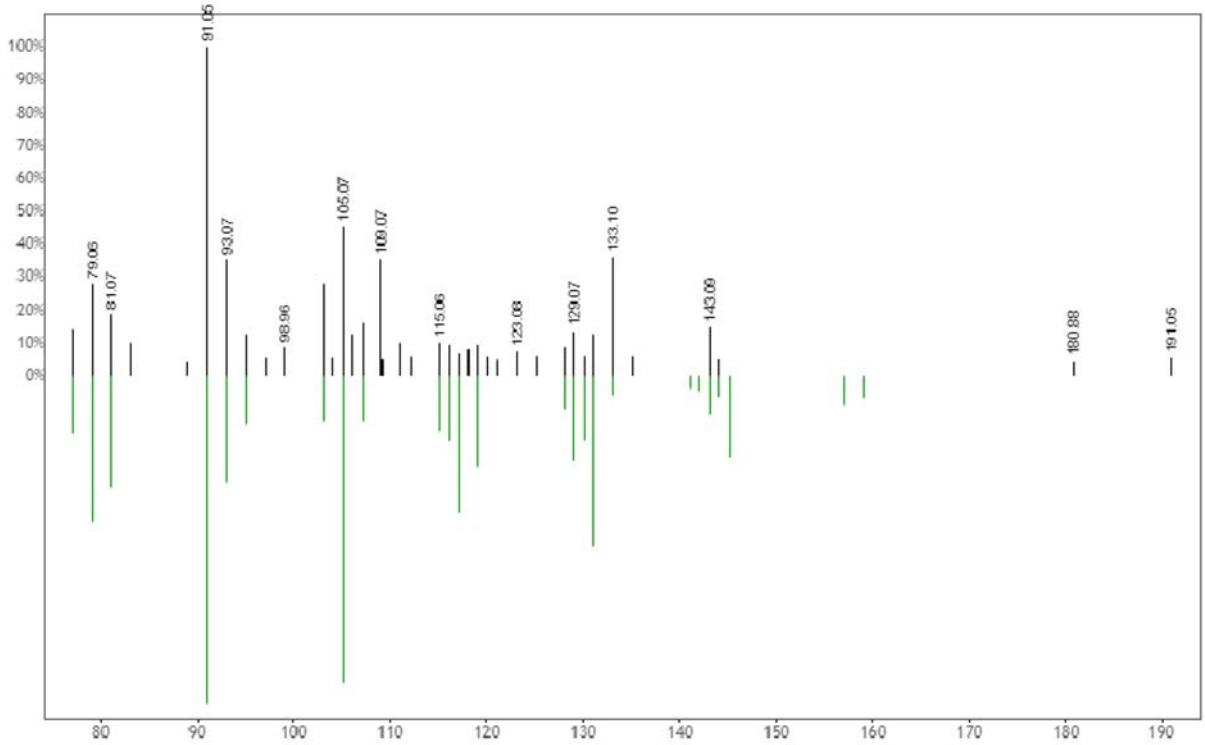

Figure 42. MS2 spectra of the feature 209.1539 annotated as costunolide

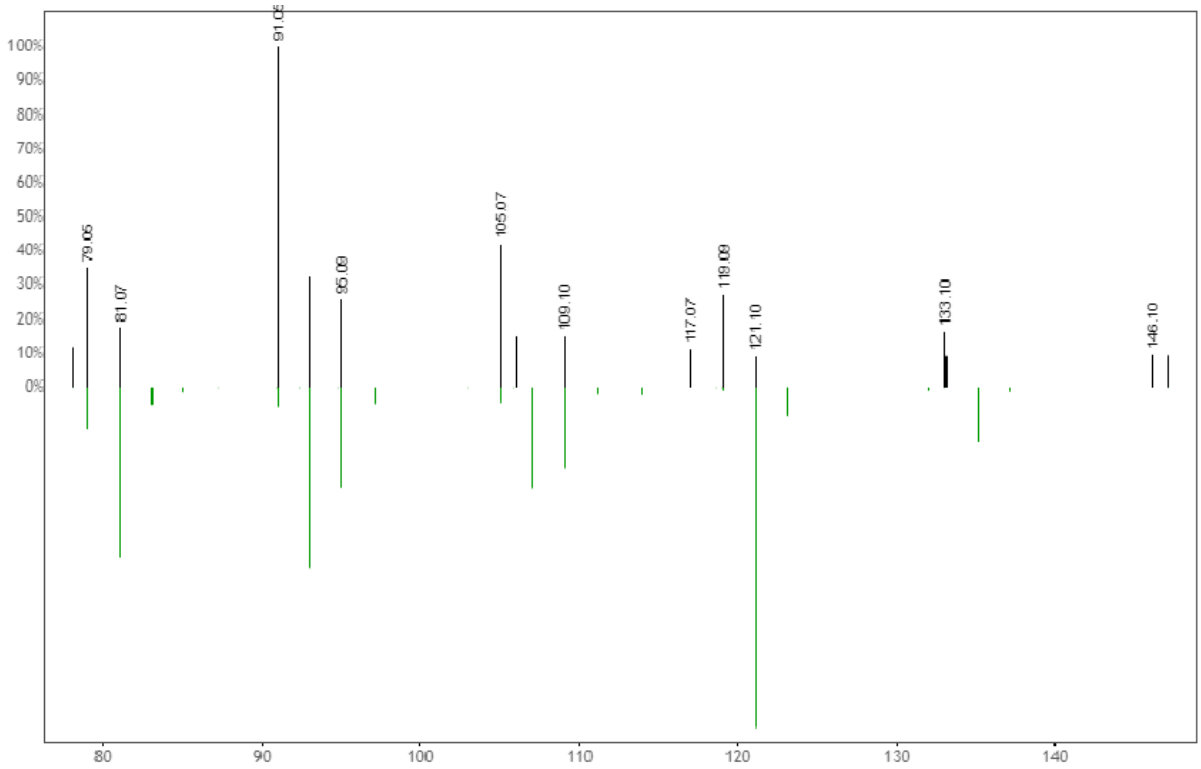

Figure 43. MS2 spectra of the feature 203.1799 annotated as bisabolol

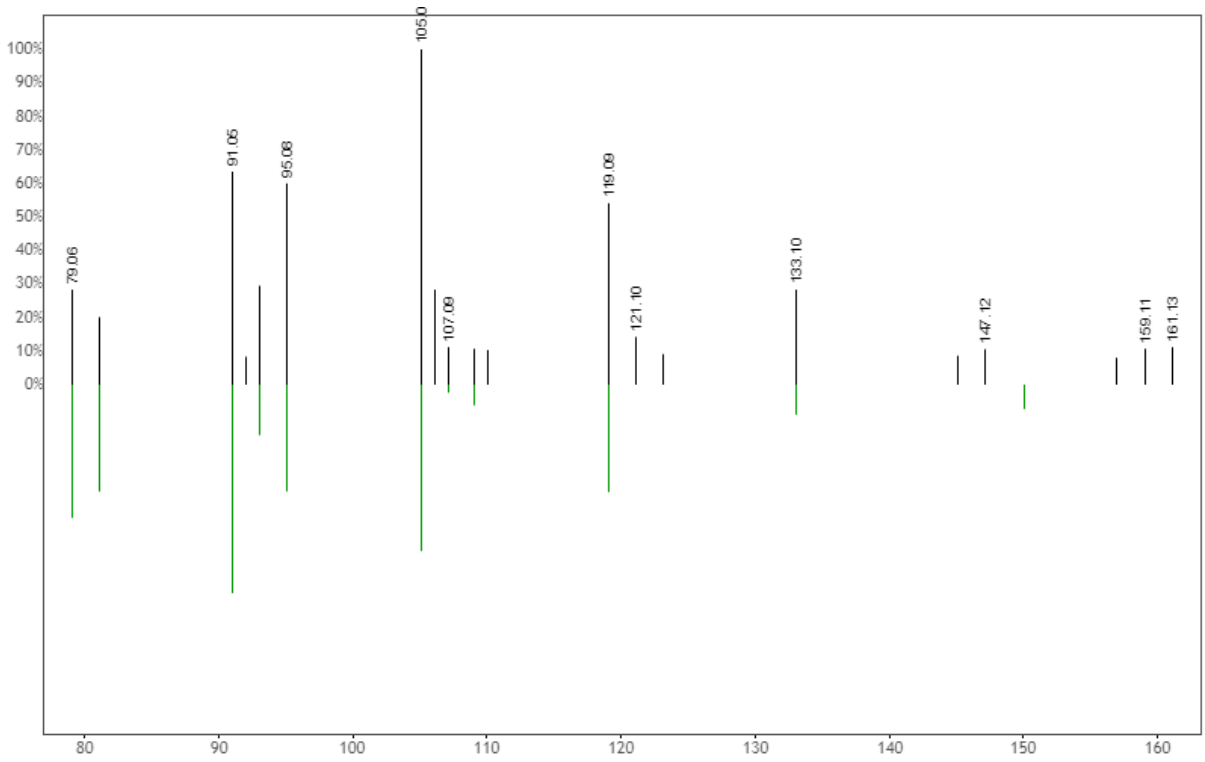

Figure 44. MS2 spectra of the feature 221.19 annotated as carophyllene epoxide

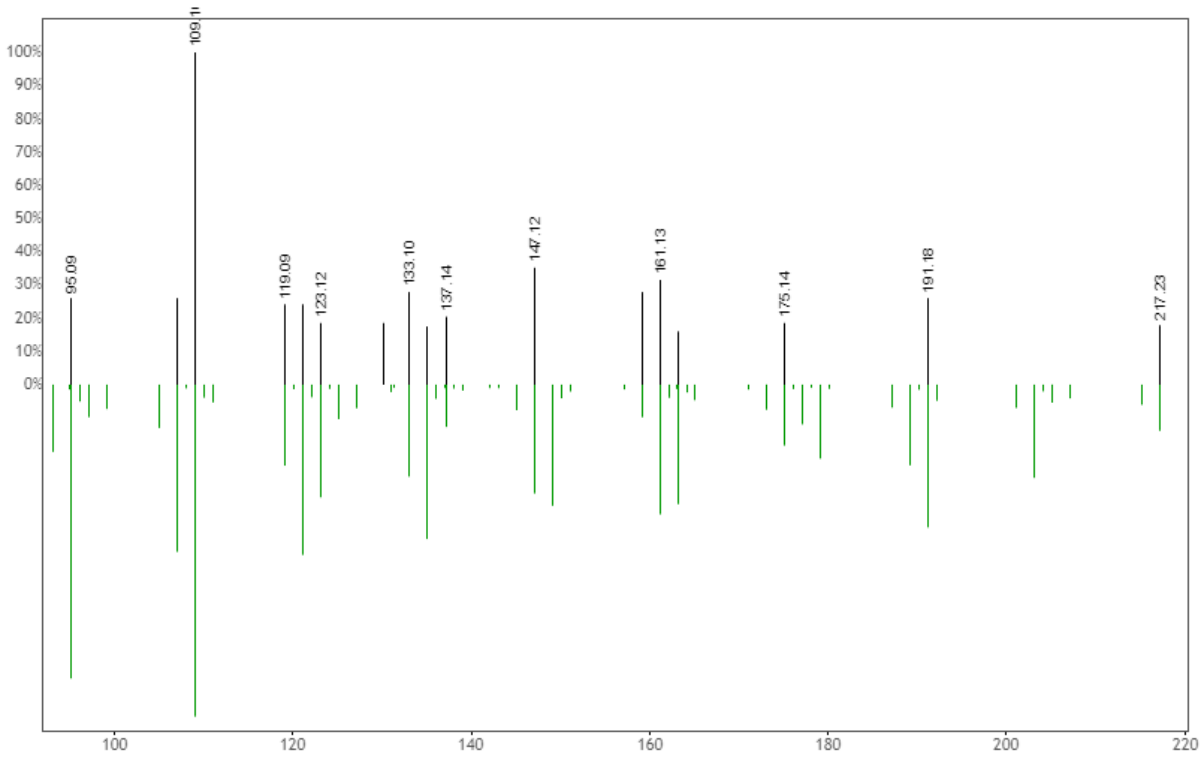

Figure 45. MS2 spectra of the feature 407.3674 annotated as a uvaol derivative**.**

.

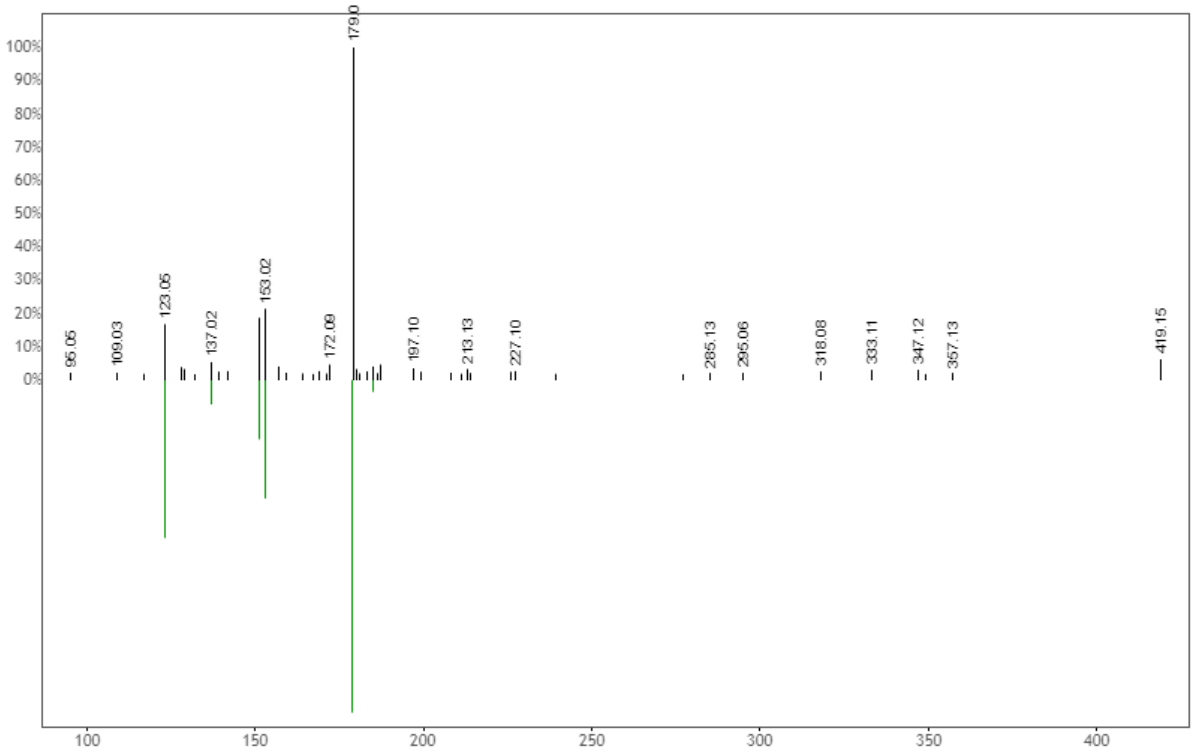

Figure 46. MS2 spectra of the feature 419.1844 annotated as a Kuwanon E derivative

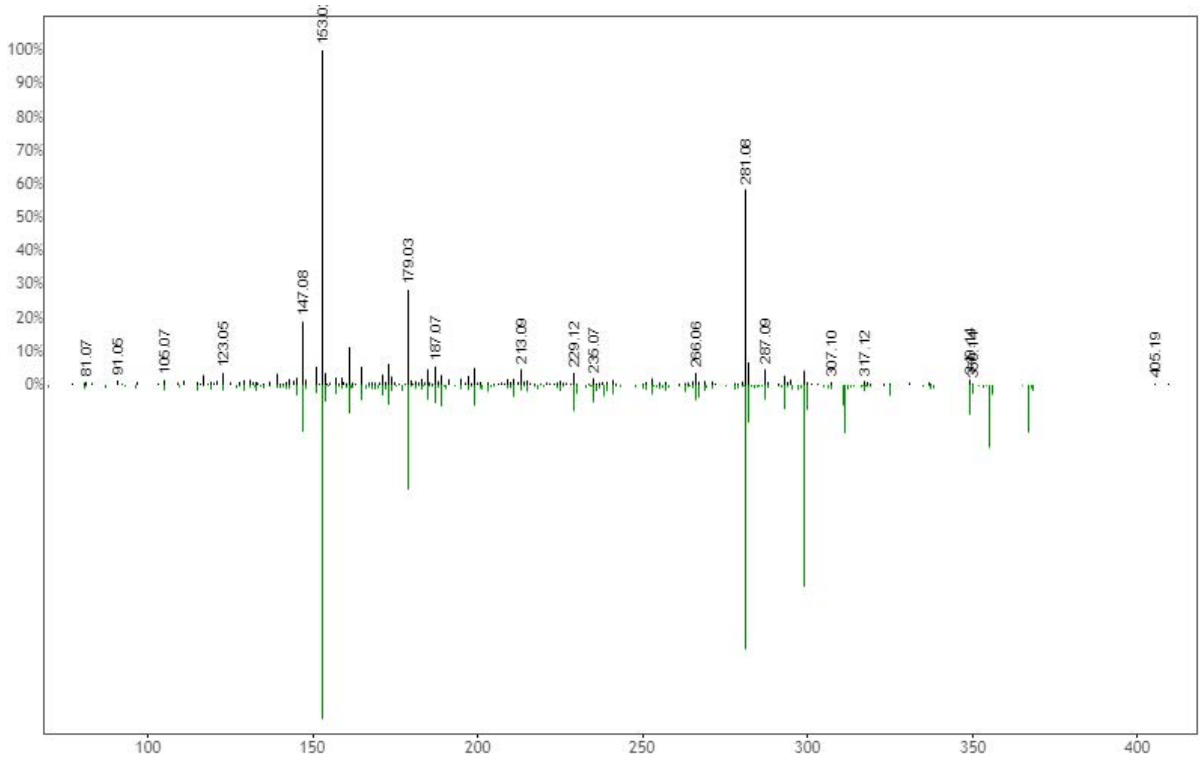

Figure 47. MS2 spectra of the feature 423.2164 annotated as Abyssinone V 4’-methyl ether

Table 15: Pharmacokinetic parameters of the isolated compounds

Compounds	mol MW	donor HB	accpt HB	QPlogPo/w	QPPCaco	QPlogBB	QPlogS	QPlogKp	QPPMDCK	QPlog Khsa	HumanOralAbsorption	PercentHumanOralAbsorption	RuleOfFive
Abssinone 4-V' methly ether	422.520	1.000	4.000	5.557	439.675	-1.433	-7.819	-2.971	203.525	1.339	1	93.834	1
Burttinone	438.519	2.000	4.750	4.920	216.440	-1.837	-7.258	-3.470	94.608	1.105	1	100.000	0
Lupeol	426.724	1.000	1.700	6.796	4565.777	0.128	-7.705	-1.914	2553.920	1.892	1	100.000	1
Stigmasterol	420.504	1.000	3.750	5.614	758.344	-1.159	-7.102	-2.162	366.860	1.218	1	100.000	1